DISSERTATION

STRUCTURAL AND FUNCTIONAL EFFECTS OF HISTONE VARIANT, H2A.Bbd, ON THE NUCLEOSOME CORE PARTICLE

Submitted by

Yunhe Bao

Department of Biochemistry and Molecular Biology

In partial fulfillment of the requirements

for the Degree of Doctor of Philosophy

Colorado State University

Fort Collins, Colorado

Spring, 2005

COLORADO STATE UNIVERSITY

March 25, 2005

WE HEREBY RECOMMEND THAT THE DISSERTATION PREPARED UNDER OUR SUPERVISION BY YUNHE BAO ENTITLED "STRUCTURAL AND FUNCTIONAL EFFECTS OF HISTONE VARIANT, H2A.BBD, ON THE NUCLEOSOME CORE PARTICLE" BE ACCEPTED AS FULFILLING IN PART THE REQUIREMENTS FOR THE DEGREE OF DOCTOR OF PHILOSOPHY.

Committee on Graduate Work

(Oren P. Anderson)

(Paul J. Laybourn)

(Olve B. Peersen)

(Laurie A. Stargell)

(Karolin Luger)
Advisor

(Marvin R. Paule)
Department Head

ABSTRACT OF DISSERTATION

Structural and Functional Effects of Histone Variant, H2A.Bbd, on the Nucleosome Core Particle

In eukaryotic cells, DNA is packaged into a protein-DNA assembly called chromatin. The basic subunit of chromatin is the nucleosome core, which is composed of 147 base pair (bp) of DNA wrapped in 1.65 turns around a histone octamer containing two copies each of the four core histone proteins (H2A, H2B, H3 and H4). Chromatin creates an impediment to the processes of DNA transcription, replication, repair and recombination. In addition to histone covalent modification and ATP-dependent chromatin remodeling, substitution of core histones by the corresponding histone variants plays an important role in transcription regulation in the chromatin context.

H2A.Bbd is only 48% conserved compared to major, replication-dependent H2A. Major sequence differences are in the docking domain that tethers the (H2A-H2B) dimer to the $(H3\text{-}H4)_2$ tetramer, and in the missing C-terminal region in H2A.Bbd. In this study, several biochemical and biophysical methods were used to investigate the effect of H2A.Bbd incorporation on the structure and stability of nucleosomes. It was found that Bbd-NCP has a more relaxed structure in which only 118+/-2 bp of DNA was protected against digestion with micrococcal nuclease. Furthermore, absence of fluorescence resonance energy transfer (FRET) between the ends of the DNA in Bbd-NCP indicated that the

distance between the DNA ends was increased significantly. The Bbd docking domain is largely responsible for this behavior, as shown by domain-swap experiments. Further, it was determined that a hybrid nucleosome, containing an H2A.Bbd-H2B dimer and an H2A-H2B dimer, is formed *in vitro*. It was found that H2A.Bbd-H2B dimers are easily depleted during *in vitro* reconstitution. *In vitro* dimer exchange experiments were used to determine that both conventional and variant histone dimers are more readily exchanged into Bbd-NCPs than into canonical NCPs. These results suggest that incorporation of H2A.Bbd into nucleosomes results in a more open structure and reduced inherent stability. This thesis work sheds light on a cellular mechanism for regulation of transcription, by changing the biochemical makeup of nucleosomes by incorporation of a special histone variant, H2A.Bbd, to reduce the inherent stability of nucleosomes and facilitate transcription.

Yunhe Bao

Department of Biochemistry
and Molecular Biology,
Colorado State University
Fort Collins, CO, 80523.
Spring, 2005

ACKNOWLEDGEMENTS

My primary acknowledgement goes to my advisor, Dr. Karolin Luger, for her consistent support and inspiration during my graduate career. Karolin is a wonderful scientist and a marvelous mentor. She was always willing and able to help me in providing direction for my work. Her love of, and enthusiasm for science has deeply influenced me.

I would also like to thank the members of my committee: Dr. Oren Anderson, Dr. Paul Laybourn, Dr. Olve Peersen, Dr. Laurie Stargell. Each of these individuals invested their time and energy in helping me. They gave me valuable suggestions and guidance throughout my research.

I am especially thankful to Kasey Konesky, Dr. Paul Laybourn, and Dr. David Tremethick for their helpful collaboration. I would like to thank Dr. Robert Woody and Dr. Jeffrey Hansen for their suggestions and inputs to my work. I would also like to thank Dr. Xu Lu from the Hansen lab for his help with analytical ultracentrifugation.

Many current and former individuals from the Luger lab provided encouraging support and friendship over the years, including: Dr. Srinivas Chakravarthy, Pam Dyer, Dr. Rajeswari Edayathumangalam, Dr. Uma Muthurajan, Dr. Youngjun park, Simona Ruso, Treresa Russell, Jay Chodaparambil, Aaron Stephan, Vidya Subramanianian, and Dr. Cindy White.

I would also like to thank my good friend, Dr. Daniel Linstedt, for his kindly reading through my thesis and offering suggestions for modifying the English structure.

Last but not least, I acknowledge the love and support of my family. My parents, Yongqing Bao and Suying Li, always encouraged me and gave me a hand when help was needed. I thank my wife, Jing Xiao, for her constant support that was critical in completing this dissertation.

TABLE OF CONTENTS

CHAPTER 1

Literature Review

1.1 Nucleosome structure

In eukaryotic cells, DNA is packaged in the nucleus by a hierarchical scheme of folding and compaction into a protein-DNA assembly called chromatin. The basic subunit of chromatin is the nucleosome core, which is composed of 147 bp of DNA wrapped in 1.65 turns around a histone octamer containing two copies each of the four core histone proteins (H2A, H2B, H3 and H4). Long arrays of nucleosomes are further coiled into a 30 nm fiber, which is compacted further into multiple higher organizational levels in an, as yet, unknown manner.

Nearly 30 years ago, Kornberg proposed that the chromatin structure is based on a repeating unit of eight histone molecules and about 200 bp DNA [Kornberg, 1974]. One year later, Oudet *et al.* provided a vivid electron microscopic image of eukaryotic genome that clearly showed the existence of uniformly sized particles on DNA, which looked like beads on a string [Oudet et al., 1975]. Micrococcal nuclease digestion of chromatin led to determination of the nucleosome core particle (NCP), with 146 bp of DNA wrapped around the histone octamer [Lohr and Van Holde, 1975; Noll and Kornberg, 1977]. These

studies provided the basis for further chromatin research (See [Kornberg and Lorch, 1999] for review).

Crystallographic studies have greatly extended our understanding of the NCP structure (for review see [Luger, 2003]). Currently, there are a number of high-resolution structures of nucleosome core particles available from different organisms [Davey et al., 2002; Harp et al., 2000; Luger et al., 1997a; White et al., 2001], reconstituted with histone variants [Suto et al., 2000], and in complex with site-specific minor groove DNA-binding ligands [Edayathumangalam et al., 2004; Suto et al., 2003]. All these NCP structures are very similar. Even the nucleosome core particle structure containing posttranslationally modified histones from chicken erythrocyte nuclei [Harp et al., 2000] shows near identical structure to that obtained from recombinant *Xenopus* histones that are free of such modifications [Luger et al., 1997a] (Fig.1.1).

The crystal structure of histone octamer and crystal structures of NCP show that each of the core histones shares a highly similar structural motif, the histone fold, which is constructed from two short α-helices and a long central helix separated by two loops (Fig. 1.2A) [Arents et al., 1991; Luger et al., 1997a]. In the NCP structure, each of the core histones exists as part of a heterotypic dimer, H2A-H2B or H3-H4. In each dimer, the two monomers are intimately associated in a head-to-tail manner termed 'handshake motif' [Arents et al., 1991], with the long central helices interacting in an antiparallel manner (Fig. 1.2 B, C). Interestingly, the histone fold has also been found in eukaryotic transcription factors [Xie et al., 1996], indicating that the histone fold is

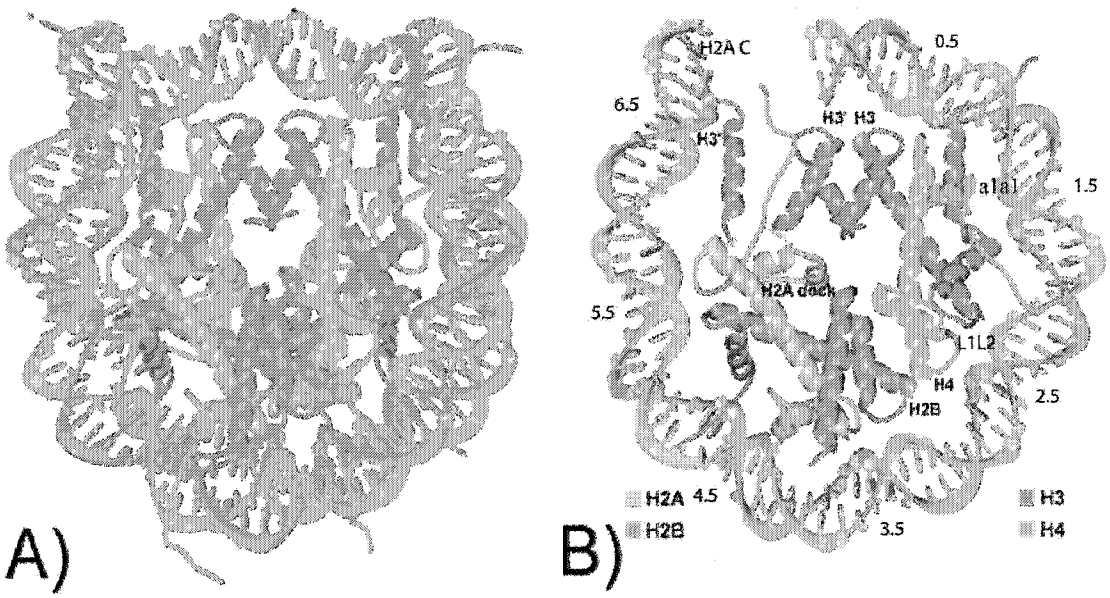

Figure 1.1: Nucleosome core particle structure
A) Overview of the nucleosome core particle structure, viewed down the superhelical axis. A non-crystallographic axis of symmetry runs vertically through the plane of the paper. Histone proteins are distinguished by different colors. B) Only one half of the DNA (73 bp) and associated proteins are shown. Regions of symmetry -related histone H3 are indicated as H3'. The H2A docking domain (H2A dock), and the H2A C-terminus (H2A C) are indicated. DNA binding motifs L1L2 and α1α1 are indicated for one H3-H4 dimer. Areas of protein-DNA interaction are numbered from the center of the DNA (superhelix axis location, SHL0.5) to the end (SHL6.5). (Figure is reproduced from Luger et al., 1997a).

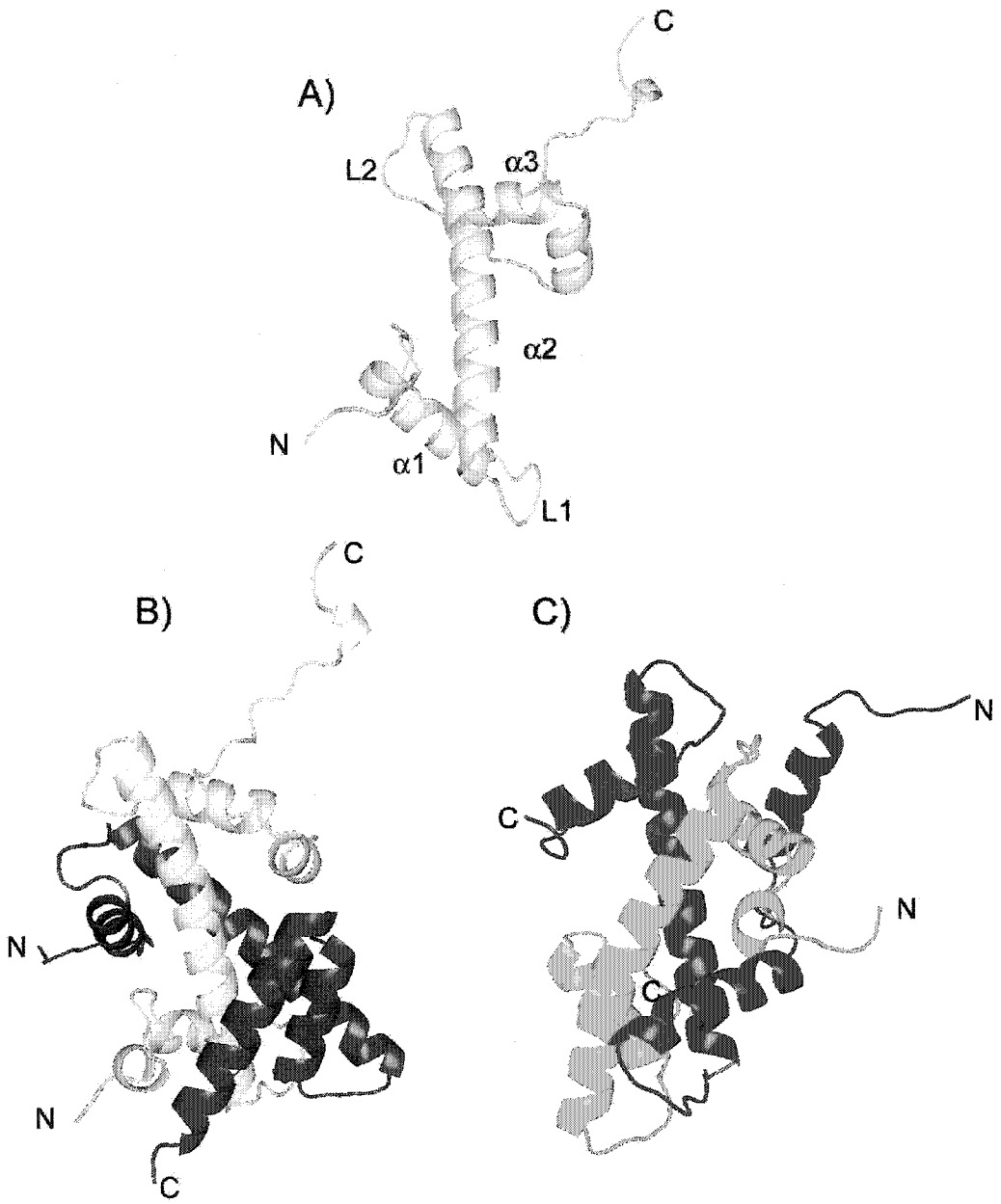

Figure 1.2: All histones share a highly similar structural motif 'histone fold' and heterodimers are associated by forming a 'handshake motif'. A) Histone H2A. All the components of the histone fold are indicated (α1, α2, α3, L1 and L2). B). Histone H2A (yellow) and H2B (red) dimer. C). Histone H3 (blue) and H4 (green) dimer.

widespread and may perform a number of roles (for review see [Ramakrishnan, 1995; Ramakrishnan, 1997]).

A 4-helix bundle formed between the H3-H4 dimers drives the formation of the tetramer, which is stable at physiological ionic strengths. This tetramer also persists in the absence of DNA [Van Holde, 1988]. It has been shown that the tetramer is involved in the initial step in nucleosome assembly, and in determining nucleosome positioning [Dong and van Holde, 1991; Hayes et al., 1991]. One H2A-H2B dimer is tethered to each side of the $(H3\text{-}H4)_2$ tetramer to form the histone octamer, which is stable both as part of the NCP and at high ionic strength. The C-terminal halves of H2B and H4 form another 4-helix bundle in association with the H2A-H2B dimer and the $(H3\text{-}H4)_2$ tetramer. Furthermore, the interactions between dimer and tetramer are also aided by the H2A ladle-shaped docking domain that guides the H3αN helix to interact with the last turn of the DNA and form a short β-sheet with the C-terminal region of H4 (Fig. 1.1) [Suto et al., 2000].

In the nucleosome core particle, the 147 bp nucleosomal DNA is wrapped around the histone octamer in 1.65 turns of a left-handed superhelix. There are three DNA binding sites formed in each heterotypic dimer: two L1L2 binding sites and one α1α1 binding site. As such, 12 of the 14 superhelix locations (SHLs: ± 0.5, ± 1.5, ± 2.5, ± 3.5, ± 4.5, ± 5.5, ± 6.5) interact with histone folds. Differences in the buried surface areas and in the number of protein-DNA contacts suggests that the binding affinities exist in the following order: SHLs ± 0.5 > ± 3.5 > ± 4.5 > ± 1.5, ± 2.5, ± 5.5 > ± 6.5 [Luger et al., 1997a; Luger and Richmond, 1998a]. In

total, there are 142 hydrogen bond interactions between protein and DNA within the 14 SHLs. About half of these hydrogen bonds are between the protein main-chain and the phosphodiester backbone atoms [Luger et al., 1997a; Luger and Richmond, 1998a]. The crystal structure shows that each histone fold pair forms a crescent shape that arcs about 28 bp of DNA in a 140° bend, leaving 4 bp linkers between. Therefore, the $(H3\text{-}H4)_2$ tetramer organizes the central 60 base pairs of nucleosomal DNA and the (H2A-H2B) dimer organizes 30 base pairs towards either end of the DNA. The last 13 base pairs of nucleosomal DNA at each terminus are organized by the H3αN helix region that does not form an intergral part of the $(H3\text{-}H4)_2$ tetramer. This H3αN helix region is apparently not able to bind DNA in the absence of the (H2A-H2B) dimer (Fig. 1.1) [Luger et al., 1997a; Luger and Richmond, 1998a].

The 1.9 Å crystal structure of the NCP provides more structural information. Over 3000 water molecules and 18 ions have been identified. Many of the water molecules act as hydrogen-bond bridges between protein and DNA, providing further stability to direct protein-DNA interactions. Additionally, they enable formation of many interactions between more distantly related elements. These solvent-mediated interactions may provide a means of accommodating structural variations in DNA to limit the sequence dependency of nucleosome positioning. More importantly, this observation suggests that the water molecules could facilitate nucleosome mobility, which plays a major role in chromatin remodeling during transcription [Davey et al., 2002].

1.2 Organization of chromatin

Linker histones, which comprise a large family of chromatin associated proteins, are present in ~ 1:1 molar stoichiometry with nucleosome in bulk chromatin *in vivo* [Van Holde, 1988]. Digestion of chromatin by micrococcal nuclease results in an intermediate, the chromatosome, which is a complex consisting of 165 bp DNA, histone octamer and linker histone H1 [Noll and Kornberg, 1977], [Simpson, 1978]. It is believed that the primary function of linker histones is to stablize the compact higher order structure of the chromatin fiber (for review see [Hansen, 2002; Widom, 1998a; Zlatanova and van Holde, 1996]). Recently, H1b, a specific isoform of linker histone, was found to be involved in gene-specific transcriptional regulation [Lee et al., 2004].

The linker histones consist of a globular domain flanked by a short N-terminal tail and a long basic C-terminal tail [Aviles et al., 1978; Hartman et al., 1977]. The crystal structure of the globular domain of histone H5 shows that the protein consists of a three-helix bundle, with a β-hairpin or "wing" at its C-terminus. This structure shows remarkable similarity to that of the DNA-binding domain of transcription factor HNF3 [Clark et al., 1993; Ramakrishnan et al., 1993].

The manner in which the linker histones interact with nucleosomes is unclear. Presently, there are two models to describe the interaction between H1 and nucleosomes. In one model, the globular domain of H1 exists outside of the DNA coils and binds to DNA where it enters and exits the nucleosome [Staynov and Crane-Robinson, 1988]. In the other model, the globular domain lies

asymmetrically inside the turns of nucleosomal DNA and contacts the core histones, especially H2A [Pruss et al., 1996]. It was shown that the linker histone H5 globular domain alone cannot stabilize chromatin folding, while a fragment containing the H5 globular domain and C-terminal tail can stabilize chromatin folding like full length H5 [Allan et al., 1986]. These results suggest that the highly basic linker histone C terminus plays a significant role in stabilization of folded chromatin fibers by binding to linker DNA [Hansen, 2002]. Interestingly, the globular domain alone is able to protect 20 bp of nucleosomal DNA, just like full length linker histones [Thomas and Wilson, 1986]. Furthermore, it has been shown that both full length linker histones and the isolated globular domains bind preferentially to four-way junctions of DNA [Varga-Weisz et al., 1993; Varga-Weisz et al., 1994]. This observation is related to another result that showed linker histones to exhibit binding preference for nucleosomes over free DNA [Hayes and Wolffe, 1993]. The implication of these results is that the globular domain of linker histones has more than one DNA-binding site and helps stabilize wrapping of peripheral nucleosomal DNA. It has also been suggested that the globular domain may mediate fiber-fiber interactions due to their ability to self-associate [Carter and van Holde, 1998; Maman et al., 1994].

In the eukaryotic cells, the nucleosome array is further folded by a hierarchical scheme of folding and compaction (Fig. 1.3). At the first level, the extended arrays of nucleosomes exhibit a beads-on-a-string conformation referred to as "10-nm-diameter filaments" [Van Holde, 1988]. However, it has been suggested that this beads-on-a-string conformation is an artifact

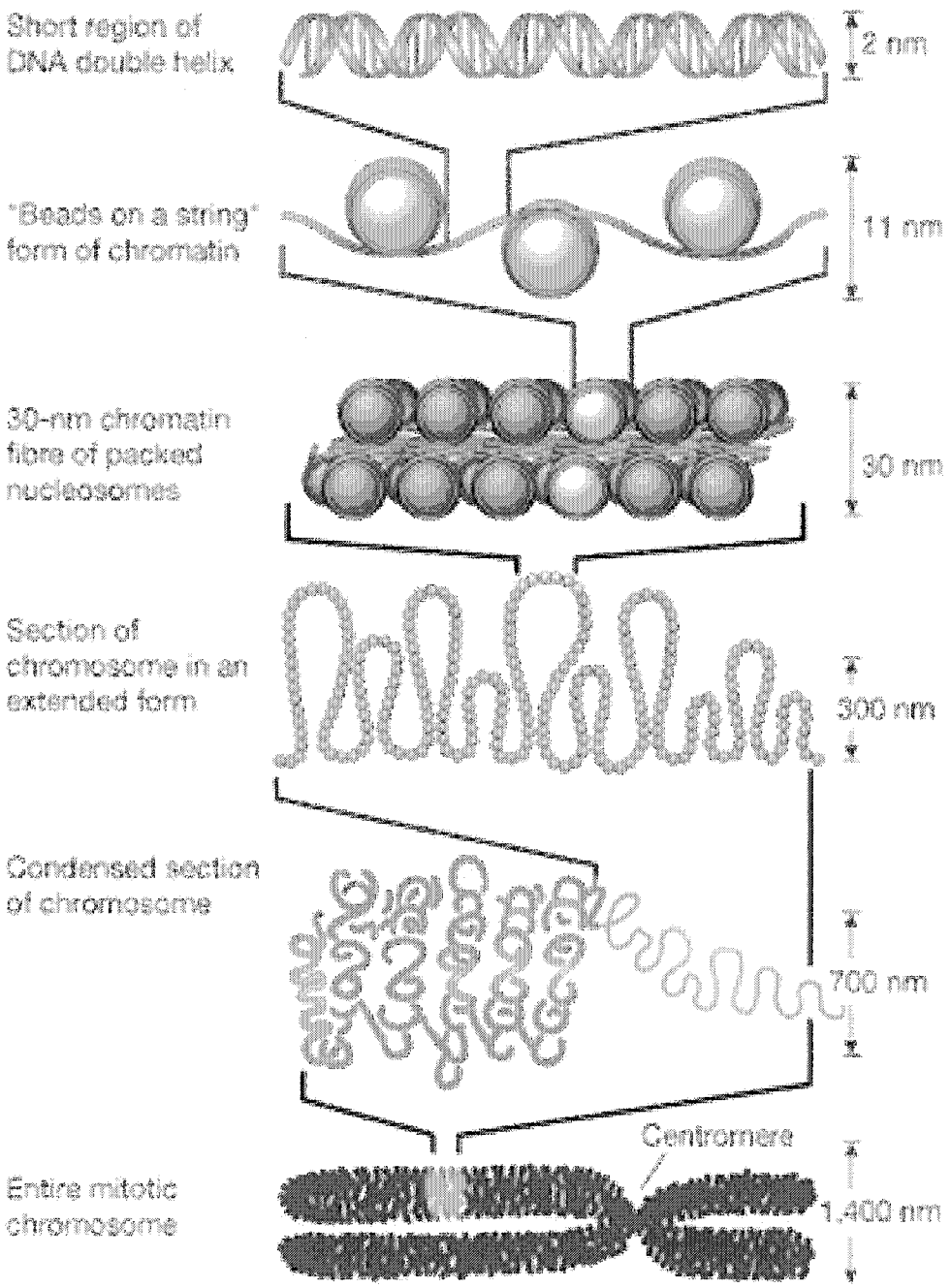

Figure 1.3: The organization of DNA within the chromatin structure. Reproduced from Alberts, B. et al. Essential Cell Biology: An Introduction to the Molecular Biology of the Cell (Garland, New York, 1998).

resulting from exposure of nucleosomal arrays to a low salt concentration *in vitro* [Hansen, 2002]. At the second level, the extended nucleosomal arrays are further folded to form irregular rod-like structures with a diameter of about 30 nm ("30-nm fiber"). This conformation has been found in nuclei. It has been suggested that much of the eukaryotic chromatin in the cell nucleus exists as the 30-nm fiber conformation [Wolffe, 1998]. Two models have been proposed to explain the arrangement of nucleosomes within the 30-nm fiber. One of these is the solenoid model with a one-start higher order helix, and the other is the irregular zigzag model with a two-start helix [Finch and Klug, 1976; Woodcock et al., 1993; Leuba et al., 1994]. Recent observations seem to favor the irregular zigzag model [Cui and Bustamante, 2000; Rydberg et al., 1998]. Using disulfide cross-linking, Dorigo and colleagues have shown that the 30-nm chromatin fiber comprises two stacks of nucleosomes in accord with the two-start zigzag model [Dorigo et al., 2004]. The 30-nm fiber is further compacted by the establishment of long-distance chromatin fiber interactions with the help of multiple chromatin-associated proteins [Adkins et al., 2004].

1.3 Nucleosome assembly

In proliferating cells, the bulk of histone synthesis occurs during the S phase of the cell cycle and is coupled to DNA synthesis. In order to maintain the chromatin structure during DNA replication, parental nucleosome segregation and de novo nucleosome assembly take place rapidly during passage of a DNA replication fork. Parental nucleosome segregation involves the transfer of pre-

existing core histones onto the new daughter strands [Krude, 1999]. However, the recycling of parental nucleosomes for re-assembly on replicated daughter DNA can only account for the assembly of half of the replicated DNA into chromatin. Therefore, the remaining complement must be assembled de novo from newly synthesized histone proteins.

The current model of de novo nucleosome assembly suggests the following sequence of reactions. First, the newly synthesized histones, H3 and H4, are associated to form tetramer and acetylated at a number of lysine residues by B-type histone acetyltransferases (B-type HATs) [Kaufman et al., 1995][Verreault et al., 1996][Parthun et al., 1996]. Subsequently, these modified $(H3\text{-}H4)_2$ tetramers are rapidly deposited on replicated daughter DNA behind the replication fork by chromatin assembly factor-1 (CAF-1). CAF-1 is found associated with acetylated $(H3\text{-}H4)_2$ tetramers and can bind directly to proliferating cell nuclear antigen (PCNA), a DNA polymerase processivity factor that forms a protein clamp around the DNA replication fork [Shibahara and Stillman, 1999; Smith and Stillman, 1991]. Next, H2A-H2B dimers are deposited by nucleosome assembly protein1 (NAP1) or other factors [Chang et al., 1997; Ito et al., 1996; Mello and Almouzni, 2001]. Finally, the acetyl groups on histones are removed by histone deacetylases and the nucleosomes are regularly spaced by ATP-dependent chromatin remodeling factors [Mello and Almouzni, 2001; Verreault, 2000]. However, the de novo nucleosome assembly pathway can only deposit histones during the DNA replication in S phase. Nucleosomes are also disassembled during the DNA repair pathway and gene expression. Thus, nucleosomes must

be able to reassemble outside of the S phase via a replication independent nucleosome assembly pathway. More interestingly, the incorporation of histone variants at specific sites during the cell cycle is also replication-independent. Three research groups have found that Swr1 complex in budding yeast is needed for specific substitution of pre-existing H2A-H2B dimers with H2A.Z-H2B dimers [Kobor et al., 2004; Krogan et al., 2003; Mizuguchi et al., 2004]. Swr1 complex contains Swi2/Snf2-related ATPase 1 (Swr1), which directly catalyzes the ATP-dependent replacement of histone H2A-H2B dimers with H2A.Z-H2B dimers [Mizuguchi et al., 2004]. These studies indicated that ATP-dependent chromatin remodeling may be intimately related to incorporation of histone variants into nucleosomes [Owen-Hughes and Bruno, 2004]. Similarly, a recent study revealed that H3.3, which is an H3 variant thought to be associated with active chromatin, is assembled into nucleosome by H3.3 specific assembly complex, the HIRA complex [Tagami et al., 2004]. Therefore, it seems like a specific protein complex is needed for the replication-independent assembly of each one histone variant into chromatin.

1.4 Alteration of nucleosome structure and transcription regulation

Chromatin helps the cell to compact and store the nuclear DNA, and also creates an impediment to the processes of DNA transcription, replication, repair and recombination. Apparently, modulation of chromatin structure plays an important role in the regulation of transcription in eukaryotes. To access the DNA

within the chromatin context, the cell has developed dedicated chromatin remodeling mechanisms, which serve to alter the chromatin structure locally to facilitate or repress DNA access. These mechanisms include: histone covalent modifications; ATP-dependent chromatin remodeling; and histone replacement by histone variants. In many cases, all of these processes may act in concert [Flaus and Owen-Hughes, 2004].

Histone tails are subject to a complex and dynamic set of post-transcriptional covalent modifications: acetylation, phosphorylation, methylation, ADP ribosylation, and ubiquitylation [Van Holde, 1988; Wolffe, 1998]. These modifications play a vital role in the modulation of chromatin dynamics and gene expression [Jenuwein and Allis, 2001; Strahl and Allis, 2000]. For example, histone acetylation is generally correlated with transcriptionally active genes. To date, many transcription coactivators, such as Gcn5p, $TAFII_{250}$, SRC-1, ACTR and CBP/P300, have been found to have intrinsic histone acetyltransferase (HAT) activity. In this process, lysine residues in the N-terminal of the core histones are acetylated. This HAT activity is essential for all these transcription coactivators to perform their transcriptional roles [Cheung et al., 2000b]. Histone lysine methylation catalysed by SET domains is involved in both transcription activation and repression: tri-methylated H3-K4 is enriched in fully activated promoters [Santos-Rosa et al., 2002]; while H3-K9 methylation is present mainly in silenced chromatin domains [Litt et al., 2001; Noma et al., 2001]. Phosphorylation of the serine 10 residue of histone H3 is crucial for chromosome condensation and a marker for activation of immediate early genes [Cheung et

al., 2000a]. Histone ubiquitylation regulates gene transcription in either a positive or a negative fashion, depending on its genomic and gene location [Zhang, 2003]. Discussion of the interplay between these distinct modifications can be found in a number of references [Berger, 2002; Kouzarides, 2002; Zhang, 2003; Zhang and Reinberg, 2001].

ATP-dependent chromatin remodeling is a fundamental process involved in all major reactions with chromatin substrate, such as the expression of genes, the duplication of the genome, the repair of DNA damage and the recombination of chromosomes [Becker and Horz, 2002]. The chromatin remodeling factors, comprised by multiprotein complexes, contain dedicated DNA-dependent ATPases of the Swi2/Snf2 subfamily [Muchardt and Yaniv, 1999; Peterson, 2000]. These enzymes couple ATP hydrolysis to alterations of the canonical nucleosome structure and further increase the accessibility of DNA elements to the regulatory proteins. The remodeling factors can be further divided into several subfamilies according to their ATPase domain structure. The four most prominent subfamilies are the SWI2, ISWI, CHD and Ino80 subfamilies. ATPases of the SWI2 subfamily are characterized by a bromodomain; ATPases of ISWI class contain SANT and SLIDE domains; ATPases of the CHD subfamily exhibit a chromodomain and PHD fingers; Ino80 type contain a split ATPase domain [Eberharter and Becker, 2004]. In vivo, the ATP-dependent nucleosome remodelling factors exhibit a diverse range of functions. For example, there is evidence for ISWI-catalysed nucleosome sliding [Fazzio and Tsukiyama, 2003]. Additionally, several groups have found the involvement of the Swr1 complex

(belongs to SWI2 subfamily) in replacing nucleosomal H2A by the H2A.Z variant in yeast [Krogan et al., 2003; Mizuguchi et al., 2004]. However, the mechanism of action of nucleosome remodeling factors is still unclear. The two most popular models are the 'Twist Diffusion' model and the 'Loop Recapture' model. The 'Twist Diffusion' model postulates that thermal energy twists DNA at the nucleosomal entry point, leading to replacement of initial DNA-histone interactions by equivalent ones involving adjacent base pairs. Both the rotational and translational position of the nucleosome would be changed when the twist diffusion occurs around the histone octamer surface [Widom, 2001]. The alternative 'Loop Recapture' model proposes that thermal energy leads to detachment of a segment of DNA at the nucleosomal entry/exit. This detached DNA segment may interact with a different position on the histone octamer, leading to a DNA loop on the nucleosomal surface. The propagation of the loop around the histone octamer surface would change the translational position of the nucleosome [Widom, 1998b].

In addition to histone covalent modification and ATP-dependent chromatin remodeling, several variants of the core histones have been identified that can substitute for the core histone and further influence nucleosome conformation and chromatin function in specific biological contexts.

1.5 Histone variants

Histone variants are distinct nonallelic forms of major-type core histones. The canonical histones are S-phase specific, that is, they are deposited during

DNA replication. The genes encoding canonical histones are present as multigene families, that is, each gene cluster typically encodes all four core histones and the linker histone H1. These S-phase-specific histones are highly expressed and incorporated into daughter DNA during DNA replication. However, histone variant genes are found outside of these gene clusters. The expression of histone variants is not restricted to the S phase of the cell cycle, and the incorporation of histone variants is replication independent. Most of the known histone variants are replacements for either H3 or H2A. An H4 variant has not been identified to date, while H2A shows the greatest variability. Histone variants are highly conserved between different species, indicating that they have evolved to accomplish important biological functions. It has been suggested that the substitution of core histones with the corresponding histone variants can generate an architecturally and functionally distinct local or global chromatin structure [Henikoff et al., 2004; Malik and Henikoff, 2003; Chakravarthy et al., 2004; Chapter 3]. Recently, histone variants of H2A and H3 have received increasing attention and moved to the forefront of chromatin research.

At least two H3 variants (H3.3 and CenH3) are found in most eukaryotic lineages. H3.3 is distinguished from canonical H3 by differences at only four positions, one in the N-terminal tail and three in the α2 helix of the histone fold domain (A31S, S87A, V89I, and M90G in Metazoans) [Malik and Henikoff, 2003]. It has been found that H3.3 is deposited by replication-independent nucleosome assembly and is targeted to transcriptionally active loci throughout the cell cycle [Ahmad and Henikoff, 2002]. In the same paper, Ahmad and Henikoff showed

that in *Drosophila melanogaster*, the three amino acid differences in the histone fold domain are critical for replication-independent deposition, while the difference in the N-terminal domain is not required [Ahmad and Henikoff, 2002]. Based on the crystal structure, these three residues could be solvent accessible [Luger, 2003; Luger et al., 1997a]. To address how histones H3 and H3.3 are deposited into chromatin, Tagami and colleagues purified the deposition machinery for these histones and found that CAF-1 and HIRA are necessary to mediate replication-dependent and replication-independent nucleosome assembly, respectively [Tagami et al., 2004]. Surprisingly, only H3.3 is present in Ascomycetes (fungi) such as *Saccharomyces cerevisiae.* Histone H3.3 is constitutively expressed in the cell cycle, and can be incorporated into the genome both during and after replication.

Centromere-specific H3s (CenH3s) are histone H3 variants that are specialized for packaging chromatin at eukaryotic centromeres, sites of spindle attachment to chromosomes that ensure their correct segregation [Palmer et al., 1991]. For example, CenpA is a centromere -specific H3 variant found in mammals and is essential for centromere assembly [Black et al., 2004; Howman et al., 2000]. CenH3s have a divergent N-terminal tail ranging from 20 to 200 amino acids in different lineages. CenH3s are only ~50% identical to H3s in the histone fold domain [Henikoff et al., 2001]. CenH3s seem to have a longer loop 1 region than the canonical H3. The crystal structure shows that Loop 1 of H3 can make specific contacts with nucleosomal DNA. This longer Loop 1 in CenH3s

may lead to a more articulated contact with DNA, providing the specificity needed for centromere targeting [Shelby et al., 1997; Vermaak et al., 2002].

To date, several H2A variants have been described (reviewed in chapter 3). H2A.X is present in nearly all eukaryotes and is implicated in DNA repair [Celeste et al., 2003b]. H2A.Z is highly conserved through most of eukaryotic evolution and has been shown to be essential in *Drosophila*, mouse and *Tetrahymena* [Faast et al., 1999; Liu et al., 1996; van Daal and Elgin, 1992]. H2A.Z is critical for maintaining a transcriptionally permissive 'open' state and preventing the spread of silent chromatin into euchromatin [Meneghini et al., 2003; Stargell et al., 1993]. MacroH2A is an unusual vertebrate-specific H2A variant, which is enriched in the chromatin of the inactive X chromosome in female mammals [the Barr body, Barr and Bertram, 1949] and in the transcriptionally silent XY body in male meiosis [Costanzi and Pehrson, 1998; Richler et al., 2000]. MacroH2A might play a role in transcriptional silencing [Angelov et al., 2003]. H2A.Bbd (Barr body deficient), another vertebrate-specific H2A variant, is enriched in transcriptionally active domains and seems to be mutually exclusive with macroH2A [Chadwick and Willard, 2001]. The H2A.Bbd sequence possesses a shorter docking domain and is quite divergent from both H2A and H2A.Z. H2A.Bbd containing nucleosomes are suggested to have 'loose' packing. The focus of this thesis is going to be on H2A.Bbd.

1.6 H2A.Bbd

Using the NIH BLAST server (http://www.ncbi.nlm.nih.gov/blast/blast.cgi), Chadwick and colleagues searched the human H2A gene family against the

human expressed sequence tag (EST) database at GeneBank and identified a novel, more distant H2A variant [Chadwick and Willard, 2001]. They investigated the chromosomal distribution of this H2A variant by immunofluorescence and fluorescence in situ hybridization and found that it is largely excluded from the Barr body, inactive X chromosome in interphase nuclei [Barr and Bertram, 1949]. Therefore, they named the protein H2A.Bbd, for H2A variant and Barr body deficient. They also showed that H2A.Bbd associates with other core histones to form nucleosomes and that the distribution of H2A.Bbd completely overlaps with acetylated forms of H4 [Chadwick and Willard, 2001]. These results raise the possibility that H2A.Bbd is enriched in nucleosomes associated with transcriptionally active regions of the genome.

H2A.Bbd is a 115 amino acid protein with a molecular weight of 12.7 KD and a pI of 10.7. It is only 48% identical to 'major H2A' in the structured region, making H2A.Bbd the most divergent histone H2A variant to date. The residues that are the targets of the post-translational modification (acetylation, phosphorylation and ubiquitination) are not conserved in H2A.Bbd [Chadwick and Willard, 2001; Jenuwein and Allis, 2001; Strahl and Allis, 2000]. This suggests that H2A.Bbd could be regulated in a different fashion compared to the other members of the H2A family. Figure 1.4 shows sequence alignment of human H2A.Bbd and canonical H2As. Based on this alignment and the knowledge of nucleosome core particle structure, the following characteristics of H2A.Bbd can be identified:

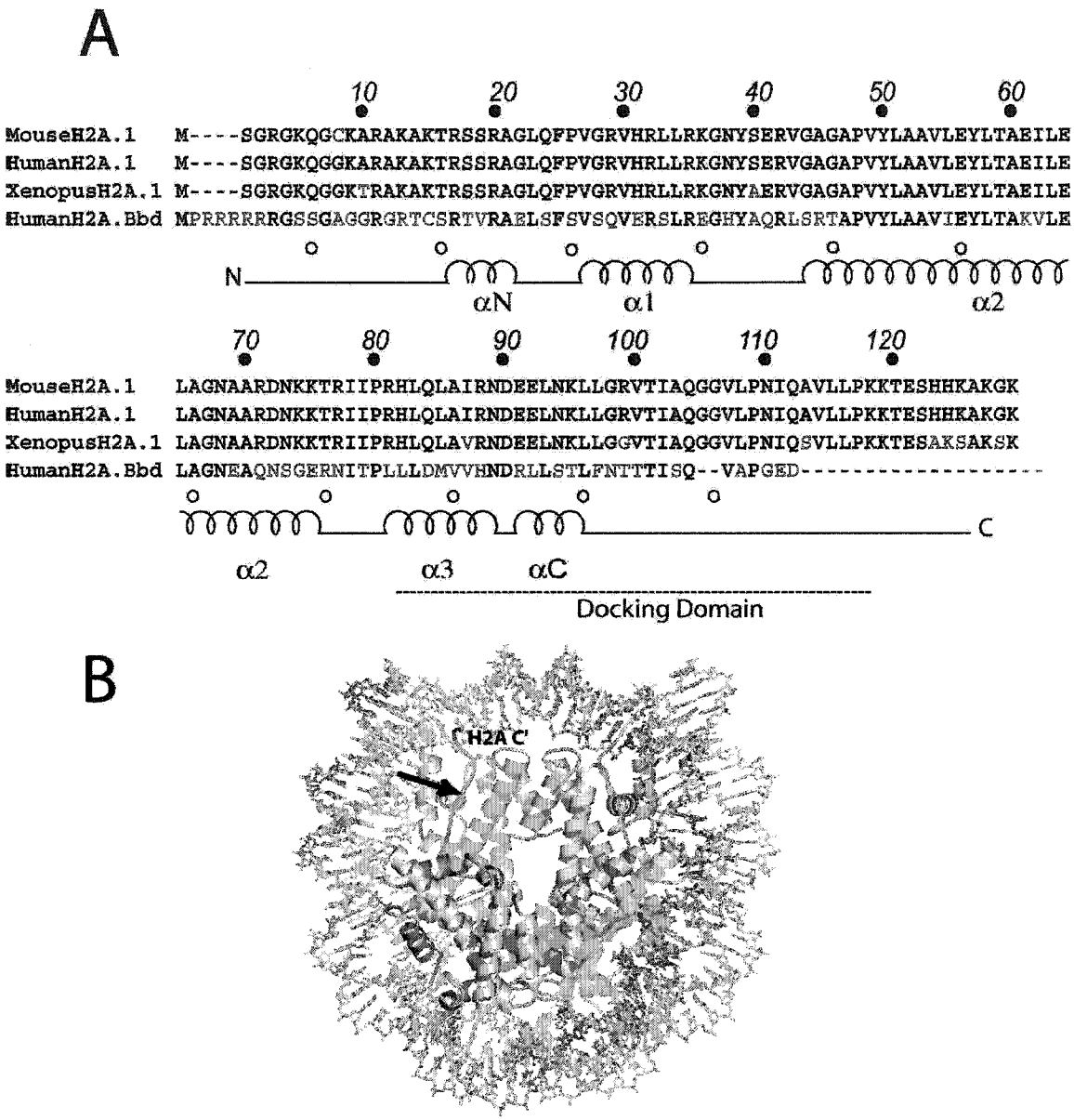

Figure 1.4: Unique features of H2A.Bbd. (A) Sequence alignment of mouse H2A.1, human H2A.1, human H2A.Bbd and X. laevis H2A. Sequence differences are shown in red. The docking domain is indicated by a dashed line. Secondary structure elements of the histone fold and extensions are indicated. (B) Structure of Xla-NCP to indicate the structural context of major sequence differences in H2A.Bbd. H2A is shown in yellow, H2B in red, H3 in blue and H4 in green. The H2A docking domain is colored orange and the H2A C-terminus (H2A C') is indicated. The black arrow indicates the approximate C-terminus of H2A.Bbd, based on the sequence alignment shown in (A). Reproduced from [Bao et al., 2004].

(1) The N terminal tail contains six additional continuous arginines, which may provide new sites for covalent modification, interaction with DNA, or other transcription factors.

(2) H2A.Bbd lacks the nonstructured C-terminus. Usually, major H2A and H2A variants have 129 or more amino acids. The C terminal tail (120-129) of H2A that is not resolved in the nucleosome structure is suggested to interact with the DNA end or interact with linker histone proteins. If a nucleosome core particle containing H2A.Bbd (Bbd-NCP) has a similar structure to that of major NCP, the C terminal end of H2A.Bbd will be at the position of H2A Q112 (Fig. 1.4). Therefore, interaction between H2A.Bbd and DNA, and/or interaction between H1 and 'variant' nucleosome may be changed, because of the absence of the H2A C terminal tail. Furthermore, the interaction between the last turn of the H3αN helix and H2A.Bbd C terminal region will also be changed.

(3) The α_2 is the most conserved region. This is not unexpected because α_2 interacts with H2B to form the dimer and is conserved in all H2A variants.

(4) The residues within the docking domain of H2A (residues 81-119) differ significantly from those of H2A.Bbd. The ladle-shaped docking domain provides a large interaction surface with the $(H3\text{-}H4)_2$ tetramer. Therefore, the stability of Bbd-NCP may be altered because of the non-conserved docking domain.

(5) The α_1 region is more acidic than that of major and other variants of H2A.

(6) There are fourteen lysine residues in major H2A, but only one lysine in H2A.Bbd. There are eleven serine residues in H2A.Bbd, but only four in major H2A. These changes make H2A.Bbd (pI 10.7) less basic than major H2A (pI 11.2). The overall interaction between H2A.Bbd containing octamer and DNA may be altered.

(7) The acidic patch on the surface of the nucleosome provides an important crystal contact with the H4 N terminal tail from a neighboring nucleosome and may be involved in nucleosome-nucleosome interaction [Luger and Richmond, 1998b; Suto et al., 2000]. However, in H2A.Bbd, three of the six conserved H2A residues that form the acidic patch are changed (H2A.1: Glu61 to Lys, Glu91 to Arg, Glu92 to Leu).

(8) In H2A.Bbd, one of the several conserved arginines (H2A.1: Arg77) that interact with the minor groove of nucleosomal DNA is changed to asparagine. Again, interaction between H2A.Bbd-octamer and DNA maybe altered.

All this information suggests that structure, stability, and function of Bbd-NCP would be different from that of major or other variant NCPs.

Recently, one group employed analytical ultra centrifugation found that, on raising the ionic strength, the decrease of $S_{20,w}$ of the Bbd-NCP was more pronounced than that of conventional NCP (predicted behaviour obtained from native NCPs), suggesting a more open structure and a lower inherent stability of the Bbd-NCP. They also found through FRAP (fluorescence recovery after photobleaching) that the photobleaching recovery for GFP-H2A.Bbd fusion within

the nuclei was much quicker than that of GFP-H2A fusion, indicating that *in vivo* H2A.Bbd is more rapidly exchanged than conventional H2A [Gautier et al., 2004].

Angelov and colleagues found that the presence of H2A.Bbd induces alterations in the structure of the H2A.Bbd nucleosome and increases the accessibility of NF-kB to nucleosomal DNA [Angelov et al., 2004]. Further, they found that irrespective of the DNA sequence used and of the starting position of the nucleosomes, H2A.Bbd nucleosomes could not be efficiently mobilized by the SWI/SNF and ACF machineries. However, their equilibrium and kinetics data suggested that the H2A.Bbd–H2B dimer exhibited a weaker interaction with the H3–H4 tetramer within the nucleosome than that of the conventional dimer, leading to a more efficient spontaneous transfer of the H2A.Bbd–H2B dimers. Interestingly, they also found that the incorporation of H2A.Bbd into the nucleosomal arrays leads to better efficiency of acetylation of the histone tails by p300. This finding was consistent with the earlier observation that the distribution of H2A.Bbd completely overlaps with acetylated forms of H4 [Chadwick and Willard, 2001]. Finally, the transcription efficiency from the H2A.Bbd templates was found to be slightly higher than that of the conventional H2A templates [Angelov et al., 2004].

In summary, these studies suggest that the incorporation of H2A.Bbd into nucleosome leads to a more open structure and a lower inherent stability of the Bbd-NCP, which might be induced by a weaker interaction between the H2A.Bbd–H2B dimer and the H3–H4 tetramer. This more open and less stable variant nucleosome facilitates the transcription process.

1.7 Nucleosome core particle containing poly (dA·dT) DNA element

The poly (dA·dT) elements (also called T-tracts) have been found to be greatly overrepresented in all eukaryotic species examined (ranging from yeast to human), and particularly enriched in promoter regions [Puhl and Behe, 1995]. It has been suggested that poly (dA·dT) promotes transcription by altering the stability or dynamics of nucleosomes, and enhancing the binding between transcription activators and their DNA targets, which lie close to the T-tracts. The mechanism of this transcription activation is not clear yet.

The poly (dA·dT) tracts have a straight and rigid DNA structure [Nelson et al., 1987], which is different from B-form DNA. Specifically, they have a narrow minor groove, 10 bp per helical turn, and additional bifurcated hydrogen bonds [Alexeev et al., 1987; Coll et al., 1987; Dickerson et al., 1982; Peck and Wang, 1981]. Thus, it has been speculated that these rigid DNA elements could not be incorporated into nucleosome core particles. Previous studies have shown that the poly (dA·dT) elements are resistant to nucleosome formation [Kunkel and Martinson, 1981; Rhodes, 1979]. Furthermore, *in vivo* yeast studies have shown that many promoter regions containing poly (dA·dT) elements (such as *HIS3*, *URA3*, *DED1* promoters) are nucleosome free [Filetici et al., 1998; Lascaris et al., 2000; Tanaka et al., 1996].

However, several research groups have recently shown that the poly (dA·dT) can be incorporated into nucleosomes both *in vitro* and *in vivo*. Using small DNA fragments from the NSR1 promoter, Losa et al. were able to

demonstrate that the naturally occurring 34 bp poly (dA·dT) tract can be folded into nucleosomes *in vitro* [Losa et al., 1990]. It has been shown that the *Saccharomyces cerevisiae* DNA topoisomerase I promoter contains a 29 bp poly (dA·dT) tract within a nucleosome core [Rubbi et al., 1997].

To date, several studies have investigated the contributions of poly (dA·dT) elements to the affinity of histone-DNA interactions. One such study has reported that incorporation of a 16 bp poly (dA·dT) element at the end and further in the middle of the nucleosomal DNA destabilized histone-DNA interactions and was accompanied by about a 1.6-fold increase in position-averaged equilibrium accessibility of nucleosomal DNA target sites [Anderson and Widom, 2001]. However, another study suggested the opposite effect, a 25 bp poly (dA·dT) tract stabilized the nucleosome [Mahloogi and Behe, 1997]. Therefore, the effects of poly (dA·dT) incorporation on histone-DNA interaction still remain uncertain.

In addition, the Thiele group found that a 16 bp poly (dA·dT) (A_{16}) element located adjacent to a metal response element (MRE) within the Amt1 gene promoter of *Candida glabrata* was incorporated into a positioned nucleosome *in vivo* [Zhu and Thiele, 1996; Liu and Thiele, 1997]. They also showed that this element was essential for rapid activation of the Amt1 promoter in response to a toxic copper level. To investigate the effects of poly (dA·dT) elements on nucleosome stability, White and Luger reconstituted nucleosomes with a 147 bp DNA containing an A_{16} element and the sequence recognition element (MRE) for Amt1 (Fig. 1.5). They reported the following effects: there was no preference for DNA sequences with or without the A_{16} element in the *in vitro* assembly system;

the DNA binding domain of Amt1 bound to nucleosome containing the A_{16} element with only a 3-fold reduction in affinity compared to that of free DNA; and, no dissociation of histones was required for Amt1 binding [White and Luger, 2004].

In order to determine the structural alteration caused by the incorporation of poly (dA·dT), we decided to study the X-ray crystal structure of the NCP containing A_{16}. With the structural data, we would be able to see whether nucleosomal DNA is distorted and more accessible to transcription factor binding. Furthermore, this nucleosome crystal structure will be the first one with a non-palindromic DNA sequence.

1.8 High-mobility group N (HMGN) proteins

The high-mobility group (HMG) proteins are chromatin binding proteins that regulate gene expression by modifying the structure of DNA and chromatin and affecting the accessibility of the nucleosomal targets to their regulatory factors. The HMG superfamily is composed of three families: HMGB (previously termed HMG1/2), HMGA (formerly HMG-I/Y), and HMGN (formerly HMG-14/-17). Each family is characterized by a distinct DNA or chromatin binding motif. The HMG-1 domain (often referred to as the HMG-1box) is the functional motif of the HMGB proteins; the AT hook is the functional motif of the HMGA group, and the nucleosomal binding domain is the functional motif of the HMGN subfamily [Bustin, 1999].

The HMGN family is comprised of small, basic proteins that bind specifically

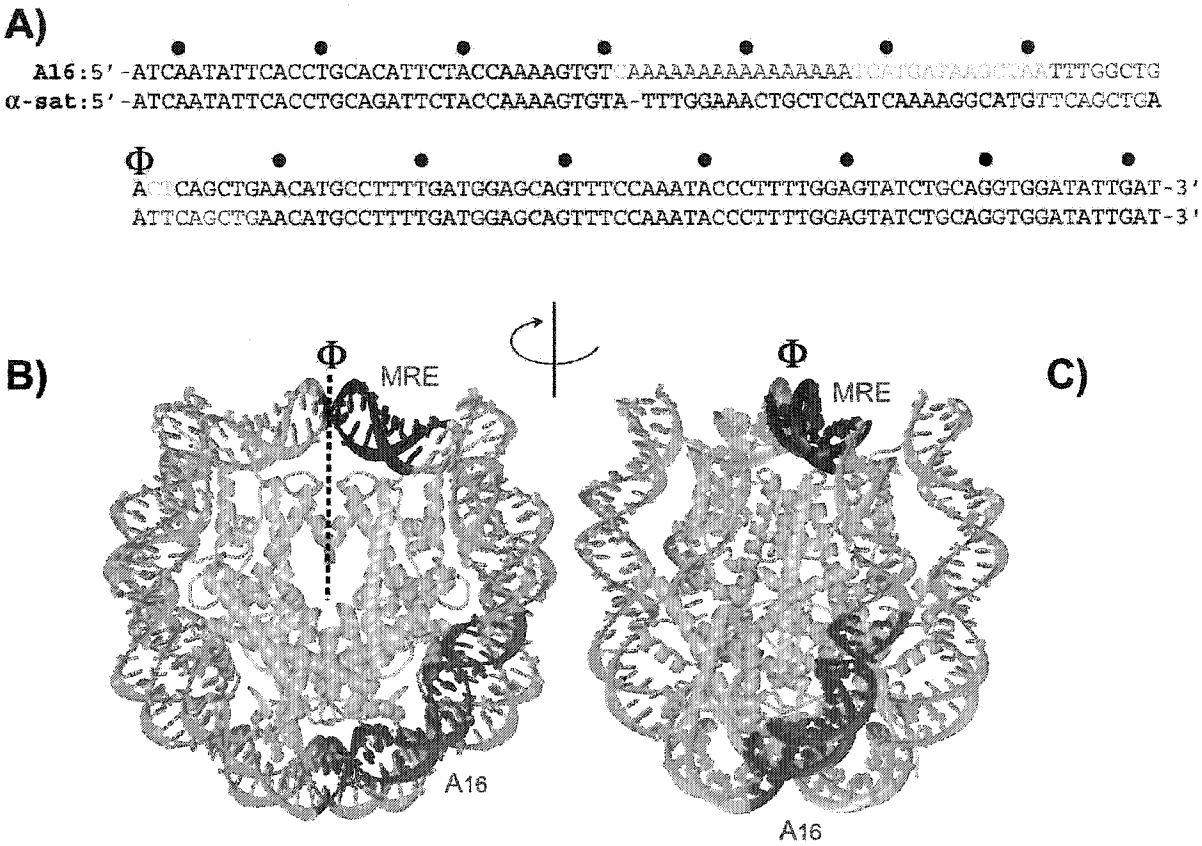

Figure 1.5: A) Sequence alignment of A16 DNA and a-satellite DNA. The A16 DNA contains the poly (dA·dT) element (blue) and the metal response element (MRE) for Amt1 (red). The region of the A16 DNA sequence that matches the rest of the Amt1 gene promoter is shown in green. The rest of the DNA sequence is identical with human α-satellite DNA, which also contains two Amt1 binding sites (red). The position of the central base pair is indicated (Φ), and 10 bp increments from the dyad are indicated by black bullets. **B) Crystal structure of the yeast NCP.** The position of the Amt1 MRE (red) and the poly (dA·dT) element (blue) are shown as they are positioned within the nucleosomal DNA based on in vivo mapping, under the assumption that the positioning of a-sat DNA has been maintained. The molecular dyad axis is indicated (Φ). **C) Side view of the crystal structure of the yeast NCP**, obtained by rotation of 50° around the y axis. Reproduced from [White and Luger, 2004].

to nucleosomes [Bustin, 2001]. They are highly conserved and found only in vertebrates. HMGN1 and HMGN2 (formerly named HMG-14 and HMG-17) have been studied extensively. These proteins have a molecular weight of~10 kDa, and contain three major functional motifs: a bipartite nuclear localization signal (NLS), a nucleosome-binding domain (NBD) and a chromatin unfolding domain (CHUD) [Bustin, 2001].

It has been shown that HMGN proteins bind specifically to the 147-base pair nucleosome core particle without any preference for the underlying sequence of DNA [Shirakawa et al., 2000]. Furthermore, HMGN1 and HMGN2 bind to nucleosomes cooperatively and form complexes containing either two molecules of HMGN1 or two molecules of HMGN2 [Postnikov et al., 1995]. The binding sites within the NCP are located in the two major grooves flanking the nucleosomal dyad axis and 25 bp from the end of the DNA [Alfonso et al., 1994; Sandeen et al., 1980]. The main HMGN region responsible for binding nucleosomes is the nucleosomal-binding domain (NBD), a positively charged stretch of approximately 30 amino acids, rich in Arg, Lys and Pro residues [Crippa et al., 1992; Trieschmann et al., 1995].

The nucleosomal binding domain anchors these HMGN proteins to the nucleosome cores to induce HMGN-dependent changes in chromatin fiber and further facilitates transcription and replication from chromatin templates [Bustin, 1999; Bustin and Reeves, 1996]. Interestingly, in all of the *in vitro* assembly systems, HMGN proteins stimulated transcription from chromatin templates but not from deproteinized DNA, leading to the conclusion that the proteins are

chromatin-specific effectors [Bustin, 2001]. However, with one exception, the stimulatory effects were observed only when the HMGN proteins were incorporated into the nucleosomes together with histones rather than were added to preassembled chromatin. This suggests that the stimulatory effects require proper placement of the proteins into nucleosomes [Bustin, 2001].

However, it has been shown by thermal denaturation, circular dichroism and nuclease digestion that the HMGN-NCP complex is more stable than NCP alone, [Bustin and Reeves, 1996]. These observations seem to be inconsistent with the reported capability of HMGN proteins to enhance transcription or replication from chromatin templates. Mounting evidence indicates that HMGN proteins de-compact chromatin by competing with histone H1 and/or interacting with the amino termini of the core histones. For example, the nucleosomal footprint of HMGN proteins has been shown to partially overlap with that of histone H1 [Alfonso et al., 1994]; site-specific crosslinking experiments have indicated that the C-terminal region of HMGN1 interacts with the amino terminus of histone H3 [Trieschmann et al., 1998]; Catez and colleagues found that members of each of the three HMG families weakened the binding of H1 to chromatin through a dynamic competition process [Catez et al., 2004]; recent result has indicated that HMGN1 modulates histone H3 phosphorylation [Lim et al., 2004].

The structure of HMGN proteins is not known. Therefore, we have set out to determine the co-crystal structure of NCP and the nucleosomal-binding domain (NBD) of HMGN. This study will shed light on the mechanism of HMGN binding

with NCP and help us to understand how the HMGN proteins de-compact chromatin fibers and participate transcriptional regulation.

1.9 Specific aims and general dissertation layout

The scope of the work outlined in this thesis investigates the structural and functional consequences of incorporating the histone variant H2A.Bbd into nucleosome core particle. H2A.Bbd possesses a shorter docking domain and is quite divergent from canonical H2A. The distribution of H2A.Bbd completely overlaps with acetylated forms of H4. Nucleosomes containing H2A.Bbd are suggested to have 'loose' packing and associated with transcriptionally active regions of the genome.

I have employed several biochemical and biophysical approaches and found that the nucleosome core particle containing H2A.Bbd possesses a relaxed structure. I performed *in vitro* domain truncation and domain swap studies to determine which region in H2A.Bbd is responsible for the structural alteration. An *in vitro* transcription assay was employed to see if chromatin containing H2A.Bbd represses transcription less efficiently than canonical chromatin. I also investigated the possibility of forming hybrid nucleosomes, nucleosomes with one H2A.Bbd-H2B dimer and one canonical H2A-H2B dimer. Complementary biochemical and biophysical techniques were used to study the stability of nucleosomes containing H2A.Bbd. I attempted to crystallize the nucleosome core particle containing H2A.Bbd reconstituted with different DNA and even H2A.Bbd derivatives. Optimization of the crystallization process is

underway. With these studies, we can better understand how the structure and stability of NCP is altered by the incorporation of H2A.Bbd into the nucleosome core particle.

The poly (dA·dT) elements have been suggested to promote transcription by altering the stability or dynamics of nucleosomes. We have employed several biochemical and biophysical approaches and found that the nucleosome core particle containing 16 bp poly (dA·dT) element (A_{16} NCP) possesses a locally distorted structure. Fluorescence resonance energy transfer analyses were performed to compare the stability of the A_{16} NCP and that of the canonical NCP. DNase I footprinting assay was employed to see whether some hypersensitive sites were created by the A_{16} element. We also performed X-ray crystallography studies on nucleosomes containing a 16 bp poly (dA·dT) element to see whether nucleosomal DNA is distorted and more accessible to transcription factor binding.

It has been suggested that the HMGN proteins are anchored to the NCPs by nucleosomal-binding domain (NBD) to induce structural changes in chromatin fiber and to facilitate transcription and replication from chromatin templates. I attempted structural studies by co-crystallization of NCP and the NBD of HMGN proteins to determine the mechanism of HMGN binding.

CHAPTER 2

Nucleosomes Containing the Histone Variant H2A.Bbd Organize Only 118 Base Pairs of DNA

This chapter was published in *The EMBO Journal*. The text of this manuscript and the figures are presented as they appeared in the journal.

The author list for this paper is as follows:
Yunhe Bao, Kasey Konesky, Young-Jun Park, Simona Rosu, Pamela N. Dyer, Danny Rangasamy, David J. Tremethick, Paul J. Laybourn, and Karolin Luger.
All experiments were performed by YB, with the exception of the chromatin assembly and the *in vitro* transcription assay, which were performed by KK. YP did preliminary FRET study within the Bbd-NCP. SR did H2A domain swap cloning. PD purified 146 bp DNA, labeled the DNA, and sub-cloned the mouse H2A. DR and DT provided the clones for mouse core histones.

2.1 Abstract

H2A.Bbd is an unusual histone variant whose sequence is only 48 % conserved compared to major H2A. Major sequence differences are in the docking domain that tethers the H2A-H2B dimer to the $(H3\text{-}H4)_2$ tetramer; in addition, the C-terminal tail is absent in H2A.Bbd. We assembled nucleosomes in which H2A is replaced by H2A.Bbd (Bbd-NCP) and found that Bbd-NCP had a more relaxed structure in which only 118±2 bp of DNA are protected against digestion with micrococcal nuclease. Absence of fluorescence resonance energy transfer between the ends of the DNA in Bbd-NCP indicates that the distance between the DNA ends is increased significantly. The Bbd docking domain is largely responsible for this behavior, as shown by domain-swap experiments. Bbd-containing nucleosomal arrays repress transcription from a natural promoter, and this repression can be alleviated by transcriptional activators Tax and CREB. The structural properties of Bbd-NCP described here have important implications for the *in vivo* function of this histone variant and are consistent with its proposed role in transcriptionally active chromatin.

2.2 Introduction

The nucleosome core particle (NCP) is the fundamental repeating unit in eukaryotic chromatin. 146 bp of DNA are wrapped in 1.65 tight superhelical turns around a histone octamer of two copies each of the four histone proteins (H2A, H2B, H3 and H4) [Luger et al., 1997a]. The H2A-H2B dimer is tethered to the $(H3\text{-}H4)_2$ tetramer by forming a four-helix bundle between the $\alpha 2$ and $\alpha 3$ helices

of H2B and H4. In addition, a spatially distinct interface is formed by the ladle-shaped docking domain of H2A that appears to guide the H3αN helix to bind the last turn of the DNA, and forms a short β-sheet with the C-terminal region of H4 [Luger et al., 1997a]. The histone octamer is not stable under physiological conditions, indicating that the H2A-H2B dimer – $(H3\text{-}H4)_2$ tetramer interaction is stabilized significantly by the interaction with DNA.

The organization of DNA into chromatin is generally repressive for DNA replication, transcription, repair and recombination. Therefore, events that alter chromatin conformation are important regulators of these processes. One mechanism to modify the biochemical make-up of the nucleosome is by incorporation of specialized histone variants into nucleosomes to generate an architecturally and functionally distinct local or global chromatin structure. Several variants of the core histone H2A have been identified that can substitute for replication-dependent H2A (reviewed in [Wolffe and Pruss, 1996]; [Malik and Henikoff, 2003]. The newest addition to this list, H2A.Bbd - first identified in humans [Chadwick and Willard, 2001] - associates with other core histones to form nucleosomes *in vivo*, and its distribution appears to overlap with that of acetylated H4. H2A.Bbd is largely excluded from the inactive X chromosome, a characteristic which gave this variant its name (Barr body deficient, Bbd) [Chadwick and Willard, 2001]. These initial findings raise the possibility that H2A.Bbd is enriched in chromatin associated with transcriptionally active regions of the genome.

H2A.Bbd is only 48% identical to major, replication-dependent H2A, making it the most specialized among all histone variants known to date (Fig. 2.1A) [Malik and Henikoff, 2003]. None of the residues that are the targets of post-translational modification in major-type H2A (acetylation, phosphorylation and ubiquitination) are present in H2A.Bbd [Chadwick and Willard, 2001; Strahl and Allis, 2000]. Based on our knowledge of nucleosome structure, major hallmarks of H2A.Bbd as compared to major H2A are (1) the presence of a continuous stretch of five arginines and the conspicuous absence of lysines in its N terminal tail, (2) the absence of a C terminal tail and the very last segment of the docking domain that is responsible for interactions with H3 in major-NCP; (3) major sequence differences in the docking domain of H2A (residues 81-119; Fig. 2.1); (4) the presence of only one lysine in H2A.Bbd compared to fourteen in major H2A, resulting in a slightly less basic protein (pI 10.7, compared to a pI of 11.2 for major H2A); and (5) the absence of the 'acidic patch' [Luger et al., 1997a] (H2A.1 Glu61 to Lys, Glu91 to Arg, Glu92 to Leu; Fig. 2.1A). These changes, either individually or in combination, may alter the interaction between the H2A.Bbd-H2B dimer and the $(H3\text{-}H4)_2$ tetramer and/or the DNA; they could change the potential of H2A.Bbd for post-translational modifications; they may modulate the ability of H2A.Bbd-containing nucleosomes to interact with linker histones; or they could affect the type of higher order structure that can be formed by these nucleosomes. All of these potential consequences would have significant implications on biological function of chromatin domains containing this histone variant.

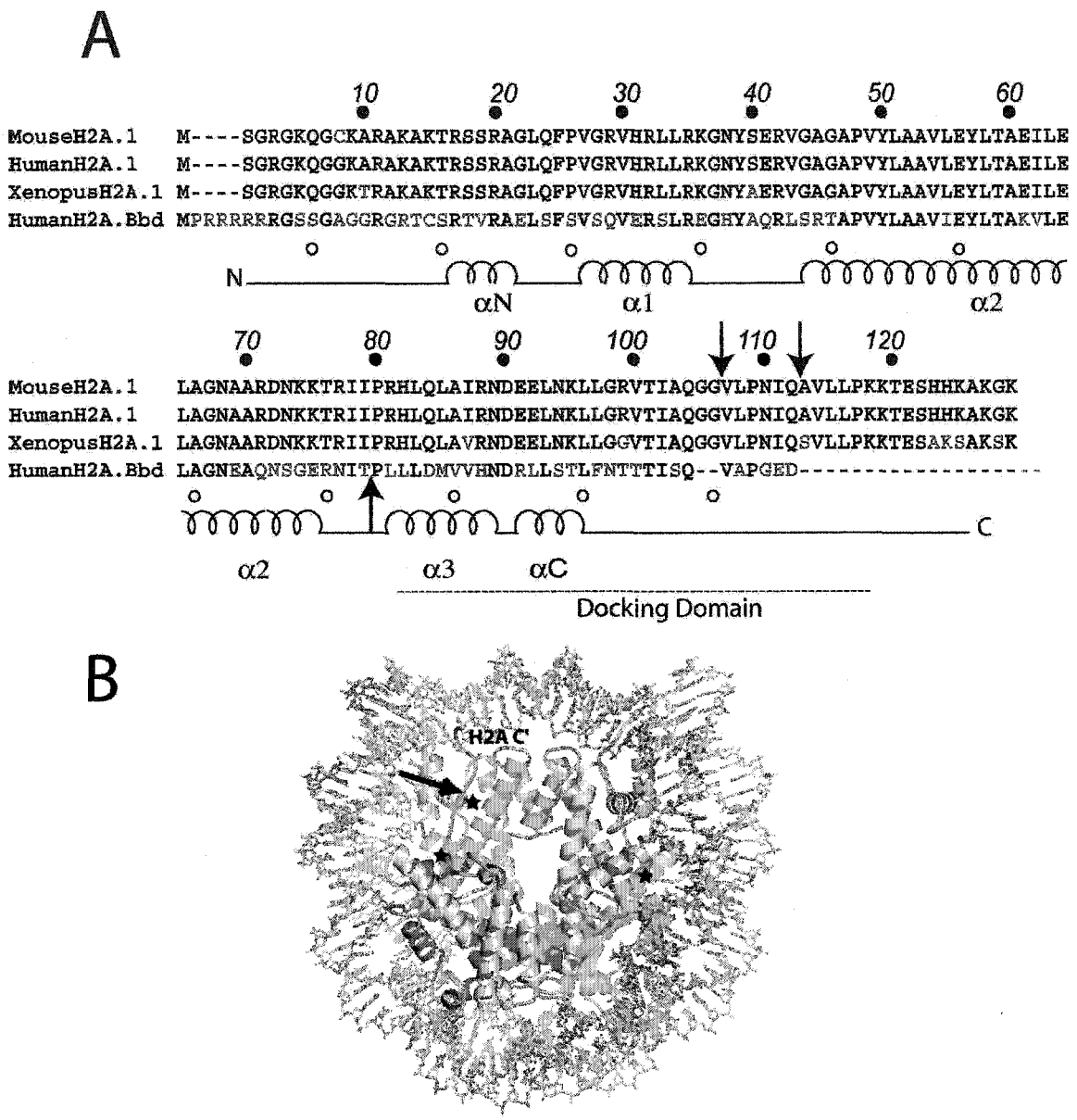

Figure 2.1: Unique features of H2A.Bbd. (A) Sequence alignment of mouse H2A.1 (gi: 121961), human H2A.1 (gi: 106265), human H2A.Bbd (gi: 15553137), and *Xenopus laevis* H2A (gi: 121966). Intervals of 10 amino acids for H2A.1 (filled circles) and H2A.Bbd (open circles) are indicated. Sequence differences are shown in red. The docking domain is indicated by a dashed line. Secondary structure elements of the histone fold (α1, α2 and α3) and extensions (αN and αC) are indicated. Truncated and domain-swapped regions are indicated by arrows. **(B)** Structure of *Xla*-NCP to indicate the structural context of major sequence differences in H2A.Bbd. H2A is shown in yellow, H2B in red, H3 in blue, and H4 in green. The H2A docking domain is colored orange and the H2A C-terminus (H2A C') is indicated. The black arrow indicates the approximate C-terminus of H2A.Bbd, based on the sequence alignment shown in (A). Sites of truncation and domain swap are indicated by a star.

To investigate the effect of H2A.Bbd incorporation on the structure and function of a nucleosome, we analyzed the properties of NCPs in which H2A has been replaced by H2A.Bbd (Bbd-NCP). We show conclusively, using two independent experimental approaches, that Bbd-NCP binds the DNA ends less tightly. To investigate which regions of H2A.Bbd are responsible for this behavior, we analyzed chimeras of H2A in which domains between Bbd and major H2A have been swapped. The ability of Bbd-containing nucleosomes to form regularly spaced arrays on plasmid DNA was also demonstrated. We found that Bbd-containing nucleosomes are spaced more closely, and that this chromatin represses transcription from a natural promoter only slightly less efficiently than chromatin reconstituted with major-type histones. This repression is alleviated upon addition of transcriptional activators Tax and CREB, and appears to be less dependent on the co-activator p300.

2.3 Materials and Methods

2.3a Cloning

The amino acid sequence of human H2A.Bbd (gi:15553137) was reverse translated into a nucleotide sequence based on an *E.coli* high codon usage table. The gene was synthesized by PCR from four overlapping oligonucleotides spanning the entire sequence [Dillon and Rosen, 1990]. The gene was flanked by NdeI and BamHI restriction sites. The PCR product was cloned into a PCR-script vector (Stratagene), and the construct was confirmed by sequencing. The

H2A.Bbd gene was subcloned into the pET-3a expression vector using the NdeI and BamHI cloning sites (Novagen). A stop codon was introduced into the coding region of *Xla* H2A at the codon following amino acid 106 or 112 by site direct mutagenesis method to obtain truncated *Xla* H2A, *Xla* $H2A_{106}$ and *Xla* $H2A_{112}$. To prepare a domain-swapped derivative of *Xla* H2A, an ApaI site (GGGCCC) was introduced into the coding region of *Xla* H2A at $I_{79}P_{80}$ (ATCCCC), resulting in a mutation of I_{79} to G_{79}; an ApaI recognize site was also introduced into the coding region for H2A.Bbd at $T_{83}P_{84}$ (ACTCCG), resulting in a mutation of T_{83} to G_{83}. Plasmids were digested with BglII and ApaI, and the sequence encoding the docking domain of H2A.Bbd was substituted for that of *Xla* H2A. Mouse genes for H2A (P22752), H2B (P10854), H3 (S06755), and H4 (S03426) were cloned using conventional strategies. Mouse H2A and H2B genes were subcloned into pET-3a vectors.

2.3b Purification of proteins and DNA

H2A.Bbd was over-expressed in BL21 (DE3) CodonPlus RIL –pLysS cells (Stratagene) for three and half hours and lysed by sonication in the presence of 0.2 mg/ml lysozyme and 0.01 mg/ml DNaseI. Standard protocols were used for further purification from inclusion bodies [Dyer et al., 2004]. Mouse core histones and H2A derivatives (Xla $H2A_{106}$, Xla $H2A_{112}$, Xla H2A/Bbd) were overexpressed in BL21 (DE3)-pLysS (Stratagene) and purified as above. 146 bp DNA was purified as described [Dyer et al., 2004]. The 196 bp DNA fragment was excised from plasmids containing 12 repeats of a 208 bp DNA fragment [Simpson et al.,

1985] using Eco RI, and the resulting fragment was purified by preparative gel electrophoresis. Drosophila NAP-1 (dNAP-1), ISWI, and Acf1 was purified as previously described [Georges et al., 2002]; [Ito et al., 1996]; [Ito et al., 1997]; [Ito et al., 2000]; CREB, Tax and p300 were purified as in [Kraus and Kadonaga, 1998].

2.3c Reconstitution and analysis of nucleosomes

Purified mouse core histones were refolded to histone octamers and purified [Dyer et al., 2004]. Mouse octamer and purified α-satellite 146 bp DNA [Luger et al., 1997a] were reconstituted to NCPs by salt gradient deposition [Dyer et al., 2004] to yield mouse-NCPs (mm-NCP). Samples were heated at 37 °C for 120 min to shift all nucleosomes to a unique position. For Bbd-NCP, $(H3\text{-}H4)_2$ tetramer, (H2A.Bbd-H2B) dimer and α-satellite 146 bp DNA were mixed in a 1:2:1 molar ratio, and reconstituted using salt gradient deposition to yield Bbd-NCPs. Samples were analyzed on a 5% polyacrylamide gel [Dyer et al., 2004]. Nucleosomal bands were excised, electro-eluted into 0.05 x TBE buffer, lyophilized, and analyzed by 18% SDS PAGE.

2.3d Micrococcal nuclease (MNase) digestion

Histone octamers, or $(H3\text{-}H4)_2$ tetramer and H2A.Bbd-H2B dimers were reconstituted with either 146 bp 5S DNA or 196 bp 5S DNA to yield NCPs (*mm*-146-NCP, Bbd-146-NCP, *mm*-196-NCP and Bbd-196-NCP, respectively). Identical amounts of *mm*-146-NCP and Bbd-146-NCP (2 μg NCP per reaction)

were digested with increasing amount of MNase (Worthington) at 37°C in 125 μl of MNase buffer (0.6 mM HEPES (pH 7.6), 52 mM KCL, 5% (vol/vol) glycerol , 1.4 % (wt/vol) polyethylene glycol and 5.4 mM $CaCl_2$) for 1.5 minutes. The reactions were stopped by transferring to tubes containing 12.5 μl TE (10 mM Tris/HCl, 1 mM EDTA, pH8.0), 12.5 μl 0.5 M EDTA, and 200 μl stop buffer (20 mM EDTA, 200 mM NaCl, 1% (wt/vol) SDS, 0.25 mg/ml glycogen). Histones were digested at 37° C for 30 min by adding 20 μl proteinase K (2.5 mg/ml). For time-course experiments, 0.15 U MNase was used to digest 10 μg NCP of *mm*-196-NCP or Bbd-196-NCP at 37° C in 625 μl MNase buffer. 122 μl aliquots were removed at 0, 2, 4, 8 & 16 minutes. The reactions were stopped and deproteinized as described above. DNA fragments were extracted, precipitated and analyzed on 10% polyacrylamide gels (in 0.5 x TBE). Gels were scanned, and the center peak for each band was plotted against the log (bp) of the marker to arrive at the actual size of the protected band.

2.3e NAP-1-dependent NCP reconstitution

Yeast NAP-1 (yNAP-1) was purified as described [McBryant et al., 2003]. Mouse octamer, $(H3\text{-}H4)_2$ tetramer, H2A-H2B dimer, and H2A.Bbd-H2B dimer that had been stored in refolding buffer (2 M NaCl, 10 mM Tris-HCl pH 7.5, 1mM EDTA, 5 mM β-mercaptoethanol) were dialyzed against 100 mM NaCl TE buffer (100 mM NaCl, 10 mM Tris-HCl pH 7.5, 1mM EDTA). The components were mixed with a 146 bp DNA fragment derived from α-satellite DNA [Luger et al., 1997b] in the presence of a two-fold molar excess of yNAP-1 over histone

octamer. The reactions were incubated at room temperature for 3 hours, followed by a one-hour incubation at 37° C. Assembled NCPs were analyzed by native PAGE.

2.3f Fluorescence resonance energy transfer (FRET)

The 5' ends of a 146 bp DNA fragment derived from the 5SrRNA gene [Richmond et al., 1988] were derivatized with 7-diethylamino-3-(4'-maleimidylphenyl) -4-methylcoumarin (CPM) and fluorescein-5-maleimide (FM), as described [Park et al., 2004b]. This pair has a Förster distance of 52 Å, the distance at which FRET is 50 % efficient. Typically, emission spectra for 0.3 μM of NCP in TE (10 mM Tris-HCL pH 7.5, 0.1mM EDTA) were measured using an AVIV Spectrofluorometer (Model ATF105). Excitation wavelength was 385 nm. 5 M NaCl was added to bring the salt concentration from 0 M to 0.38 M, 0.71M, 1M, 1.25M, 1.47M and 1.67M, respectively, and spectra were taken after a five minute equilibration period. Ratios of fluorescence intensities were plotted as described.

2.3g Reconstitution of nucleosomal arrays

H2A.Bbd-H2B dimers and mouse $(H3\text{-}H4)_2$ tetramers were combined in a 2:1 molar ratio and assembled into chromatin using a recombinant assembly system. Core histones were incubated with dNAP-1 (2.4-fold molar excess dNAP-1 over core histones) on ice for 30 min in 25 mM HEPES (K+, pH7.6), 0.05 mM EDTA and 5% glycerol. ACF (Acf1/ISWI) was added to the core

histone/dNAP-1 mix (1:10 molar ratio of ACF to octamer), followed by the addition of an ATP-regenerating system (3 mM ATP, 30 mM phosphocreatine, 1 μg/mL creatine phosphokinase). Supercoiled plasmid DNA (p-306/G-less) was added to assembly reactions and incubated for 4-18 h at 27°C under final conditions of 10 mM HEPES (K+, pH 7.6), 50 mM KCl, 5 mM $MgCl_2$, 5 % glycerol, 1 % polyethylene glycol, and 0.01 % NP-40. Assembly reaction volumes were scaled to 150 ng of plasmid DNA in a 7 μL volume (amount added to typical transcription reaction). However, actual reaction volumes ranged from 50-200 μL. Supercoiled p-306/G-less contains the HTLV-1 natural promoter sequence (-306 to –1 relative to transcriptional start site) cloned into pUC13, which encompasses the three viral cyclic-AMP response elements (vCREs) upstream of the core promoter and a 380 nucleotide G-less cassette [Anderson and Widom, 2000]. Mouse octamers were assembled into chromatin using the same system. Micrococcal nuclease digestion was performed on 2.1 μg of assembled DNA (98 μL assembled chromatin). First, chromatin samples were incubated wtih 135 μl MNase buffer at 37°C for 5 min. Digestion was initiated by addition of 0.12 U of MNase at 37°C and 60 μl aliquots were removed after 1, 2, 4, and 8 minutes of digestion. Nucleic acids were analyzed on a 1.2 % agarose gel followed by SYBR® gold staining and STORM (Molecular Dynamics) imaging. Gene Ruler 100 base pair plus markers (Fermentas) were used as DNA size standards.

2.3h *In vitro* transcription assays

In vitro transcription reactions from assembled chromatin were conducted as previously described [Georges et al., 2002] with the following modifications. Preinitiation complexes were formed using 67 fmol of p-306/G-less (150 ng of assembled p-306/G-less in a 7 μL volume) in the presence or absence of exogenous Tax (6 nM), CREB (6 nM), and p300 (6 nM) in a 30 μL final volume. All reactions contained 50 μM acetyl CoA and 40 μg CEM (HTLV-1 negative T-cell line) nuclear extract. Transcription data was collected using STORM phosphorimaging and quantified by Image Quant 5.1. Transcript levels were normalized to the recovery standard. Fold activation was determined relative to basal transcription (no added activators) for each array.

2.4 Results

2.4a H2A.Bbd does not refold to a histone octamer with the other three core histones

The histone variant H2A.Bbd co-localizes with the other three core histones *in vivo,* but to date, no *in vitro* analysis of H2A.Bbd containing nucleosomes exists. To address whether purified recombinant H2A.Bbd can replace histone H2A to form a histone octamer, equimolar amounts of denatured human H2A.Bbd, mouse H2B, H3, and H4 (and, in a control reaction, mouse H2A, H2B, H3, and H4) were refolded by dialysis against a buffer containing 2 M salt. Note that the sequences of H2A.Bbd from mouse and humans are virtually identical

(D. J. T., unpublished observations). The refolded histone complexes were purified by size exclusion chromatography. Major-type mouse histones, just as those from *Xenopus laevis,* readily refold to a histone octamer, as demonstrated by a single peak at the appropriate elution volume (Fig. 2.2A) and by the presence of a full complement of all four histones in the peak (Fig. 2.2B). However, replacement of major H2A with H2A.Bbd in the refolding reaction results in two peaks that elute in the position of the H2A-H2B dimer and $(H3\text{-}H4)_2$ tetramer (Fig. 2.2A) [Dyer et al., 2004]. Analysis of the fractions by SDS PAGE confirmed that the first tetramer peak contains histone H3 and H4, while the second peak contains H2A.Bbd and H2B (Fig. 2.2B).

Histone octamers are not stable under physiological conditions in the absence of DNA. High ionic strength is required to maintain the protein complex in the absence of the counterbalancing charges provided by the DNA. Nevertheless, crystallographic studies have shown that histone – histone interactions within the histone octamer at high ionic strength are virtually identical to those observed in the NCP at low salt [Chantalat et al., 2003; Luger et al., 1997a]. Thus, our results indicate that the incorporation of H2A.Bbd results in a destabilized interface between the H2A.Bbd-H2B dimer and the $(H3\text{-}H4)_2$ tetramer.

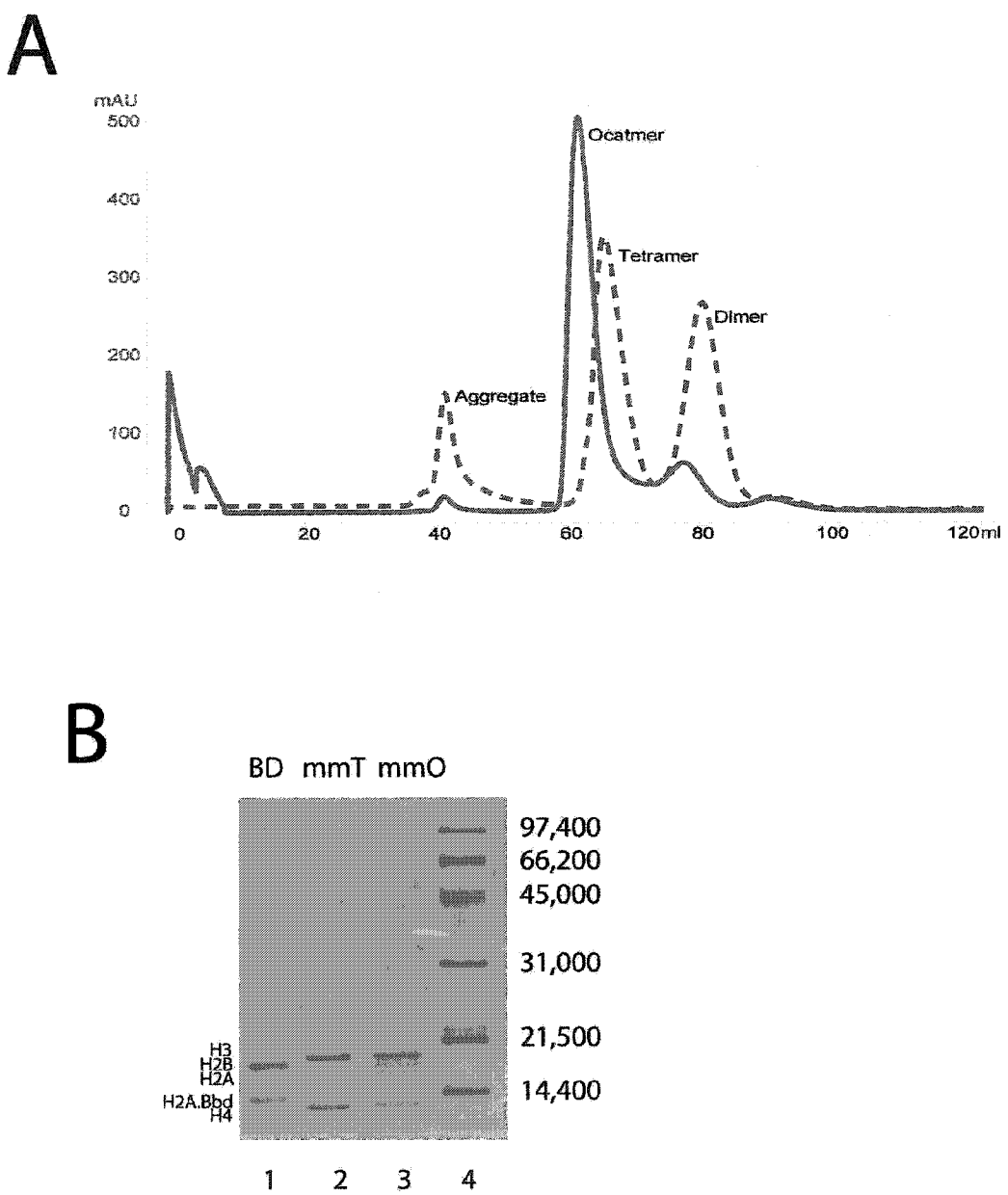

Figure 2.2: H2A.Bbd does not refold to a histone octamer with H2B, H3, and H4. (A) Gel filtration of refolding reactions from mouse histones (octamer, solid line), and mouse H3, H4, H2B, and H2A.Bbd (tetramer and dimer, dashed line). **(B)** Fractions containing mouse tetramer (*mm*T, lane 1), H2A.Bbd-H2B dimer (BD, lane 2), and mouse octamer (*mm*O, lane 3) were analyzed by 18% SDS-PAGE, stained with coomassie brilliant blue.

2.4b H2A.Bbd forms nucleosome core particles with slower electrophoretic mobility

Mouse histone octamer and a 146 bp α-satellite DNA fragment were combined to yield mouse nucleosome core particle (*mus musculus* NCP, or *mm*-NCP) by salt gradient deposition [Dyer et al., 2004]. Nucleosomes containing *Xenopus laevis* histones were reconstituted similarly, yielding *Xla*-NCPs. Reconstitution from *Xla* octamer and DNA results in a heterogeneous population of NCPs with respect to the position of the DNA on the histone octamer [Dyer et al., 2004]. A simple heating step (37-55° C for 20-180 min) is usually sufficient to convert this mixture to a uniquely positioned species which is suitable for biochemical studies and crystallization. Analysis by gel electrophoresis under native conditions shows that *mm*-NCP (Fig. 2.3A, lanes 5 and 6) behaves very similar compared to *Xla*-NCP (Fig. 2.3A, lane 1, 2). This is expected, since the four core histones are highly conserved between these two species (H2A: 92.3%, H2B: 92.8%, H3: 95.5%, H4: 100%).

To reconstitute nucleosomes containing H2A.Bbd, H2A.Bbd-H2B dimers, $(H3\text{-}H4)_2$ tetramers and α-satellite 146 bp DNA were mixed in a 2:1:1 ratio, and dialyzed as described above. The thus obtained Bbd-NCPs behave quite differently upon analysis by native PAGE (Fig. 2.3A, lanes 3 and 4). Two bands (the upper being much more prominent than the lower) were consistently obtained that migrate slower than *Xla*-NCP or *mm*-NCP, and neither their position nor their relative distribution changes upon heat treatment (Fig. 2.3A,

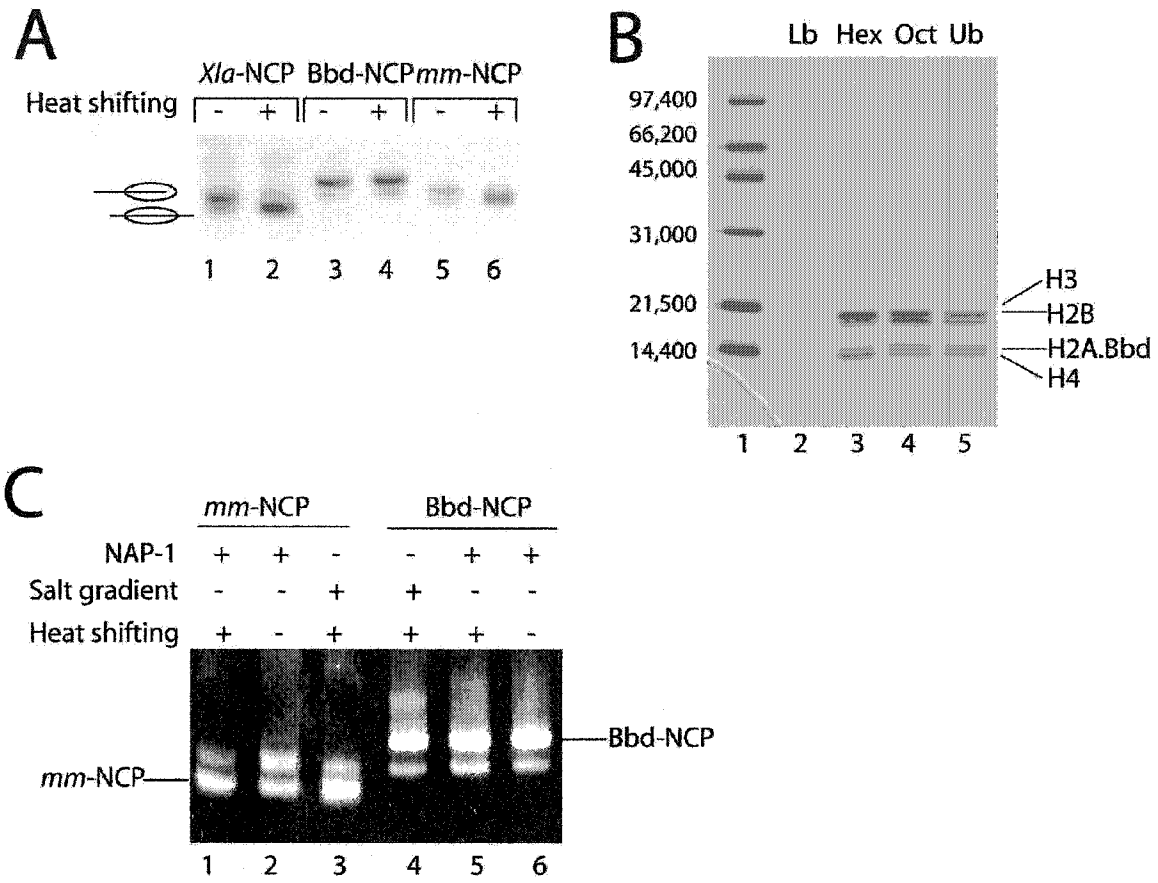

Figure 2.3: Bbd-NCP is structurally altered. (A) Salt gradient reconstituted *Xla*-NCP (lanes 1 and 2), Bbd-NCP (lanes 3 and 4), and *mm*-NCP (lanes 5 and 6), before (-) and after (+) a 1 hour incubation at 37°C, were analyzed by 5 % native PAGE and stained with coomassie blue. **(B)** Analysis of the histone content of the two Bbd-NCP nucleosomal bands. The upper band (Ub; lane 5) and lower band (Lb; lane 2) of Bbd-NCP were excised from the native gel and analyzed by 18% SDS-PAGE. H2A.Bbd-H2B dimer : $(H3\text{-}H4)_2$ tetramer mixtures of 2:1 (Oct, lane 4) and 1:1 (Hex, lane 3) were used as controls. **(C)** yNAP-1 - reconstituted *mm*-NCP (lane 1 and 2) and Bbd-NCP (lane 5 and 6) were compared with salt gradient reconstituted NCPs (lanes 3 and 4, respectively) on a 5% native gel, stained with ethidium bromide.

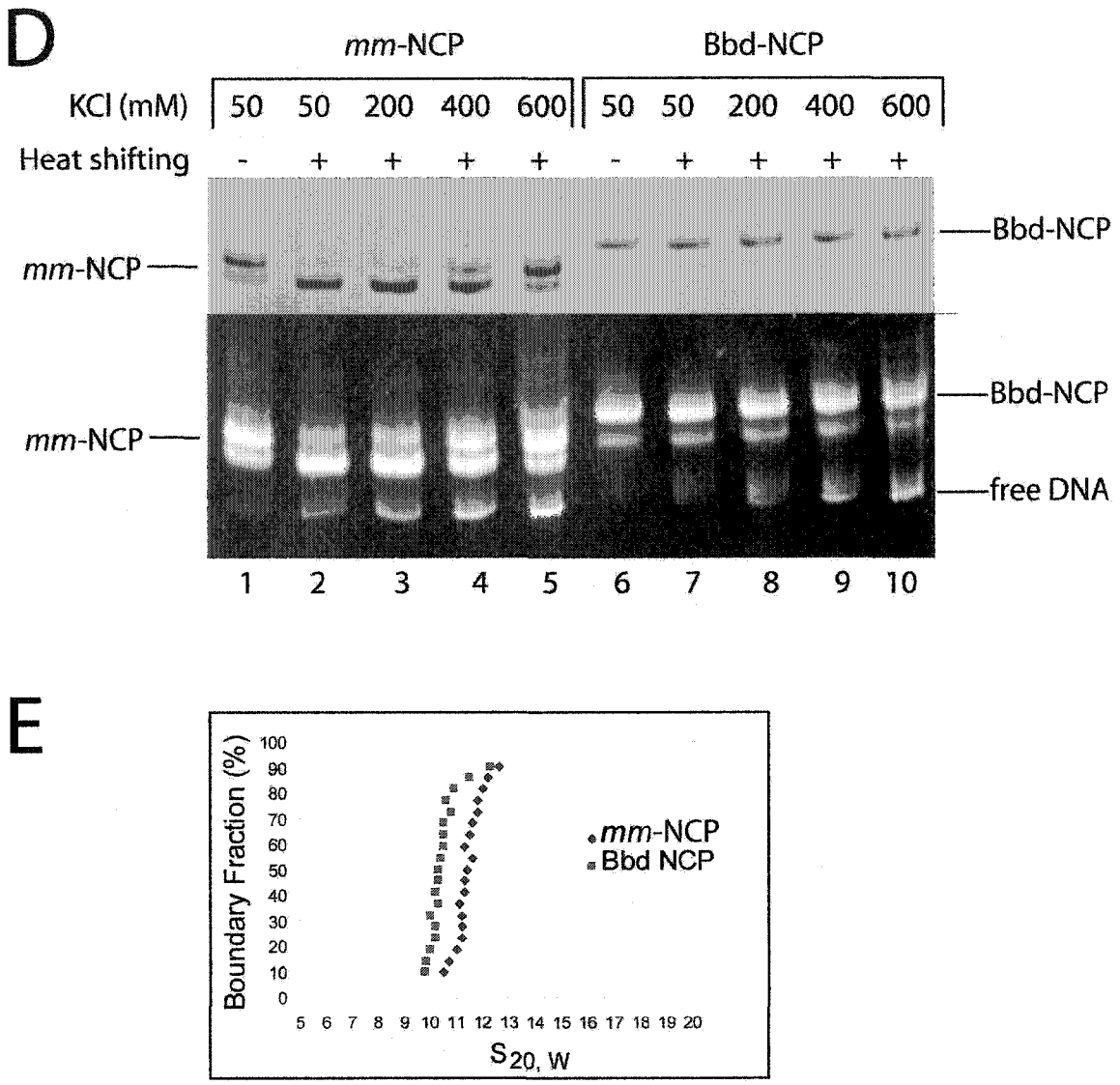

Figure 2.3: Bbd-NCP is structurally altered. (D) Stability of *mm*-NCP and Bbd-NCP at elevated ionic strength. Heat-shifted NCPs (lane 2 and 7) were incubated at 37°C for 1 hour in the presence of 200, 400 and 600 mM KCl (lane 3, 4, 5 and 8, 9, 10). **(E)** The integral distributions of sedimentation coefficients, G(s), obtained for Bbd-NCP and *mm*-NCP after analysis of sedimentation velocity boundaries [van Holde and Weischet 1978].

compare lanes 3 and 4). To rule out that these differences were the result of variations in the assembly method, i.e. by using separately purified H2A.Bbd-H2B dimer and $(H3\text{-}H4)_2$ tetramers instead of histone octamer during reconstitution, we reconstituted *mm*-NCP from separately refolded (H2A-H2B) dimer and $(H3\text{-}H4)_2$ tetramer. Analysis by native PAGE clearly showed that such nucleosomes were indistinguishable from *mm*-NCP obtained from histone octamer (not shown).

We next determined whether both bands obtained upon reconstitution of Bbd-NCP contained a full complement of histones. We excised the two bands individually and analyzed their content by SDS PAGE (Fig. 2.3B). The ratio of the four histones in the upper band was determined to be ~1:1:1:1 based on a comparison with a 'mock-octamer' (a precise mixture of independently refolded tetramer and Bbd dimer at a 1:2 ratio, compare lanes 4 and 5 of Fig. 2.3B). No depletion of either H2A.Bbd or H2B is evident, as seen in a comparison with lane 3, showing a 1:1 mixture of tetramer and dimer. Unfortunately, the bands are too closely spaced to allow quantization. The lower band of Bbd-NCP was analyzed similarly (Fig. 2.3B, lane 2), however, this species could never be obtained to sufficient amounts to draw a definitive conclusion.

To exclude that the observed results were an artifact of salt-dependent reconstitution (resulting, perhaps, from differences in the affinities of the various histone sub-complexes for DNA at various salt concentrations during the salt gradient), we used yeast Nucleosome Assembly Protein 1 (yNAP-1) to reconstitute nucleosomes under physiological conditions, at 100 mM NaCl. We

have shown previously that yNAP-1 has a similar affinity for H2A.Bbd-H2B and (H2A-H2B) dimers (Y-J. P., unpublished observations). For both *mm*-NCP and Bbd-NCP, identical results were obtained upon reconstitution with yNAP-1 and by salt-gradient (Fig. 2.3C, compare lanes 1 with 3; and 4 with 5), proving that the observed Bbd-NCP species forms independently of the assembly pathway.

Our findings that Bbd-NCP contains stoichiometric amounts of the four histones to form a structurally altered NCP is formally consistent with a non-native particle in which histones are bound to DNA without forming a histone octamer (for example, a 'tetrasome' particle to which two (H2A.Bbd-H2B) dimers are bound by weak electrostatic interactions. DNase I footprinting is not suited to rule out this possibility, since a 10 bp pattern is not necessarily indicative of an intact NCP (for example, [Kerrigan and Kadonaga, 1992]). We therefore assayed the integrity of Bbd-NCP in the presence of increasing ionic strength, under the assumption that non-native charge-charge interactions between histones and the DNA would not be able to withstand elevated ionic strength [Brooks and Jackson, 1994]. We incubated the shifted *mm*-NCP and Bbd-NCP in the presence of 200, 400 or 600 mM KCl at 37° C for one hour (Fig. 2.3D). As demonstrated previously [Muthurajan et al., 2003], the translational position of the histone octamer with respect to the DNA changes upon increased ionic strength in NCPs reconstituted with major-type histones (compare, for example, Fig. 2.3D, lanes 2 and 5). Only small amounts of DNA are liberated in the process (Fig. 2.3D, lower panel). Although no redistribution of bands takes place in Bbd-NCP, the complex is stable even at 600 mM salt, and similarly small amounts of DNA are liberated

upon incubation at elevated ionic strength. We thus conclude that Bbd-NCP forms a reasonably stable particle that is stabilized by similar interactions as those observed in canonical NCPs.

The altered electrophoretic behavior of Bbd-NCP could be caused by changes in either charge, nucleosome structure, or both. H2A.Bbd is less basic than mouse H2A (with a pI of 10.7 versus 11.2) and has a lower molecular weight, and therefore Bbd-NCP would migrate faster than *mm*-NCP if the two nucleosomes exhibited identical structures. Thus, changes in shape must be responsible for the slow electrophoretic mobility of Bbd-NCP. This was verified by analytical ultracentrifugation. The sedimentation coefficients were 11.6±0.3 for *mm*-NCP, and 10.5±0.3 for Bbd-NCP (Fig. 2.3E). This 9.5 % difference in S-values, which is observed over the entire sedimentation boundary, is significant and reproducible. From the relation $S = M (1- u\rho) / Nf$, we calculated that the frictional coefficient of Bbd-NCP has increased by 9%. Based on the molecular weight and sedimentation coefficient, we calculate that f/fo (where fo is frictional coefficient for a sphere) for Bbd-NCP is 1.662, and f/fo for *mm*-NCP is 1.521, indicating that Bbd-NCP has a more elongated shape than *mm*-NCP.

2.4c The DNA ends are less constrained in Bbd-NCP

One simple hypothesis to explain the observed characteristics of Bbd-NCP is that the DNA is less constrained in these particles. Fluorescence resonance energy transfer (FRET) is a powerful tool to determine the distance between two regions within a macromolecular complex. We used this method to test our

hypothesis, and to further characterize the structural changes within Bbd-NCP. Nucleosomes exhibit a compact structure at low salt concentration, with the two ends of the DNA at a distance of ~ 60 Å, but the DNA begins to partially dissociate from the surface of the histone octamer at increased salt concentrations [Park et al., 2004b]. We labeled the two 5' ends of a 146 bp DNA fragment derived from the 5S rRNA gene [Richmond et al., 1988] with fluorescein (FM, acceptor) and coumarin derivatives (CPM, donor) and reconstituted the labeled DNA into *mm*-NCP and Bbd-NCP. We note that the presence of the fluorescent probes does not compromise electrophoretic migration of the samples (data not shown; and [Park et al., 2004b]). Samples used for FRET studies were devoid of free DNA, and Bbd-NCP samples usually had a very prominent upper band, and very little of the lower band described above.

Fluorescence was excited at 385 nm, and emission spectra for *mm*-NCP and Bbd-NCP at increasing ionic strength were measured. For *mm*-NCP we observed a pronounced signal at the acceptor emission wavelength (520 nm) upon excitation of donor emission (Fig. 2.4A). Within *mm*-NCP, FRET between the DNA ends occurs up to a salt concentration of 0.38 M NaCl, but is lost if the ionic strength is further increased, confirming earlier results with *Xla*-NCP [Park et al., 2004b] (Fig. 2.4C). In striking contrast, no FRET is observed in Bbd-NCP even at low ionic strength (Fig.2.4B), as seen by an absence of fluorescence acceptor emission. Since FRET is concomitant with decreased donor emission, we plotted the ratios between fluorescence emission at 520 nm and 480 nm for each NCP and for free labeled DNA at several salt concentrations (Fig. 2.4C). In

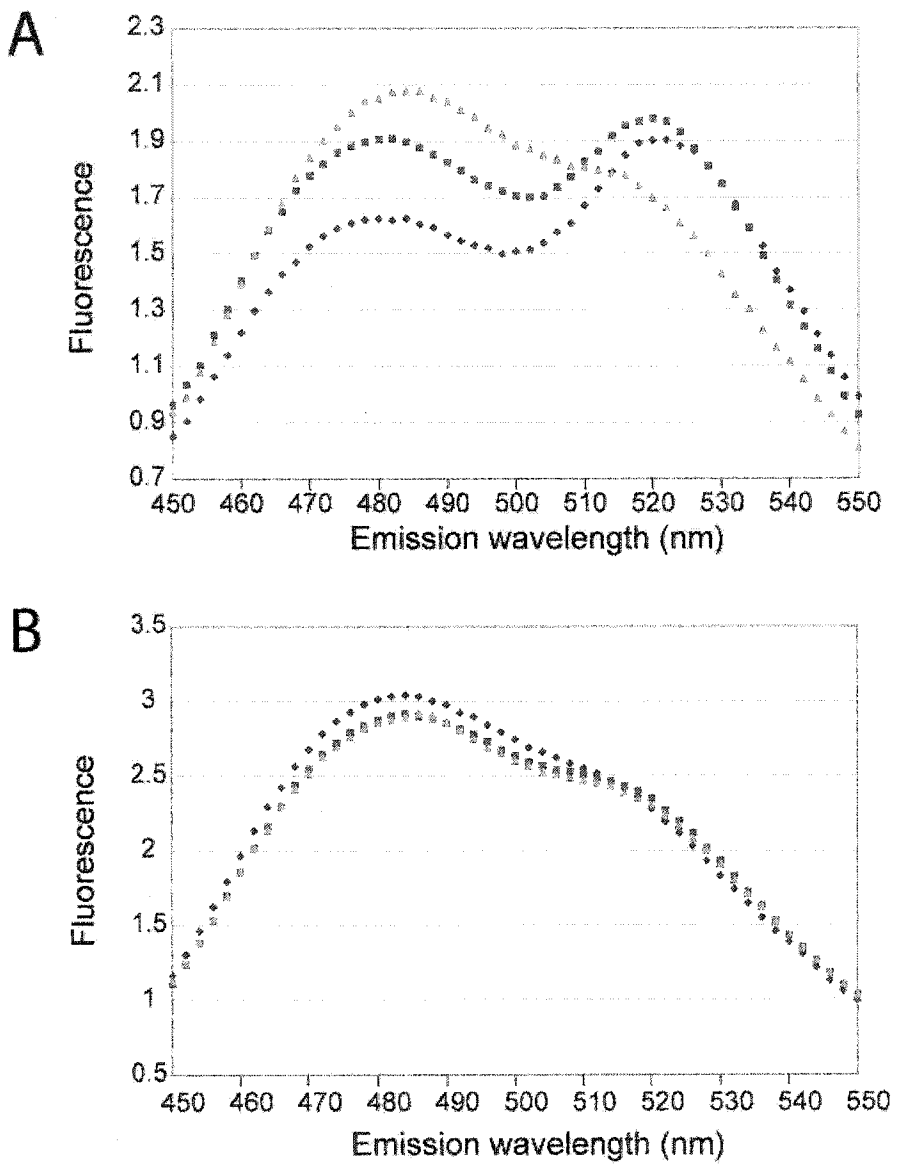

Figure 2.4: Fluorescence resonance energy transfer (FRET) between the two ends of nucleosomal DNA shows that the DNA in Bbd-NCP is less tightly bound. Fluorescence was excited at 385 nm, emission spectra were measured from 450 nm to 550 nm for *mm*-NCP (A) and Bbd-NCP (B) at increasing ionic strengths. Only spectra taken at 0 M, 0.38 M, and 1 M NaCl are shown (diamonds, squares, and triangles respectively).

C

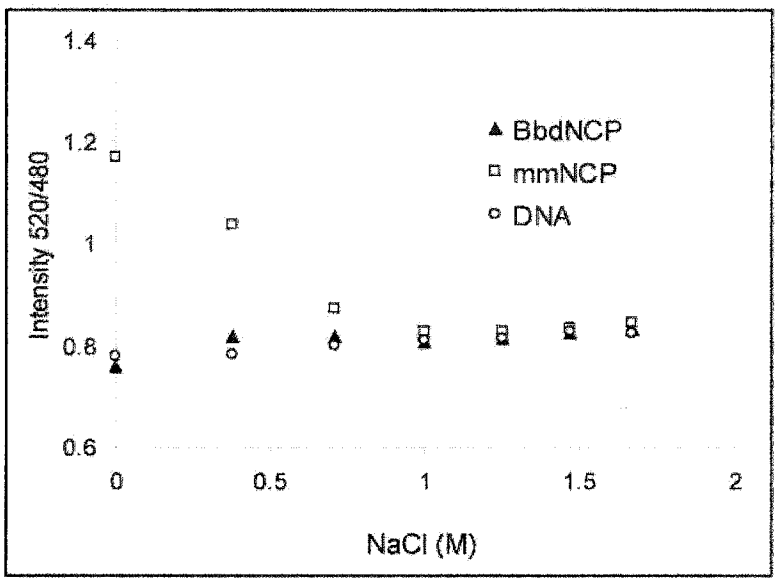

Figure 2.4: Fluorescence resonance energy transfer (FRET) (C) Ratios of fluorescence intensities (520 nm / 480 nm) for *mm*-NCP, Bbd-NCP and labeled DNA at indicated salt concentrations (squares, triangles, and circles respectively) are plotted.

NCP-Bbd, no change in this ratio is observed over the entire salt range measured, as is the case for free DNA. These results were confirmed by monitoring FRET between the DNA end and the $(H3\text{-}H4)_2$ tetramer, with the same results (data not shown). Thus, our results strongly indicate that the ends of DNA in Bbd-NCPs are partially dissociated from the surface of the histone octamer, resulting in a less compact structure. This is a consistent explanation for the observed slower electrophoretic mobility, and the decreased S-value.

2.4d Only 118±2 bp of DNA are protected against micrococcal nuclease digestion in Bbd-NCP

The NCP was originally defined as a stable intermediate from chromatin digestion with MNase [Simpson, 1978]. Thus, completely folded NCPs reconstituted with 146 bp of DNA should be quite resistant towards digestion, but nucleosomes with only loosely organized DNA ends should be much more susceptible. Mouse octamer [or $(H3\text{-}H4)_2$ tetramer and H2A.Bbd-H2B dimers] were reconstituted onto either 146 bp 5SDNA or 196 bp 5SDNA [Georgel et al., 1993] to yield nucleosomes (*mm*-146-NCP, Bbd-146-NCP, *mm*-196-NCP and Bbd-196-NCP, respectively). Identical amounts of *mm*-146-NCP and Bbd-146-NCP were incubated with increasing amounts of MNase, and the de-proteinized DNA fragments were analyzed on a 10% polyacrylamide gel. A comparison of Fig. 2.5A and 5B shows that Bbd-146-NCP is digested much more rapidly than *mm*-146-NCP under identical conditions, confirming that the DNA in Bbd-NCPs is

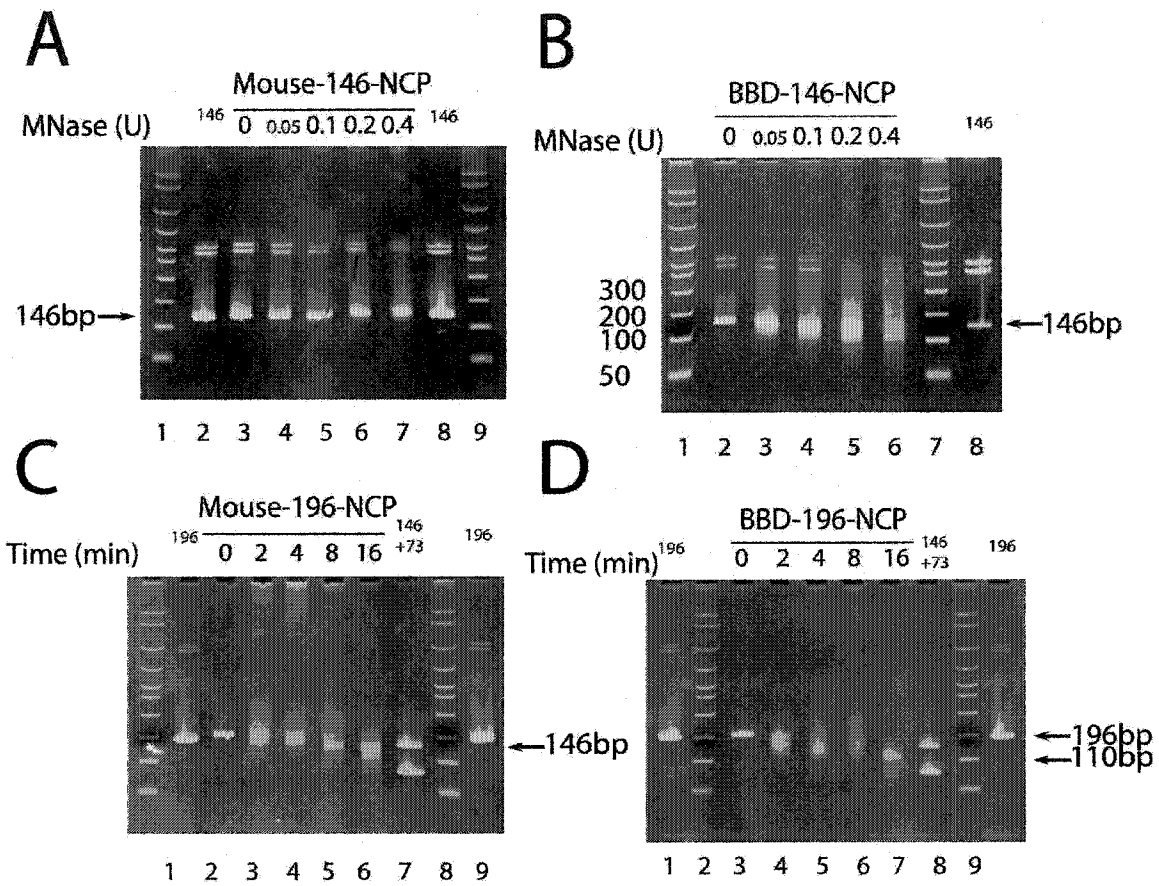

Figure 2.5: Bbd-NCPs are less resistant against Micrococcal Nuclease (MNase) digestion. Identical amounts (2 μg) of *mm*-146-NCP **(A)** and Bbd-146-NCP **(B)** were digested with increasing amount of MNase (0, 0.05, 0.1, 0.2, 0.4 U) for 1.5 min. Deproteinized samples were analyzed by 10 % PAGE, stained with ethidium bromide. For time courses, 10 μg of *mm*-196-NCP **(C)** and Bbd-196-NCP **(D)** were incubated with the same amount of MNase (0.15U) for the indicated times. 2 μg of sample was removed at 0 min, 2min, 4 min, 8 min and 16 min, and the deproteinized samples were analyzed by 10 % PAGE. The 146 bp 5sDNA (146), 196 bp 5sDNA (196) and mixtures of 146 bp and 73 bp α-satellite DNA (146 +73) were loaded as controls, as indicated. DNA size markers are given.

relatively less protected from MNase digestion. An intermediate band of ~118 bp is clearly observed at higher MNase concentrations (Fig. 2.5B, lane 6).

To more precisely define the number of base pairs that are actually protected by Bbd-NCPs, we performed a time course of MNase digestion with nucleosomes reconstituted on longer DNA fragments. Fig. 2.5C and D show that digestion of *mm*-196-NCP results in a pronounced stop at ~146 bp, as expected. In contrast, no stop at 146 bp is observed in Bbd-196-NCP, but instead MNase generates a DNA fragment of 118±2 bp in length. Thus, compared to canonical nucleosomes, the terminal ~14 bp of the 146 bp nucleosomal DNA are not protected against digestion, under the assumption that the DNA is symmetrically positioned on the surface of the histone octamer.

2.4e The absence of the C-terminal tail in H2A.Bbd is not responsible for the relaxed structure of Bbd-NCP

One of the obvious differences between H2A and H2A.Bbd is the absence of the basic C-terminal histone tail (which is in a perfect position to organize the terminal regions of the DNA; Fig. 2.1B) in the latter (Fig. 2.1A). C-terminally truncated *Xla* H2A constructs were generated by introducing a stop codon after amino acid 112 (*Xla* $H2A_{112}$, Fig. 2.1). As an additional control, a stop codon was also introduced after amino acid 106, in essence removing the entire 'stem' of the ladle-shaped docking domain (*Xla* $H2A_{106}$, Fig.2.1). Unexpectedly, both purified truncated histones, together with the three other core histones, could be refolded to histone octamers using standard procedures (not shown). This indicates that

the C-terminal portion of the H2A docking domain and the C-terminal tail is not responsible for stabilizing histone – histone interactions within the histone octamer, despite the presence of several hydrogen bonds between this region and H3 αN and H3 α2 observed in published nucleosome structures (reviewed in [Luger, 2003]).

We next reconstituted NCPs with these truncated H2A versions. To maintain consistency with Bbd-NCP reconstitutions, $(H3\text{-}H4)_2$ tetramer and *Xla* $H2A_{112}$-H2B dimers (or *Xlα* $H2A_{106}$-H2B dimers) were reconstituted with 146 bp 5S DNA in a 1:2:1 molar ratio to yield mutant NCPs (*Xla* $H2A_{112}$-NCP and *Xla* $H2A_{106}$-NCP, respectively), using salt gradient deposition. The resulting nucleosomes were analyzed by native PAGE. Fig. 2.6 shows that *Xla* $H2A_{112}$-NCP behaves very similarly to *Xla*-NCP. Nucleosomal bands can be shifted almost completely to a band that migrates only slightly slower than *Xla-NCP* (Fig. 2.6A, compare lanes 4 and 5 with lanes 6 and 7). *Xla* $H2A_{106}$-NCP migrates somewhat slower, and can be partly shifted (Fig. 2.6A, lane 2, 3). Both truncated nucleosomes are much more similar to full length *Xla*-NCP and *mm*-NCP in their electrophoretic behavior than to Bbd-NCP. Consistent with this observation, *Xla* $H2A_{106}$-NCPs and *Xla* $H2A_{112}$-NCP exhibit a similar degree of resistance towards digestion with MNase as does *Xla*-NCP (Fig. 2.6B, D, and E), and are both much more resistant than Bbd-NCPs (Fig. 2.6C).

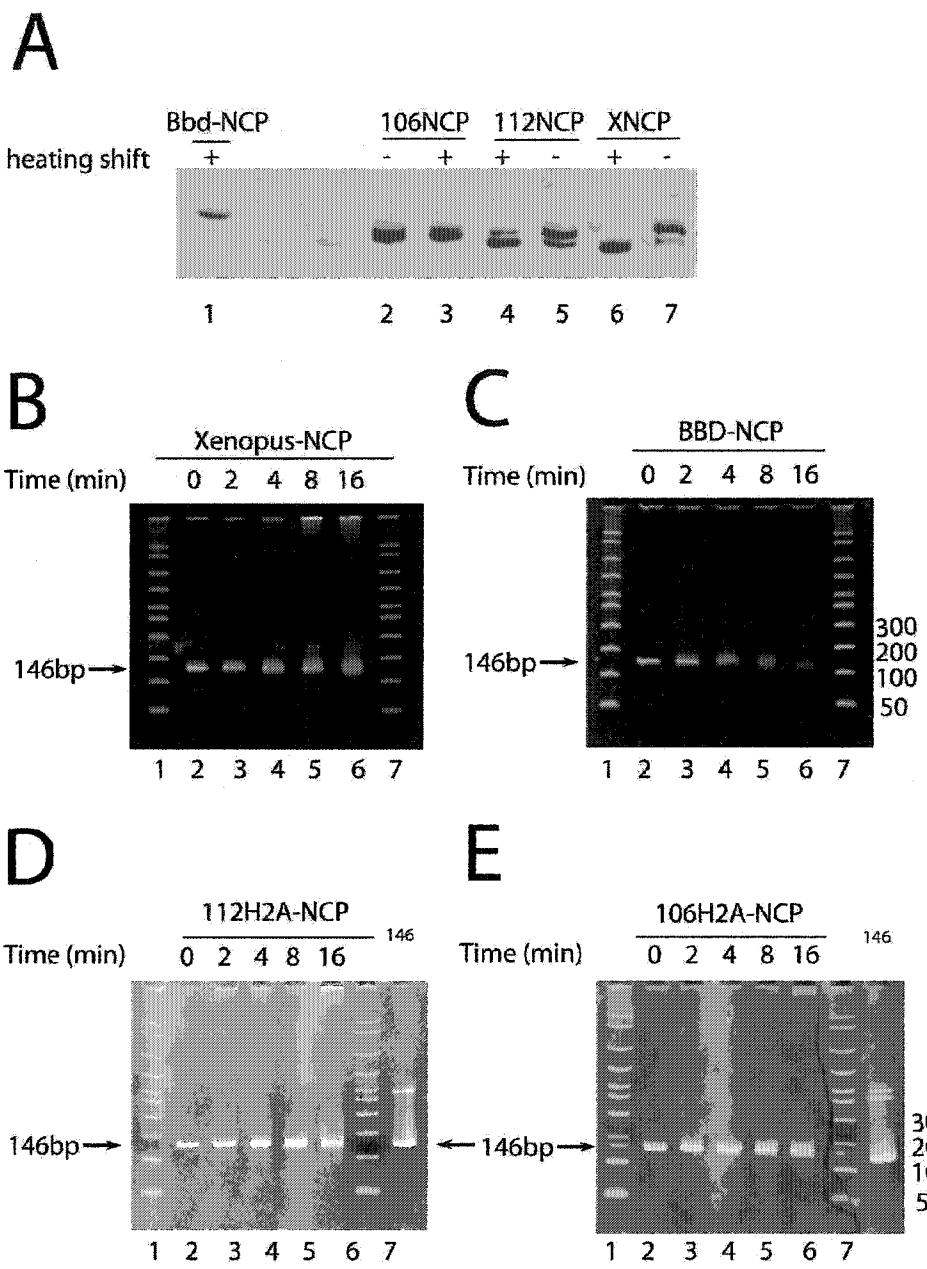

Figure 2.6: *Xla* $H2A_{106}$-NCP and *Xla* $H2A_{112}$-NCP behave like wild type *mm*-NCP. (A) Salt gradient reconstituted Bbd-NCP (lane 1), *Xla*-NCP (lanes 6 and 7), *Xla* $H2A_{106}$-NCP (106NCP, lanes 2 and 3), and ***Xla*** $H2A_{112}$-NCP (112NCP, lanes 4 and 5), before (-) and after (+) a 1 hour incubation at 37°C, were analyzed by 5 % native PAGE, followed by staining with coomassie blue. **(B-E):** micrococcal digestion of mutant nucleosomes: 10 μg of *Xla*-NCP **(B)**, Bbd-NCP **(C)**, *Xla* $H2A_{112}$-NCP **(D)** and *Xla* $H2A_{106}$-NCP **(E)** were digested with 0.15 U of MNase. Aliquots of 2 μg were removed after 0, 2, 4, 8, and 16 min. 10% PAGE was used to check the deproteinized DNA fragments. 146 bp 5sDNA (146) was loaded as indicated (D and E, lanes 8).

2.4f Changes in the docking domain are responsible for the altered conformation of Bbd-NCP

Having established that the C-terminal end of the H2A docking domain is not involved in organizing the DNA ends, we turned our attention to the H2A docking domain, where the majority of sequence differences between H2A and H2A.Bbd are clustered. A derivative of *Xla* H2A was prepared in which the original docking domain (from the C-terminal end to I_{79}, Fig. 2.1A) was replaced with the Bbd docking domain (*Xla* H2A/Bbd). This histone chimera combines two features of interest in H2A.Bbd (the absence of the C-terminal tail and the H2A.Bbd-specific sequence variations in the docking domain) but maintains the sequence of *Xla* H2A in all other regions. Just like H2A.Bbd, this chimeric *Xla* H2A/Bbd histone cannot be refolded to a histone octamer upon combination with the three other histones, but instead forms *Xla* H2A/Bbd-H2B dimers and $(H3\text{-}H4)_2$ tetramers (data not shown).

$(H3\text{-}H4)_2$ tetramers and *Xla* H2A/Bbd-H2B dimers were reconstituted with 146mer DNA to form *Xla* H2A/Bbd-NCP, using salt gradient deposition. Analysis of the reconstituted products by gel electrophoresis shows that *Xla* H2A/Bbd-NCP (Fig. 2.7A, lanes 4 and 9) migrates much slower than *Xla*-NCP (Fig. 2.7A, lane 1, 2), even somewhat slower than Bbd-NCP (Fig. 2.7A, lanes 7 and 8). Also, just like Bbd-NCP, *Xla* H2A/Bbd-NCP does not reposition upon heat treatment (Fig. 2.7A, compare lanes 4 and 9, and lanes 7 and 8). FRET analysis of *Xla* H2A/Bbd-NCPs confirmed that this is because the ends of the DNA are

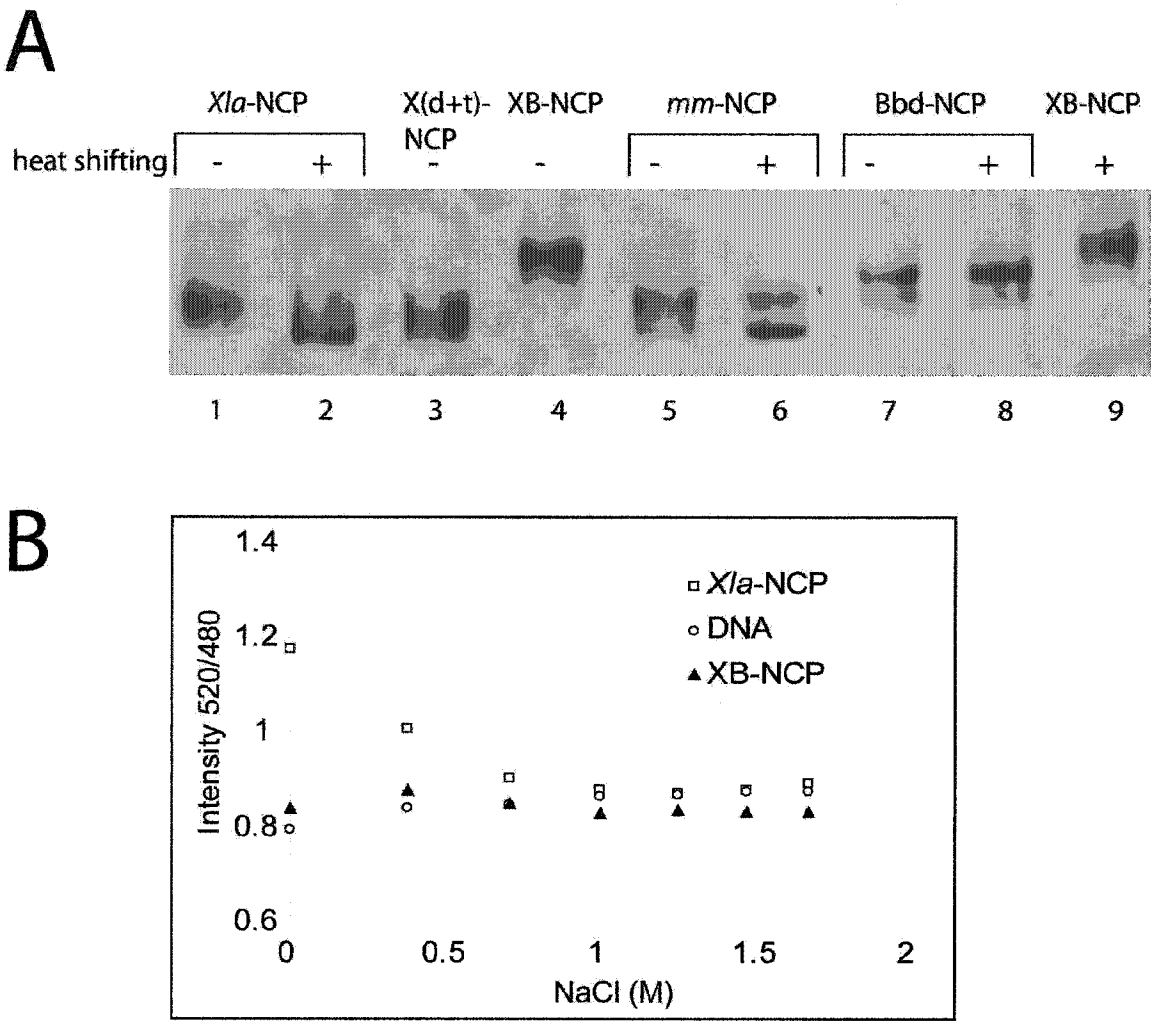

Figure 2.7: The H2A.Bbd docking domain is responsible for the relaxed structure of Bbd-NCP. (A) Salt gradient reconstituted *Xla*-NCP (lanes 1 and 2), *Xla*-NCP reconstituted from (H2A-H2B) dimer and $(H3\text{-}H4)_2$ tetramer (X(d+t)-NCP; lane 3), *Xla* H2A/Bbd-NCP (XB-NCP, lanes 4 and 9), *mm*-NCP (lanes 5 and 6), and Bbd-NCP (lanes 7 and 8), before (-) and after (+) 1hour incubation at 37°C, were analyzed by 5 % native PAGE, stained by coomassie brilliant blue. **(B)** Analysis by FRET. Ratios of fluorescence intensity at 520 nm and 480 nm for *Xla*-NCP, XB-NCP and labeled DNA at indicated salt concentrations (squares, triangles, and circles respectively). Data points were taken from spectra similar to those shown in Fig. 2.4A and B.

beyond the critical Förster distance, resulting in the absence of FRET even at low ionic strength, as has been observed in Bbd-NCP. Ratios of fluorescence intensities at 520 nm and 480 nm are plotted in Fig. 2.7B. Together, the analysis of derivative and chimeric nucleosomes indicate that the region between amino acids 79 and 105 (in *Xla* H2A numbering, Fig. 2.1A) appears to be mainly responsible for either directly or indirectly organizing the ~14 penultimate bp of nucleosomal DNA.

2.4g H2A.Bbd – containing nucleosomal arrays repress transcription from a natural promoter

Having defined the structural changes in H2A.Bbd-containing mono-nucleosomes, we wanted to investigate whether this histone variant could be efficiently assembled into nucleosomal arrays. H2A.Bbd-H2B dimers and mouse $(H3\text{-}H4)_2$ tetramers were assembled onto supercoiled plasmid DNA containing a highly inducible natural promoter (p-306/G-less), using a previously described recombinant assembly system [Georges et al., 2002]. Recombinant mouse histone octamers and native *Drosophila* histones were assembled as controls. The quality of assembled chromatin and nucleosome spacing were checked by MNase digestion (Fig. 2.8A). H2A.Bbd (together with the other three mouse histones) was assembled into regularly spaced nucleosomal arrays, comparable in quality to the control arrays. However, a Bbd-containing nucleosomal array produces digestion ladders with a repeat length of ~126 bp, whereas

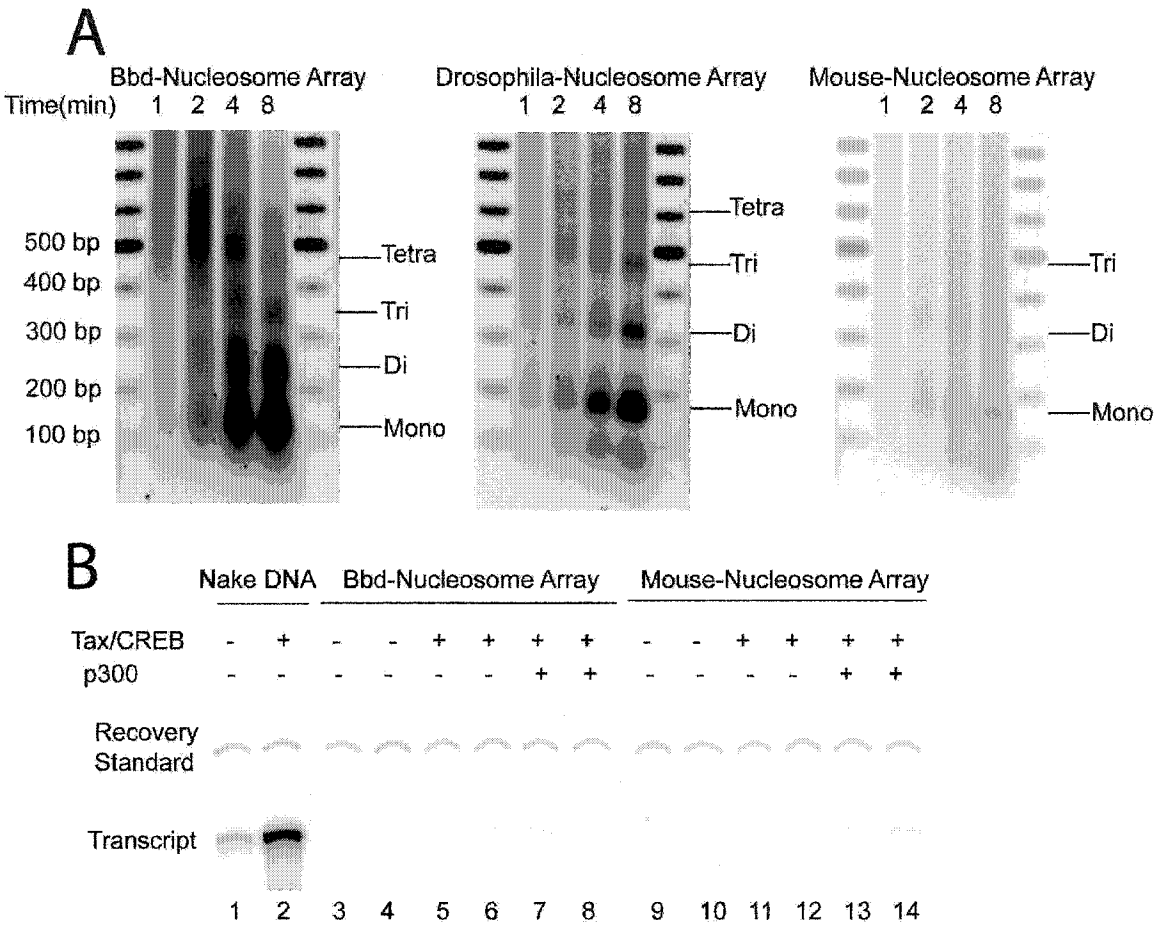

Figure 2.8: Bbd-containing nucleosomal arrays repress basal transcription. (A) 2.1μg of assembled Bbd-, mouse-, and *Drosophila*-nucleosomal arrays were digested with 0.12 U of MNase. Aliquots of 0.5 μg were removed after 1, 2, 4, and 8 min, deproteinized, and analyzed on 1.2 % agarose gels. **(B)** *In vitro* transcription reactions for naked DNA, Bbd-nucleosomal arrays and mouse-nucleosomal arrays are shown. Tax/CREB and p300 was added as indicated above the lanes. Recovery standard and transcript are indicated to the left.

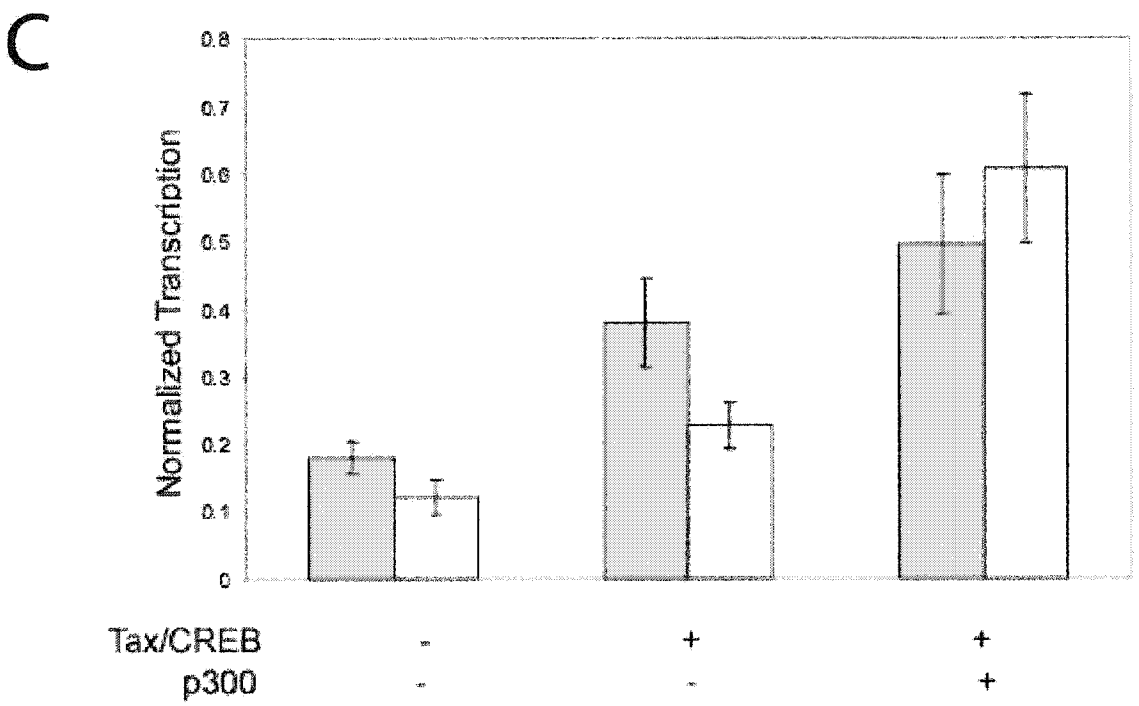

Figure 2.8: Bbd-containing nucleosomal arrays repress basal transcription. (C) Results from three transcription assays (from three independent chromatin assembly reactions) were quantified by ImageQuant 5.1 and normalized compared to the recovery standard. Transcripts from mouse and Bbd-nucleosomal arrays are shown by white and gray bars, respectively.

nucleosomal arrays reconstituted with either mouse or *Drosophila* histones produce ladders with a repeat length of ~170 bp.

Further, we wanted to know whether such arrays would repress transcription by RNA polymerase II *in vitro* and whether this repression could be alleviated by the action of transcription activators and co-activators, using the well-defined HTLV-LTR *in vitro* system [Georges et al., 2002]. In this system, nucleosomal arrays efficiently inhibit basal transcription, and this repression is relieved in a Tax/CREB/p300 – dependent manner. Bbd-containing nucleosomal arrays inhibit transcription slightly less efficiently than mouse arrays (Fig. 2.8B, compare lane 3 and 4 with 9 and 10). Tax/CREB – dependent activation is essentially the same (2-fold versus 1.9 fold), however, the effect of p300 was not as pronounced as in mouse nucleosomal arrays (1.3 vs. 2.7-fold activation; Fig. 2.8C).

2.5 Discussion

The incorporation of histone variants via replication-independent assembly mechanisms has emerged as an important pathway by which eukaryotic cells locally or globally modify chromatin structure to regulate transcription, repair, and replication. Histone variants differ from major-type histones in their amino acid sequence, in their expression patterns, and in their pattern of incorporation into chromatin [Malik and Henikoff, 2003; Rangasamy et al., 2003]. They are as diverse in function as they are in their amino acid sequence: whereas some are targeted to specialized chromatin regions (for example, the centromeric histone

H3 variant; [Sullivan, 1998], others, such as H2A.X, serve as markers for chromatin regions where DNA repair is required [d'Adda di Fagagna et al., 2003], or play more ill-defined roles in transcription regulation and chromatin higher order structure organization [Chadwick and Willard, 2001; Chadwick and Willard, 2002; Fan et al., 2002; Perche et al., 2000]. With the notable exception of H2A.Z [Fan et al., 2002; Suto et al., 2000], very little biophysical data is available on the effect of any of these histone variants on nucleosome and chromatin structure.

Of all the histone variants, H2A.Bbd is the most specialized in terms of amino acid sequence, and the least-well understood in terms of function. Here we have shown that the interaction between the $(H3\text{-}H4)_2$ tetramer and the H2A.Bbd-H2B dimer is weakened compared to that observed between the H2A-H2B dimer and the $(H3\text{-}H4)_2$ tetramer. Domain swap experiments demonstrate that this is due to the sequence differences in the 'base' of the H2A ladle-shaped docking domain. *In vivo*, the weaker interaction between the histone sub-complexes within H2A.Bbd-nucleosomes may facilitate the dissociation of the H2A.Bbd-H2B dimer from chromatin, either spontaneously or assisted by transcription-related factors such as FACT [Belotserkovskaya et al., 2003], histone chaperones [Akey and Luger, 2003], or ATP-dependent chromatin remodeling factors [Becker and Horz, 2002], consistent with its proposed localization in transcriptionally active chromatin [Chadwick and Willard, 2001].

We showed by native PAGE, FRET, and micrococcal nuclease digestion that only 118±2 bp of DNA are bound firmly in Bbd-NCP, as opposed to the 147 bp that are tightly organized in canonical NCPs. These results are consistent with

a significantly decreased S-value of the variant particle. Several lines of evidence argue that the observed species is a bona-fide nucleosome rather than a $(H3\text{-}H4)_2$ tetramer - DNA complex with H2A.Bbd-H2B dimers non-specifically bound. First, Bbd-NCP contains stoichiometric amounts of the four histones. Second, identical complexes are obtained by two independent methods; salt-dependent reconstitution and chaperone-mediated reconstitution under physiological conditions. Third, Bbd-NCP exhibits normal stability in the presence of elevated ionic strength. Finally, we observe that H2A.Bbd –containing nucleosomal arrays exhibit a significantly shorter repeat length (and thus higher nucleosome density). These arrays significantly repress basal transcription, and this repression is relieved in a Tax/CREB-dependent manner.

We demonstrated that the H2A.Bbd docking domain is responsible for the looser DNA organization observed in Bbd-NCP, whereas the missing C-terminal tail plays only a minor role in organizing the 14 penultimate base pairs of nucleosomal DNA. In a structural context, our results suggest that the contact that is made at SHL ±5.5 (which is organized by the H2A.Bbd-H2B dimer) is still intact, whereas the penultimate contact between the H3 αN-helix must be significantly weakened. We interpret these results as evidence that the H2A docking domain (in particular the circular base of the ladle-shaped sub-structure) is responsible for orienting the H3 αN helix for proper interactions with the DNA, consistent with the role of this particular region in stabilizing the histone octamer.

To date, this is the first histone variant that forms nucleosomes with such unusual structural properties. H2A.Z, macroH2A, or centromeric H3 all form tightly folded nucleosome core particles in our *in vitro* reconstitution system ([Suto et al., 2000]; and S. Chakravarthy & K.L., unpublished observations). Dependent on the prevailing histone variant, different physiological outcomes may be obtained since two histone variants may have opposite effects on chromatin structure. For example, whereas H2A.Bbd destabilizes nucleosomal structure, H2A.Z appears to be stabilizing [Park et al., 2004b]; the effect of the incorporation of other histone variants into nucleosomes is not known. The structural properties of Bbd-NCPs described here have important implications for the *in vivo* function of this histone variant. The evidence for the involvement of H2A.Bbd in transcriptionally active chromatin is indirect and mainly stems from the observation that H2A.Bbd co-localizes with acetylated H4 [Chadwick and Willard, 2001]. However, consistent with this hypothesis, the observed weakened interaction between the H2A.Bbd-H2B dimer and $(H3\text{-}H4)_2$ tetramer, and the less efficient organization of the DNA ends should present a less formidable obstacle for the advancing RNA polymerase. It is also interesting to speculate that H2A.Bbd containing nucleosomes may be less dependent on histone modifications and chromatin remodeling. The fact that none of the residues that are the usual targets of posttranslational modification in major H2A are present in H2A.Bbd indicates potential consequences for the histone code [Strahl and Allis, 2000] in H2A.Bbd-containing chromatin regions. This hypothesis is supported by our finding that transcriptional activation in Bbd-containing arrays are less

dependent on p300 than arrays reconstituted with major-type histones. However, more experiments are needed to investigate the role of H2A.Bbd in particular and of histone variants in general in modulating transcriptional properties of selected genes.

In summary, we have shown how the replacement of H2A with the histone variant H2A.Bbd alters the conformation of the nucleosome in a way that is consistent with a role in facilitating the transcription process. Clearly, histone variants provide an important alternative way to modulate chromatin structure in addition to, or without the continued need of histone modifying enzymes.

2.6 Acknowledgements

We thank Xu Lu and Jeffrey Hansen for help with analytical ultracentrifugation, and Srinivas Chakravarthy for critical reading of the manuscript. Supported by a grant from the Human Frontiers Science Program (HFSPO) to K.L. and D.J.T, and by NIH grant # 61909 to K.L.

CHAPTER 3

Structural Characterization of Histone H2A Variants

The contents of this chapter were published in *the 69th Cold Spring Harbor Symposia for Quantitative Biology: Epigenetics*.

The author list for this paper is:

Srinivas Chakravarthy, Yunhe Bao, Victoria A. Roberts, David Tremethick, and Karolin Luger. YB contributed the data on H2A.Bbd.

3.1 Introduction

Eukaryotic DNA associates with an equal amount of protein to form chromatin, the fundamental unit of which is the nucleosome core particle (NCP). An NCP consists of two copies each of the four core histones H2A, H2B, H3, and H4. This histone octamer binds 147 base pairs of DNA around its outer surface in 1.65 tight superhelical turns [Luger et al., 1997a; Richmond, 2003](Fig. 3.1a). Linker histones and other non-histone proteins promote or stabilize the folding of nucleosomal arrays into superstructures of increasing complexity and largely unknown architecture [Hansen, 2002]. Covalent modification of the core histones and variations in the fundamental biochemical composition of nucleosomes distinguish transcriptionally active from inactive chromatin regions, by either changing the structure of the nucleosomes, by altering their ability to interact with other protein factors, or by modifying their propensity to fold into varying degrees of higher order structures (or by any combination of the above). Studying the mechanism for establishing distinct chromatin domains is essential to understanding differential regulation of gene expression and all other DNA-dependent processes. Much progress has been made in this direction in the past few years.

Substitution of one or more of the core histones with the corresponding histone variants has the potential to exert considerable influence on the structure and function of chromatin. Histone variants are distinct non-allelic forms of conventional, major-type histones that form the bulk of nucleosomes during replication and whose synthesis is tightly coupled to S-phase. Histone variants

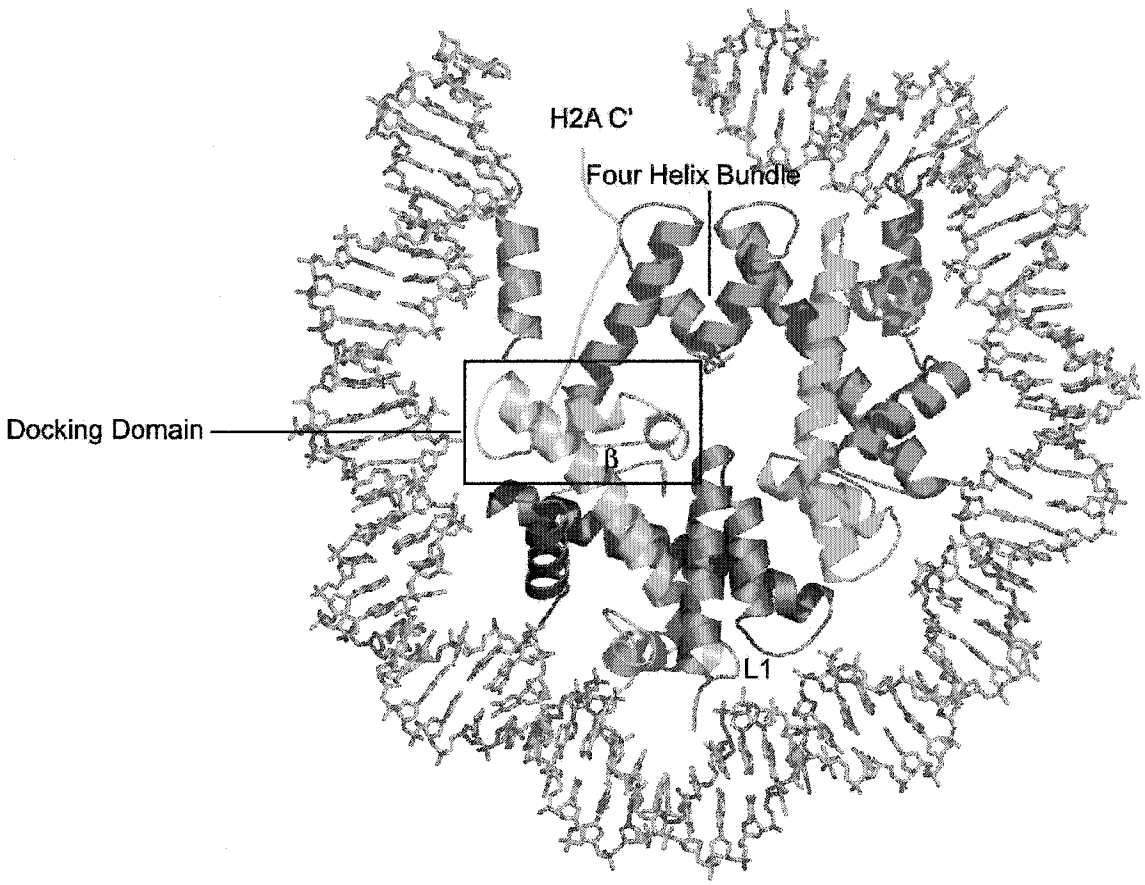

Figure 3.1: Histone H2A variants. a. Overview of nucleosome structure. Only 74 base pairs of DNA and associated proteins are shown. H2A is shown in yellow, H2B in red, H3 in blue, and H4 in green. The axis of non-crystallographic symmetry is indicated by a dashed line. The four-helix bundle structure formed by the two H3 molecules and the H2A docking domain are boxed, other structural features are indicated.

B.

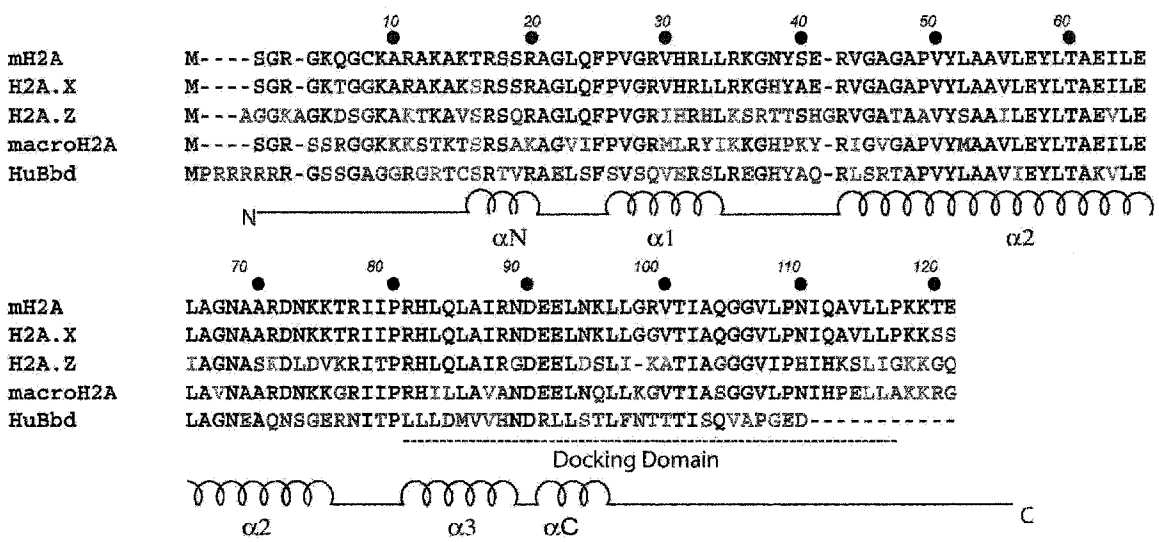

Figure 3.1: Histone H2A variants. b. Sequence alignment of the histone domain of human H2A.X, mouse H2A.Z, mouse macroH2A, and mouse H2A.Bbd with major-type mouse H2A. Bullets indicate every tenth residue in major H2A. Identical residues are indicated in black, similar residues in blue and different residues in red. Also indicated are the secondary structure elements of the histone fold (α1, α2, and α3) and the loops and extensions (L1, L2, αN, and αC).

are characterized by a completely different expression pattern that is not restricted to S-phase. They are found in most eukaryotic organisms, and are expressed in all tissue types (unlike some H2B isoforms that are only found in specialized tissues such as testes). Compared to their major-type counterparts, histone variants exhibit moderate to significant degrees of sequence homology (Fig. 3.1b). H2A.X (82 %) and H3.3 (~96%) are the least divergent of all histone variants. H2A.Z (~ 60 %), macroH2A (~ 65 %), H2A.Bbd (40 %), and CenpA which has a 93 amino acid domain that is 62 % identical to H3 [Palmer et al., 1991; Sullivan et al., 1994] are increasingly divergent in their histone moiety from H2A and H3, respectively. As is the case with histones in general, the structured regions of the histones (encompassing histone folds and extensions) are more conserved than the histone tails. The structured region of H2A.X is 97% conserved to its major-type H2A counterpart, that of macroH2A 70%, H2A.Z 66%, and H2A.Bbd 48%, respectively. MacroH2A is unique in that it contains an additional non-histone like domain that is connected to the histone-homology domain by a flexible linker [Pehrson and Fried, 1992]. All histone variants are highly conserved between different species. In many cases, they are even more conserved than their major-type paralogs [Sullivan et al., 2002], indicating that they all have evolved to fulfill important functions that cannot be accomplished by major-type H2A and H3, as has been demonstrated for H2A.Z [Clarkson et al., 1999; Faast et al., 1999; van Daal and Elgin, 1992].

While the *modus operandi* of most of histone variants remains unknown they are all characterized by unique *in vivo* localization patterns, which in turn

shed light on their putative function. H2A.X is distributed throughout the genome. It is implicated in double stranded DNA repair [Celeste et al., 2003b; Rothkamm and Lobrich, 2003], and is necessary for programming DNA breakage that occurs in developing lymphozytes [Bassing et al., 2003]. The presence of H2A.Z within euchromatin plays a role in preventing silencing from spreading into regions of the chromosome that are normally transcriptionally active [Meneghini et al., 2003]. Interestingly, H2A.Z can co-exist with Sir proteins at the telomere [Krogan et al., 2003]. Most recently, H2A.Z has also been shown to play a role in chromosome segregation [Rangasamy et al., 2004]. MacroH2A is found at the inactive X-chromosome of adult female mammals, which consists predominantly of heterochromatin and is transcriptionally inactive [Costanzi and Pehrson, 1998], while H2A.Bbd co-localizes with hyper-acetylated histone H4, indicating that it might be associated with actively transcribed chromatin [Chadwick and Willard, 2001]. The histone H3 variant H3.3 is thought to be associated with active chromatin, and CENP-A is a major component of centromeric heterochromatin [Ahmad and Henikoff, 2002; Vermaak and Wolffe, 1998].

Here we will summarize and review available structural information on nucleosomes and chromatin containing histone H2A variants, and will attempt to explain how structure relates to their varied function. We note that an exhaustive review of all biological and functional data would clearly exceed the scope of this manuscript. We will present a hypothesis why 'true' histone variants have only been identified for histone H2A and H3, and show data in support of our

hypothesis that particular regions in the H2A amino acid sequence appeared to have been targets during the evolution of H2A histone variants.

3.2 Why are there no H4 and H2B histone variants?

All known true histone variants are replacements for either histone H3 or H2A (reviewed in [Henikoff et al., 2004; Malik and Henikoff, 2003]). From a structural vantage point, we hypothesize that this is the case because only H3 and H2A are engaged in homotypic interactions (Fig. 3.2). In contrast, neither H4 nor H2B interact with the other H4 or H2B molecule within the histone octamer. A four-helix bundle formed by residues from the two H3 chains holds together the $(H3\text{-}H4)_2$ tetramer, which is stable in the absence of DNA under physiological conditions (Fig. 3.2a, b). This interface, which is characterized by a combination of salt bridges, ionic interactions, and some hydrophobic contacts [Luger et al., 1997a] has been proposed many years ago to be conformationally flexible, especially in the absence of the (H2A-H2B) dimers [Chen et al., 1991; Hamiche et al., 1996], but see also [Protacio and Widom, 1996]. In contrast, the interface formed between two H2A molecules is quite small and only exists in the context of a folded nucleosome (Fig. 3.2c, d). It is however the only point of contact between the two (H2A-H2B) dimers in a nucleosome, and thus may be in part responsible for highly cooperative incorporation of the two H2A-H2B dimers, as well as for tethering the two gyres of the DNA superhelix together. Intriguingly, major sequence differences between H3 and the centromeric H3

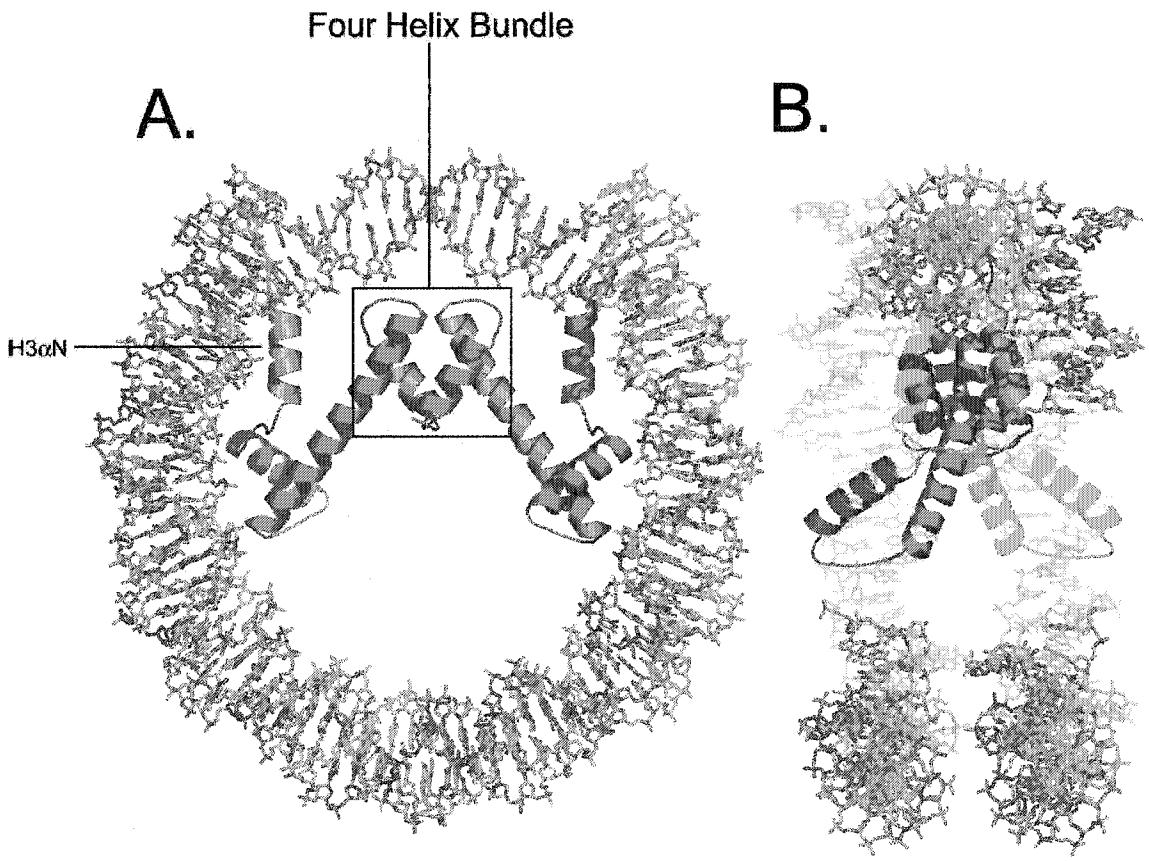

Figure 3.2: H3 and H2A fulfill special roles within the NCP. a. Structure of the NCP viewed down the superhelical axis. Only the two H3 chains are shown. **b.** The same structure is shown after rotation by 90 ° around the y-axis, with parts of the DNA omitted for clarity.

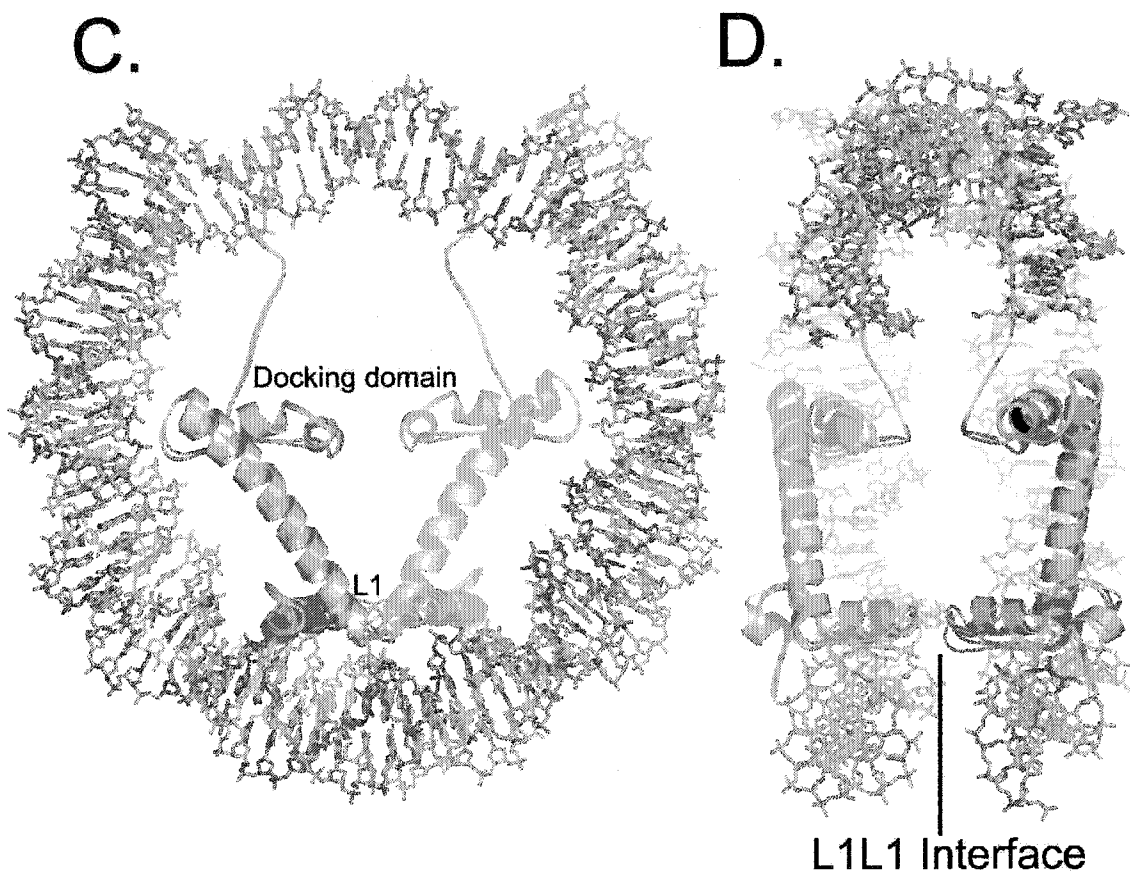

Figure 3.2: H3 and H2A fulfill special roles within the NCP. c. Structure of the NCP viewed down the superhelical axis. Only the two H2A chains are shown. The structures of NCPs containing major-type H2A from *Xenopus laevis* (yellow; pdb entry code 1AOI), H2A.Z (grey; pdb entry code 1F66), and macro-H2A (wheat; S. C., unpublished data) have been superimposed. **d.** the structures displayed in c, shown in the same orientation as b.

variant are found in this four-helix bundle region [Black et al., 2004; Shelby et al., 1997]. Similarly, variability among the many H2A variants themselves, and differences between variants and major-type H2A are found in the L1 loop (Fig. 3.1b). This suggests that sequence variability in these regions of self-interactions may serve to ensure that only nucleosomes with two identical H2A or H3 'flavors' are formed. Equally likely, these interfaces may preclude the formation of such nucleosomes, and may instead favor the incorporation of a major-type histone H3 with variant H3, or major-type H2A with variant H2A, respectively, as will be shown below.

A second common feature of H3 and H2A that is not shared by H4 and H2B is the fact that they both are involved in the organization of more than the requisite ~ 70 base pairs of DNA that are bound by a canonical histone fold dimer [Luger and Richmond, 1998a], due to quite extended regions in both H3 and H2A outside the histone fold. The N-terminal helix of H3 (αN) is positioned to interact with the penultimate turn of the DNA double helix before it exits the confines of the nucleosome (Fig. 3.1a and 3.2a). It is held in position by the H2A docking domain [Bao et al., 2004]. The C-terminal tail of H2A is poised to interact with linker DNA that extends beyond the 147 nucleosomal base pairs (Fig. 3.1a and 3.2c).

Thus, unlike H2B and H4, replacement of H3 and H2A with histone variants has the potential to affect DNA organization (or exit angle) at the penultimate 15 base pairs of nucleosomal DNA, with potential implications for higher order structure. As pointed out above, sequence variations that are

specific to either H3 or H2A variants have the potential to increase the pool of theoretically possible nucleosomes, in being able to choose their interaction partners. Finally, in light of the current models for linker histone binding to the nucleosome [Angelov et al., 2001; Crane Robinson, 1997], histone H1 and its variants and isoforms are more likely to interact with H3 and H2A than with H2B and H4. One intriguing (but as yet untested) model for how histone variants exert their function in chromatin may be by modulating the interaction between the nucleosome and linker histones or non-histone architectural chromatin proteins, such as HP1. For example, it is conceivable that nucleosomes harboring certain H2A or H3 variants may be unable to interact with linker histones or other architectural proteins, or that they may prefer certain H1 isoforms over others, with profound effects on gene regulation and / or chromatin higher order structure.

3.3 Structural characteristics of nucleosomes and chromatin containing histone H2A variants

3.3a H2A.X

Amino acids (1-120) of H2AX are very similar in sequence to major H2A; indeed, with an only two amino acid difference in the structured domain it is safe to assume that the structural properties of a mono-nucleosome are likely to remain unaffected. The two sequence changes in the structured domain of H2A.X are in the L1 loop and in the docking domain, respectively, and are also

found to distinguish macroH2A from major-type H2A (H2A N38 to H, and R99 to G, Fig. 3.1b).

The C-terminal domain of H2A.X is phosphorylated, and it is this phosphorylated form of this variant that is implicated in DNA repair [Celeste et al., 2003b]. One possible mode of H2A.X action could be via recruitment of repair proteins to the site of DNA-damage. It is indeed found that formation of Nbs1, 53bp1, and Brca1 foci at the damage sites is severely impaired in H2A.X -/- cells, as well as suppressing genomic instability [Celeste et al., 2003a].

3.3b H2A.Z

H2A.Z, which is essential in *Drosophila*, mouse and *Tetrahymena* [Faast et al., 1999; Liu et al., 1996; van Daal and Elgin, 1992] is the histone variant whose structure and function is perhaps best studied among all histone variants. While not being essential in budding yeast, H2A.Z (Htz1) functions to prevent the spread of heterochromatin into euchromatin [Meneghini et al., 2003] and plays a role in transcription with a function that is partially redundant with specific chromatin remodeling complexes.

The crystal structure of an NCP in which major H2A is replaced by H2A.Z reveals no major differences in the path of the DNA superhelix or in the nature of protein-DNA interactions [Suto et al., 2000]. While tyrosine quenching revealed no major change in nucleosome stability *in vitro*, a more sensitive fluorescence resonance energy transfer (FRET) approach [Park et al., 2004b] revealed that

the sequence changes of H2A.Z result in subtle stabilization of the (H2A-H2B) dimer interaction with the $(H3\text{-}H4)_2$ tetramer-DNA complex upon increasing ionic strength (Fig. 3.3).

Amino acid changes in the H2A.Z docking domain also contribute to an extended acidic patch, which is a prominent feature of the nucleosome surface [Suto et al., 2003]. The docking domain is the region that is essential for *Drosophila* development [Clarkson et al., 1999]. This region of H2A.Z (and the N-terminal tail) has been shown to interact with the pericentric heterochromatin-binding protein INCENP [Rangasamy et al., 2003], a protein critical for proper chromosome segregation. Thus, it appears that subtle sequence differences between major-type H2A and H2A.Z bear a direct relevance to its ability to interact with non-histone proteins.

Restriction digest analysis of an *in vitro* chromatin model system (H2A or H2A.Z nucleosome arrays assembled on a DNA template that contains 12 repeats of a 208 base-pair nucleosome positioning sequence) in combination with sedimentation velocity studies established that H2A and H2A.Z nucleosomes assemble with comparable affinity [Fan et al., 2002]. Consistent with the increase in nucleosome core stability, H2A.Z arrays are more regularly spaced than H2A arrays. Sedimentation velocity analysis at elevated salt concentrations was used to determine that H2A.Z facilitates intramolecular folding of nucleosome arrays resulting in the formation of a folded state (55S). This folded state is thought to reflect the canonical 30nm fiber. On the other hand H2A.Z is found to hinder the oligomerization mediated by interactions

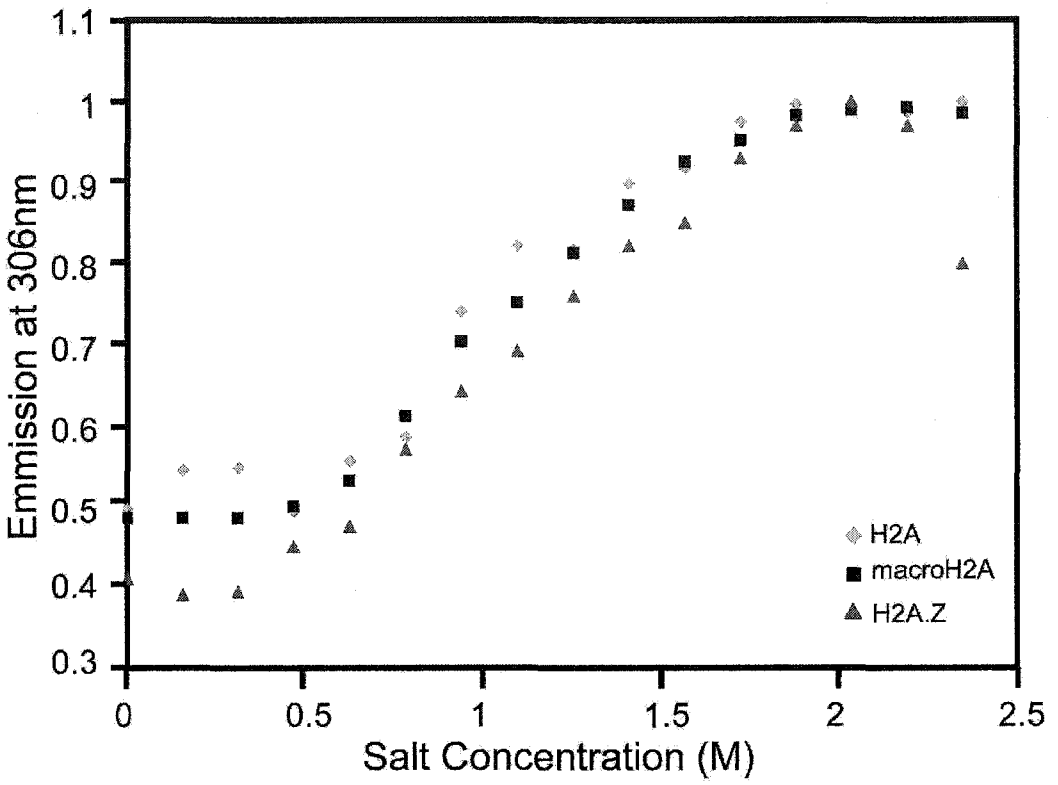

Figure 3.3: The tyrosine fluorescence quenching profile shows no pronounced differences in the overall stability of macro-NCP, H2A.Z-NCP, and major-NCP. Tyrosine quenching profiles in response to increased ionic strength for nucleosomes in which the histone domain of macroH2A, or H2A.Z has replaced major H2A. Values have been normalized using the formula $\mathbf{A_n=A/A_h}$, where A_n is the normalized value, A is the observed signal and A_h is the highest signal observed. Diamonds: major-NCP, squares: macro-NCP; triangles: H2A.Z-NCP.

between nucleosome arrays [Fan et al., 2002]. Therefore, H2A.Z arrays form higher-order chromatin structures that are distinctly different from H2A arrays. Consistent with this, H2A.Z is located at constitutive heterochromatin in mammalian cells and is required for faithful chromosome segregation [Rangasamy et al., 2003; Rangasamy et al., 2004]. Taken together, H2A.Z may have a dual role in modulating the recruitment of non-histone proteins and in chromatin fiber folding. These features would enable H2A.Z to play a role in a number of different processes that include gene expression and mitosis.

3.3c MacroH2A

MacroH2A is perhaps the most unusual of all histone variants due to its large size (~370 amino acids and a molecular weight of 42 kDa) and tripartite structural organization. The N-terminal third (amino acid 1-122) is ~64 % identical to major H2A [Pehrson and Fried, 1992]. This region is followed by a highly basic stretch (amino acid 132-160), which is homologous to the C-terminus of linker histone H1 (57 % identical to sea urchin H1γ over 30 residues; [Pehrson and Fried, 1992]. Amino acids 161-370 form a tightly folded domain whose high-resolution structure we have determined recently (G.S.Y.K. Swamy and S. C, unpublished data). The structure of an NCP in which H2A has been replaced by the histone domain of macro-H2A shows that the significant differences in sequence are accommodated with surprisingly minor structural changes (S. C. et al., unpublished data, Fig. 3.2c, d). The most pronounced structural divergence is found in the L1 region of macroH2A. Changes in the

electrophoretic behavior of mono-nucleosomes containing the H2A-like domain of macroH2A, and in the stability of the histone octamer at decreased ionic strength and in the absence of the stabilizing influence of the DNA were observed. A mutant of major-type H2A in which four amino acid in the L1 loop of major-type H2A (38 - NYAE – 41) were replaced with the corresponding amino acids from macroH2A (38 – HPKY – 41) was shown to confer all *in vitro* characteristics of macro-H2A containing octamer and NCP onto major-type H2A (S.C. et al., unpublished data).

Despite the pronounced effect on histone octamer stability, preliminary data show that the overall stability of the nucleosome in response to increased ionic strength is not affected (Fig. 3.3). However, given our results with H2A.Z-containing nucleosomes [Park et al., 2004b], it is possible and even likely that more subtle changes exist. It should be pointed out that since the first and foremost task of histone variants is to form nucleosomes, subtle changes are expected at most, but clearly these differences are fundamental to the function of histone variants.

MacroH2A- containing chromatin has been shown to be inhibitory to transcription *in vivo* [Perche et al., 2000]. Furthermore, macroH2A containing mono-nucleosomes are not remodeled by SWI/SNF, and are unable to bind transcription factors [Angelov et al., 2003]. More precisely, the non-histone domain or the flexible linker (or both) were responsible for the inability of these variant nucleosomes to bind the transcription factor NF-kappaB. In contrast, the histone-like domain of macroH2A was shown to be responsible for the inability of

macro-H2A-containing nucleosomes to be remodeled [Angelov et al., 2003]. It will be of interest to see whether the L1 loop alone can confer this inhibition of chromatin remodeling and transcription to nucleosomes. The key location of the L1 loop within the NCP structure (where it seemingly holds together the two gyres of the DNA double helix) certainly makes this region a prime candidate to affect the dynamic motions of the NCP that are associated with chromatin remodeling.

MacroH2A displays a very unique nuclear localization pattern. While it is expressed in equal quantities in both males and females [Rasmussen et al., 1999] in almost all the higher eukaryotes, it is enriched in the inactive X-chromosome (Xi) of adult female mammals manifested as a Macro Chromatin Body (MCB) [Costanzi and Pehrson, 1998; Hoyer-Fender et al., 2000]. Various GFP-tagged constructs have been used to determine the importance of the histone and the non-histone domain in the localization of macroH2A to the inactive X-chromosome [Chadwick et al., 2001]. The histone domain alone (without N- and C-terminal tails) fused to GFP was found to form the Xi associated MCB with efficiencies comparable to full-length macroH2A. Of the 19 amino acids that are different in macroH2A compared to major H2A no single amino acid could be attributed this function by point mutation studies. On the basis of preliminary analysis of the crystal structure of macroH2A mono-nucleosomes and biochemical studies of L1 mutants of major H2A it seemed likely that the L1 loop is crucial for the localization on the Xi. This hypothesis has been tested experimentally (S. C. et al., unpublished data).

MacroH2A is gradually emerging as a "family" of variants. At least two different genes are known to encode this protein with significant variations in sequence but the same basic structural organization (H2A1 and macroH2A2, respectively). MacroH2A1 has two splice-variants (macroH2A1.1 and macroH2A1.2), which are non-identical in a very small region of the non-histone region starting at amino acid 195 [Pehrson et al., 1997]. MacroH2A2 is overall 68% identical to macroH2A1.2. The histone region is 84% identical to that of macroH2A1 and only 66% identical to major H2A. The sequence of the macroH2A2 L1-loop (TFKY) seems to be a convolution between that of major H2A (NYAE), and macroH2A (HPKY). The basic region is the most varied and is only 25% identical to that of macroH2A1, whereas the non-histone region is 64% identical to that of macroH2A1.2. MacroH2A1.2 and macroH2A2 display very similar (and sometimes overlapping) nuclear localization patterns, at least at a global level, and the functional relevance of the sequence differences remains unclear [Chadwick et al., 2001; Costanzi and Pehrson, 2001].

3.3d H2A.Bbd

The structured region of H2A.Bbd is only 48% identical to that of major H2A, making H2A.Bbd the most divergent histone H2A variant known to date. So far, this histone variant has only been identified in humans and mice. Major hallmarks of the amino acid sequence of H2A.Bbd as compared to that of major H2A are (1) the presence of a continuous stretch of five arginines and the conspicuous absence of lysines in its N terminal tail, (2) the absence of a C

terminal tail and the very last segment of the docking domain; (3) major sequence differences in the docking domain of H2A; (4) the presence of only one lysine in H2A.Bbd compared to fourteen in major H2A, resulting in a slightly less basic protein (pI 10.7, compared to a pI of 11.2 for major H2A); and (5) the absence of the 'acidic patch' [Luger and Richmond, 1998b] on the docking domain (Fig. 3.1b).

We found that mono-nucleosomes containing H2A.Bbd had a more relaxed structure with less tightly bound DNA ends [Bao et al., 2004]. Only 118±2 bp of DNA are protected against digestion with micrococcal nuclease, in contrast to 146 bp in canonical nucleosomes. These results are consistent with the observed more rapid exchange of GFP-H2A.Bbd *in vivo* [Gautier et al., 2004]. Intriguingly, we also found a lower repeat length in micrococcal nuclease digestion of nucleosomes reconstituted onto plasmids using a recombinant *in vitro* assembly system [Georges et al., 2002] (136 bp as opposed to ~160 bp for major nucleosome arrays), which suggests that the H2A.Bbd nucleosomes are deposited at a higher density. At this high density, H2A.Bbd represses transcription comparable to H2A. Intriguingly, domain swap experiments (in which the H2A docking domain was exchanged with that of Bbd) show that the H2A.Bbd docking domain is largely responsible for its behavior. The conservation of the histone-fold together with the nuclear localization pattern suggests that H2A-Bbd alters chromatin structure at the nucleosomal level, giving rise to transcriptionally active domains [Chadwick and Willard, 2001].

3.4 Evolutionary targets in the histone fold of H2A variants

Sequence comparisons (Fig. 3.1b) together with analysis of the two available crystal structures of nucleosomes containing histone variants [Suto et al., 2000]; S. C., unpublished data) and analysis of biochemical and biophysical data from ours and several other laboratories show that histone variants are true replacement histones in that they can form functional nucleosomes and chromatin. The majority of structural and functional changes in histone H2A variants reside in the docking domain and in the L1 loops, with the latter being more structurally divergent than the former.

3.4a The multi-functional H2A docking domain

The docking domain is involved in interactions between the H2A-H2B dimer and the $(H3\text{-}H4)_2$ tetramer, and harbors three of the seven residues that form the 'acidic patch' on the surface of the nucleosome [Luger and Richmond, 1998b]. Thus, sequence divergence in this region may affect the stability of the H2A variant-H2B dimer / $(H3\text{-}H4)_2$ tetramer interface, as has been observed for H2A.Z [Park et al., 2004b], which will have effects on chromatin remodeling and transcription. The inefficient organization of the penultimate ~ 15 – 20 base pairs of nucleosomal DNA can also be a consequence of relatively minor sequence changes in this domain, as described for H2A.Bbd [Bao et al., 2004]. Changes in amino acid sequence may also alter the surface of the nucleosome, with important implications for the ability of nucleosomes to interact with other factors or to form more compact higher order structures. It is interesting to note that

while the acidic patch is decreased in H2A.Bbd (not shown), its size is actually increased in H2A.Z [Suto et al., 2000], and expanded towards the C-terminal end of the docking domain in macroH2A (Fig.3.4).

3.4b The H2A L1 loop may select for the second H2A-H2B dimer

The L1 loops of the two H2A moieties within the nucleosome are involved in the formation of the L1L1-interface, which is the only site of interaction between the two H2A-H2B dimers in the nucleosome. The L1L1-interface is responsible for the cooperative incorporation of the two H2A-H2B dimers. It may also stabilize the two gyres of the nucleosome core particle (Fig. 3.2d). Altering the biochemical nature of this interface should therefore result in an altered response to the transcriptional machinery and to chromatin remodeling factors, as well as determine the histone composition of the nucleosome.

There is no experimental evidence for the tacit assumption that one nucleosome contains, for example, two H2A.Z-H2B dimers. It is theoretically possible to have a nucleosome in which only one of the H2A moieties has been replaced by its corresponding variant, resulting in a nucleosome with one $(H3\text{-}H4)_2$ tetramer, one major H2A-H2B dimer and one variant H2A-H2B dimer. From a nucleosomal viewpoint, the primary determinant of the composition of a given nucleosome must be the compatibility of the L1-loop of major H2A with those of different H2A variants. To investigate this possibility *in vitro,* we performed salt-gradient reconstitutions with mixtures of $(H3\text{-}H4)_2$ tetramer, (H2A-H2B) dimers, and H2A.Z-H2B dimers (Fig. 3.5); or with H2A.Bbd-H2B dimers (Fig. 3.6). We

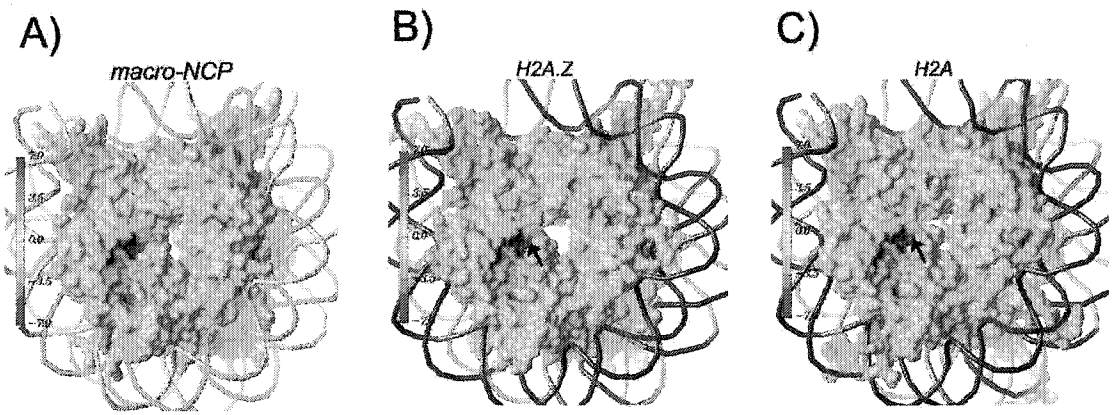

Figure 3.4: Subtle changes in the molecular surface of macro-NCP compared to H2A.Z-NCP and major-NCP. a. macro-NCP; **b**, H2A.Z-NCP; **c**, major-NCP. The electrostatic potential ranges from +7.0 (blue) to -7.0 (red) kcal/mol/e (color bar), shown is the value at the solvent-accessible surface (out 1.4 Å, the radius of a water molecule, from the molecular surface) mapped back on to the molecular surface. Molecular surfaces were calculated with the program MSMS [Sanner et al., 1996] using a 1.4 Å probe sphere. The acidic patch that provides an essential crystal contact with the N-terminal tail of histone H4 of a neighboring nucleosome core particle is indicated by a black arrow. Panels b and c are taken from [Suto et al., 2000], with permission.

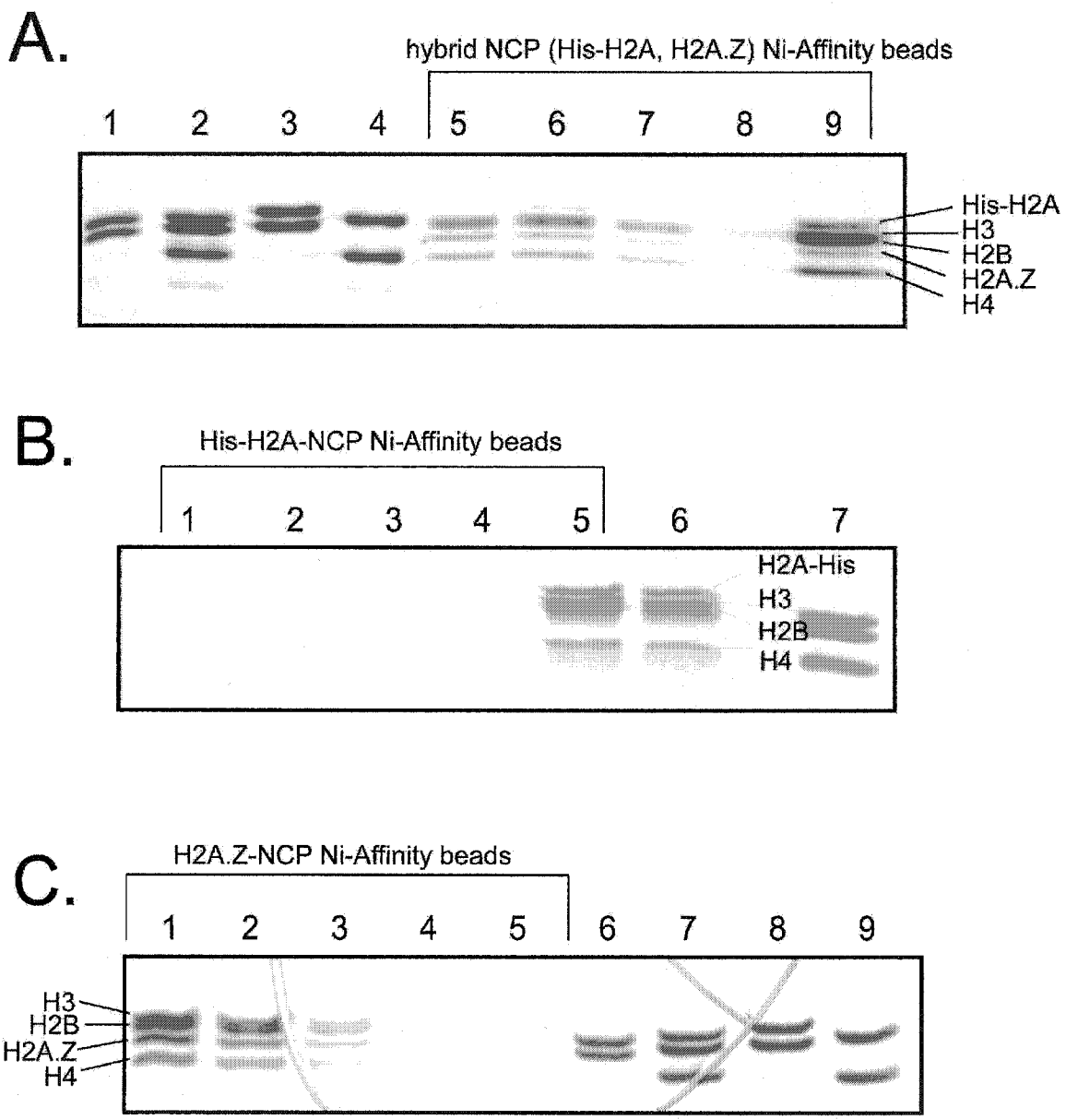

Figure 3.5: H2A.Z can form hybrid nucleosomes with major-type H2A. a. Lane 1: H2A.Z-H2B dimer. Lane 2: Histone octamer with untagged H2A. Lane 3: His-tagged H2A-H2B dimer. Lane 4: H3-H4 tetramer. Lane 5-8: flow-through and washes with 5 mM imidazole of NCP reconstituted from a mixture of H2A.Z, His-tagged H2A, H2B, H3, and H4 after a two-hour incubation with Ni-NTA beads. Lane 9: Elution with 1 M imidazole. **b.** Control with his-tagged H2A NCP. Lanes 1-4: flow through and washes with 5 mM imidazole after a two-hour incubation of His-tagged H2A NCP to Ni-NTA beads. Lane 5: Elution with 1 M imidazole. Lane 6: Onput. Lane 7: Histone octamer with untagged H2A. **c.** Control with untagged H2A.Z nucleosomes. Lanes 1-4: Flow through and washes with 5 mM imidazole after 2 hrs binding of H2A.Z NCPs to Ni-NTA beads. Lane 5: Elution with 1 M imidazole. Lane 6: H2A.Z-H2B dimer. Lane 7: Histone octamer with non His-tagged H2A. Lane 8: His-tagged H2A-H2B dimer (His-tagged H2A – upper band, H2B lower band). Lane 9: H3-H4 tetramer. All gels shown here are 18% SDS-PAGE gels stained with coomassie brilliant blue.

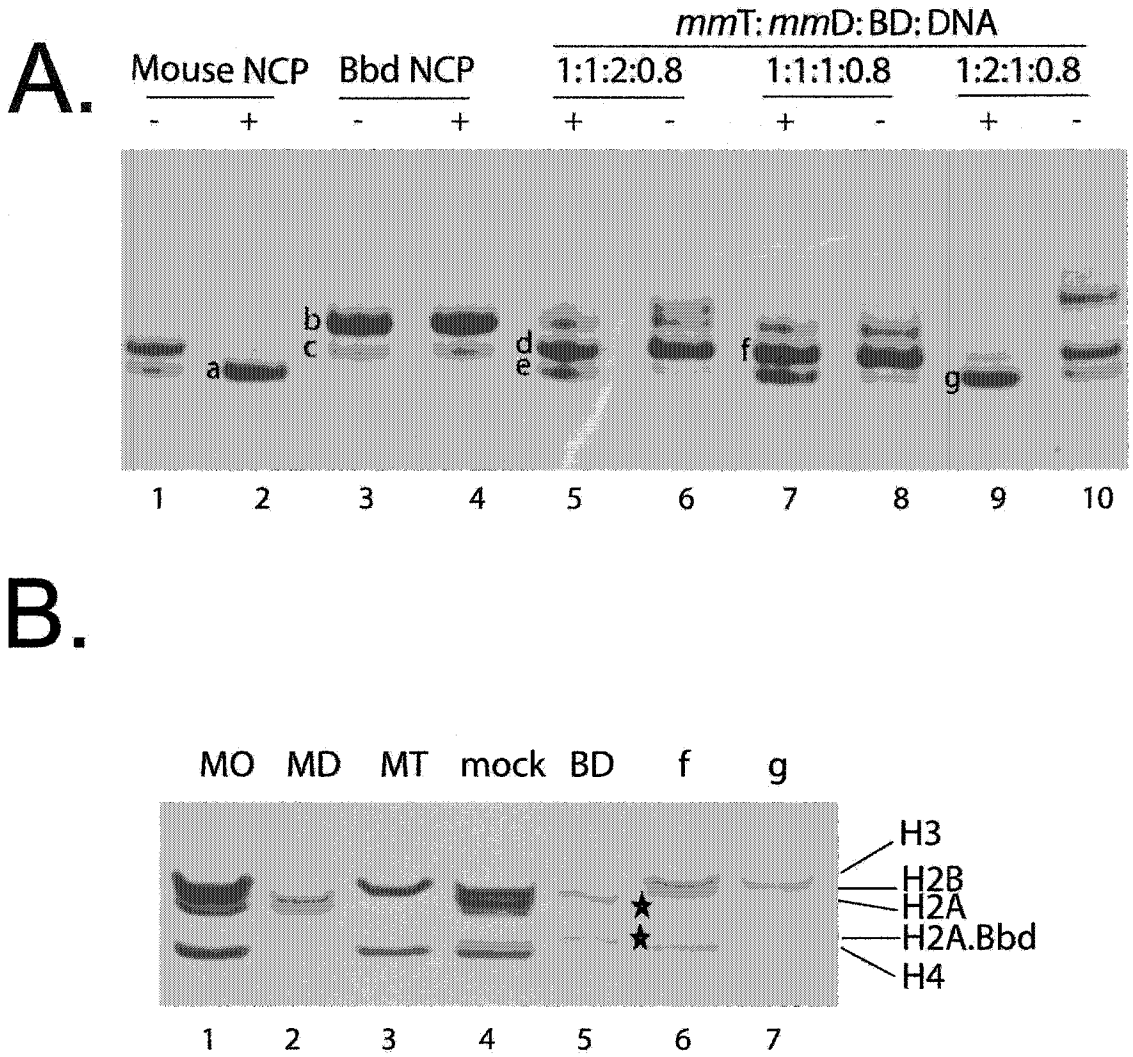

Figure 3.6: H2A.Bbd can form hybrid nucleosomes with major-type H2A. a. Salt gradient reconstituted mouse NCP (*mm*-NCP; lanes 1 and 2), Bbd-NCP (lanes 3 and 4) and hybrid NCPs (lanes 5-10), before (-) and after (+) a 1 hour incubation at 37°C, were analyzed by 5 % native gel and stained by coomassie brilliant blue. Ratios between mouse (H3-H4)2 tetramer (*mm*T), mouse (H2A-H2B) dimer (*mm*D), H2A.Bbd-H2B dimer (BD), and DNA for 'hybrid NCP' reconstitution are indicated. Bands that were subsequently excised from the gel for further analysis are labeled from a-g. **b.** Bands f, g (Fig. 3.6a) were analyzed by 18% SDS-PAGE, stained with coomassie brilliant blue. Mouse H2A and H2A.Bbd are indicated by stars. Mouse octamer (MO, lane 1), MD (lane 2), *mm*T (lane 3), *mm*T:*mm*D:BD mixtures of 1:1:1 (mock, lane 4) and BD (lane 5) are shown as controls.

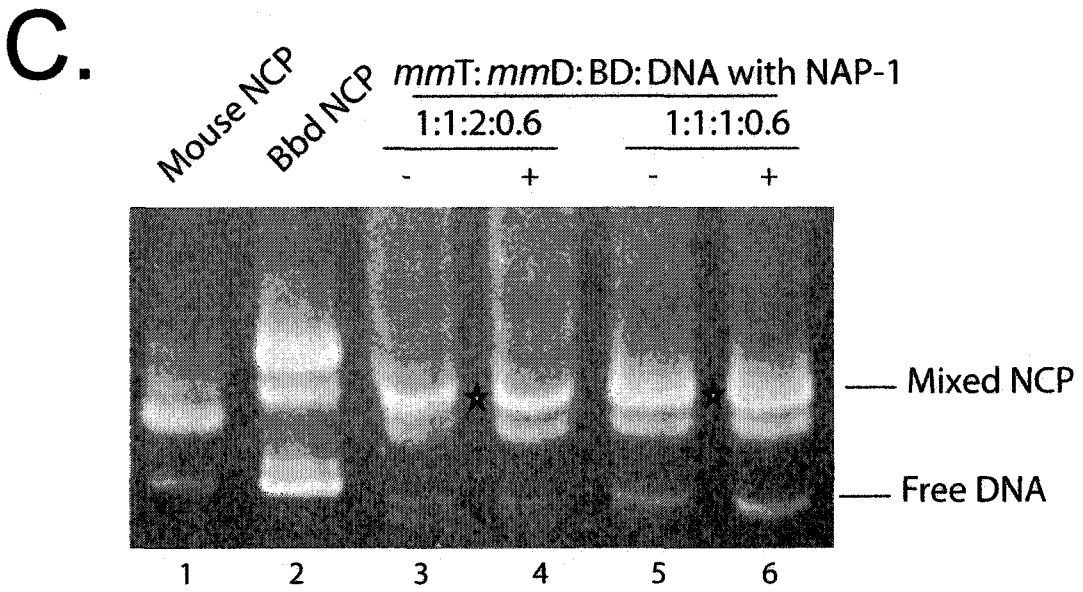

Figure 3.6: H2A.Bbd can form hybrid nucleosomes with major-type H2A. c. Hybrid NCPs are also obtained with yNAP-1 – dependent nucleosome assemblies. yNAP-1 – reconstituted NCP (reconstituted at indicated ratios) were compared with NCP reconstituted over a salt gradient on a 5% native gel. The gel was stained with ethidium bromide. Hybrid NCP is indicated by asterisks.

used either nickel-affinity chromatography to isolate nucleosomes containing his-tagged H2A (Fig. 3.5), or gel elution of 'mixed nucleosome bands' (Fig. 3.6), followed by analysis of the histone content by SDS PAGE. Using these two approaches, we could show that while all histone H2A variants are capable of forming hybrid nucleosomes (Fig. 3.5 and 3.6), the propensity to do so clearly differs between macroH2A, H2A.Z, and H2A.Bbd.

Intriguingly, hybrid nucleosomes reconstituted from a mixture of H2A-H2B dimers and H2A.Bbd-H2B dimers together with $(H3\text{-}H4)_2$ tetramer protect only ~130 bp of DNA against digestion with micrococcal nuclease, that is ~ 20 base pairs more than nucleosomes containing two H2A.Bbd chains, and ~ 15 base pairs less than canonical nucleosome (not shown). The ability of H2A.Bbd to form hybrid nucleosomes is independent of the assembly pathway, since the same end result is obtained by yNAP-1 – dependent assembly under physiological ionic strength (Fig. 3.6C).

Our results clearly indicate the possibility that variants may be combined with major-type histone H2A in a single nucleosome, thus generating yet another level of structural and functional heterogeneity. The specific nature of the different L1L1-interfaces and their potential influence on the accessibility of nucleosomal DNA will become more obvious in light of future structural studies. How would such nucleosomes be assembled *in vivo*? Histone H2A-H2B dimers are in rapid exchange even in the absence of transcription and replication [Kimura and Cook, 2001; Louters and Chalkley, 1985]. Recently discovered histone-variant specific assembly factors for H2A.Z [Kobor et al., 2004; Krogan et

al., 2003; Mizuguchi et al., 2004] promote the replacement of one or both H2A-H2B dimer with a H2A.Z – H2B dimer. ATP-dependent chromatin remodeling factors are also capable of actively exchanging histone variant dimers into folded nucleosomes [Bruno et al., 2003]. Since it is unlikely that both dimers are exchanged at the same time, the final 'equilibrium' makeup of a particular nucleosome will be determined by the L1 loop, and by the relative availability of major-type and variant histones.

3.5 Conclusions and Outlook

Histone variants are receiving an ever increasing amount of attention, but much needs to be done before we reach a complete understanding of their role in the complex biology of chromatin. *In vitro,* structural and biophysical analysis of nucleosomes containing H2A.Bbd and CenpA (in addition to the already available structures for H2A.Z and macroH2A containing nucleosomes) will provide further insight into the ways in which nucleosome structure and dynamics is affected by histone variants. These studies will also have to be expanded to take into the account the possible existence of hybrid nucleosomes. Second, we will need to extend our investigations to include model nucleosomal arrays, as demonstrated for H2A.Z [Fan et al., 2002]. Third, the interaction of variant-containing chromatin to interact with various linker histones and non-histone proteins needs to be investigated. Fourth, more systematic analyses are needed to study the dynamic behavior of variant-containing nucleosomes and chromatin in the presence of various chromatin remodeling factors (see, for example,

[Bruno et al., 2004]). Finally, the transcriptional properties of variant-containing nucleosomes from several model promoters will have to be scrutinized carefully *in vitro*.

In vivo, the challenges are perhaps even greater. For example, knock-out models are available for only few histone variants. Second, we need to investigate the distribution of histone variants at the single-nucleosome (and sub-nucleosome) level at a variety of chromatin loci. This represents a technical challenge that may not be easily overcome. Third, the pathways by which variant nucleosomes (or hybrid nucleosomes) are assembled needs to be further investigated. Finally, the ability of histone variants to be post-translationally modified must be scrutinized. Combined, these studies are likely to yield a picture of mind-boggling complexity that probably will approach or even exceed that of the histone modification network. Doubtlessly, histone variants add an entirely new dimension to the 'histone code'.

CHAPTER 4

Nucleosomes Containing H2A.Bbd are More Dynamic Than Conventional Nucleosomes

In the biochemical and biophysical studies outlined in chapter 2, we found that Bbd-NCP possesses a relaxed structure and that the interaction between H2A.Bbd dimer and $(H3H4)_2$ tetramer is weak. These results suggest that the Bbd-NCP has a low inherent stability. To test this hypothesis, we set out to compare the relative stability of Bbd-NCP and conventional NCP. The data shown in this chapter will be written up for submission to *the Journal of Biological Chemistry* as referenced below.

Yunhe Bao and Karolin Luger. Nucleosomes Containing H2A.Bbd are More Dynamic Than Conventional Nucleosomes

4.1 Abstract

The incorporation of H2A.Bbd into nucleosomes has been suggested to lead to a relaxed structure and a low inherent stability, and to facilitate the transcription process. In this study, it was found that H2A.Bbd dimers were spontaneously removed from nucleosomes containing H2A.Bbd (Bbd-NCP) reconstituted *in vitro*. Furthermore, both conventional and variant histone dimers were found to be more easily exchanged into Bbd-NCPs than into canonical NCPs. It was also shown that Bbd-NCP was formed spontaneously at 20°C and 37°C without the driving force of salt gradient or histone chaperone protein. These results suggest that H2A.Bbd-H2B dimers are highly dynamic and move in and out of NCPs spontaneously. In vivo, the H2A.Bbd-H2B dimer depletion would increase accessibility of the nucleosomal DNA to transcription factors and facilitate the transcription process, and would provide an opportunity for other histone dimers to be exchanged into nucleosomes.

4.2 Introduction

Eukaryotic genome DNA is organized in a protein-DNA complex structure called chromatin. The basic subunit of chromatin is the nucleosome core particle (NCP), which is composed of 147 bp of DNA wrapped in 1.65 turns around a histone octamer containing two copies of each of the four histone proteins (H2A, H2B, H3 and H4). The $(H3\text{-}H4)_2$ tetramer organizes the central ~70 base pairs of nucleosomal DNA, and the (H2A-H2B) dimer organizes ~40 base pairs towards either end of the DNA [Luger et al., 1997a]. Chromatin helps the cell to compact

and store the nuclear DNA, and also creates an impediment to the processes of DNA transcription, replication, repair and recombination. Surprisingly, chromatin is highly dynamic despite the high degree of DNA compaction. To access the DNA within the chromatin context, the cell has developed dedicated chromatin remodeling mechanisms, which serve to alter the chromatin structure locally to facilitate or repress DNA access. These mechanisms include: histone covalent modifications; alteration of chromatin conformation through the action of ATP-dependent chromatin remodeling factors; and, histone replacement by histone variants. In many cases, all of these processes may act in concert [Flaus and Owen-Hughes, 2004].

It has been found that histone components of chromatin, especially histone H2A-H2B dimers, are exchanged rapidly in transcriptionally active chromatin [Jackson, 1990; Kimura and Cook, 2001]. Depletion of H2A and H2B has also been found in transcriptionally active chromatin [Baer and Rhodes, 1983]. It has been reported that FACT (facilitates chromatin transcription) complex destabilizes nucleosomal structure so that one histone H2A-H2B dimer is removed during transcription elongation [Belotserkovskaya et al., 2003]. *In vitro* studies have revealed that RNA polymerase II alone is also able to displace H2A-H2B dimers during transcription elongation [Kireeva et al., 2002]. The histone chaperone nucleosome assembly protein 1 (NAP-1) from yeast was found to reversibly remove and replace histone H2A-H2B dimers or histone variant dimers from assembled nucleosomes *in vitro* [Park et al., 2004a]. All these data suggest

that the exchange and/or depletion of histone H2A-H2B dimers play an important role in transcription regulation.

Histone variants are distinct nonallelic forms of major-type core histones and are incorporated in replication-independent assembly pathways. It has been suggested that the substitution of core histones with the corresponding histone variants can generate an architecturally and functionally distinct local or global chromatin structure [Henikoff et al., 2004; Malik and Henikoff, 2003; Chakravarthy et al., 2004, Chapter 3]. H2A.Bbd is a histone H2A variant, which is largely excluded from the inactive X chromosome. It is only 48% identical to 'major H2A', making H2A.Bbd the most divergent histone H2A variant to date. It was found that nucleosomes containing H2A.Bbd (Bbd-NCP) have a more relaxed structure in which only 118+/-2 bp of DNA were protected against digestion with micrococcal nuclease [Bao et al., 2004]. Results of an *in vivo* FREP study suggested that H2A.Bbd was more rapidly exchanged than conventional H2A [Gautier et al., 2004]. The transcription efficiency from the H2A.Bbd templates was found to be slightly higher than that of the conventional H2A templates [Angelov et al., 2004; Bao et al., 2004]. All these studies suggest that the incorporation of H2A.Bbd into nucleosome leads to a more open structure and a lower inherent stability of the Bbd-NCP. This lower stability might be induced by a weaker interaction between the H2A.Bbd–H2B dimer and the H3–H4 tetramer. The more open and less stable nucleosome variant facilitates the transcription process.

The stability of Bbd-NCP was investigated in this research. It was found that H2A.Bbd dimers were easily depleted during *in vitro* reconstitution. Bbd-NCP was shown to form spontaneously *in vitro* in a matter of minutes, even at 20°C. Further, it was shown that both conventional and variant histone dimers were more readily exchanged into Bbd-NCPs than into canonical NCPs. These results suggest that H2A.Bbd-H2B dimers are highly dynamic and move in and out of NCPs, spontaneously.

4.3 Materials and Methods

4.3a Purification of proteins and DNA

122 bp DNA was designed and prepared as described previously [Dyer et al., 2004]. 146 bp α-sat DNA was prepared in a similar manner. Human H2A.Bbd and mouse histones were over-expressed in bacteria and purified using previously published protocols [Bao et al., 2004; Dyer et al., 2004]. GST-NAP1 was expressed in BL21 (DE3) cells and purified as described previously [McBryant et al., 2003].

4.3b Salt gradient reconstitution of NCP

Mouse core histones were refolded into histone octamers and purified by gel filtration [Dyer et al., 2004]. Mouse octamer and purified α-satellite 146 bp DNA were reconstituted into NCPs by salt gradient deposition [Dyer et al., 2004] to yield mouse-NCPs. $(H3\text{-}H4)_2$ tetramer, (H2A.Bbd-H2B) dimer and α-satellite 146 bp DNA or 122 bp DNA were mixed in a 1:2:1 molar ratio (or the ratio

marked in figures), and reconstituted using salt gradient deposition to yield Bbd-NCPs. Samples were analyzed on a 5% polyacrylamide gel (acrylamide : bis-acrylamide 60:1) in 0.2 x TBE, run at a constant 150 V at 4°C, and bands were visualized with ethidium bromide staining. Bbd-NCPs were subjected to heat shifting (37°C and 55°C for 1hour).

4.3c 2D gel analysis of lower band of Bbd-NCP

Nucleosomal bands on 5% polyacrylamide gel were excised, electro-eluted into 0.05 x TBE buffer, concentrated by Vivaspin 10K MWCO PES concentrator, and analyzed by 18% SDS polycacrylamide gel. Proteins were visualized by applying coomassie blue stain.

4.3d Bbd-NCP reconstitution in 100 mM KCl TE buffer

Labeled H2A.Bbd-H2B dimer and $(H3\text{-}H4)_2$ tetramer were dialyzed against the buffer A, containing 100 mM KCl, 20 mM Tris-HCl (pH 7.5), 1 mM EDTA, and 1 mM DTT at 4 °C. Subsequently, the dimers, tetramers and 146 bp DNA were mixed at 2:1:0.8 (or 0.5) molar ratio in the buffer A to produce final concentrations of DNA of 0.56 μg/μl (for 2:1:0.8) or 0.35 μg/μl (for 2:1:0.5). The mixtures were incubated at 4° and 20°C for 90 min (or 45 min), and at 37°C for indicated times. Samples were analyzed on a 5% polyacrylamide gel in 0.2 x TBE, run at a constant 150 V at 4°C, and bands were visualized on a transilluminator and then with ethidium bromide staining.

4.3e Histone labeling with fluorescent dye

H2B T112C and H4 E63C were unfolded in 6 M guanidinium HCl (20 mM Tris/HCl, pH 7.5, 0.4 mM TCEP), and Alexa Fluor 488 or Alexa Fluor were added at a 2:1 (dye:protein) molar ratio. The mixtures were incubated at room temperature overnight. Labeled histones were then separated from unreacted dyes by a Sephadex G-25 spin column.

4.3f Dimer exchange within NCPs with and without GST-yNAP1

The electroeluted purified Bbd-NCP (or mouse-NCP), Alexa Fluor 488 labeled H2A.Bbd-H2B dimer (or H2A-H2B dimer), and GST-yeast NAP1 were mixed at a 1:4:8 molar ratio in buffer A and incubated at 4°C overnight. The samples were analyzed by 5% native PAGE. The gels were visualized on a transilluminator and then with ethidium bromide staining.

4.4 Results

4.4a Depletion of Bbd dimers occurred spontaneously in Bbd-NCP

H2A.Bbd–H2B dimers, $(H3–H4)_2$ tetramers and α-satellite146 bp DNA were mixed in a 2:1:1 ratio and reconstituted by the salt gradient method [Dyer et al., 2004]. The salt gradient reconstitution results in a heterogeneous population of NCPs related to the position of the DNA on the histone octamer. A simple heating step (37–55°C for 20– 180 min) is usually sufficient to convert this mixture to a uniquely positioned species. The salt reconstituted Bbd-NCPs

behaved differently upon analysis by native PAGE (Fig. 4.1A, lanes 2, 3 and 4). Two bands were formed in Bbd-NCP and migrated at a slower rate than Xenopus-NCP (Fig. 4.1A, lane 1, [Bao et al., 2004]). Their position and their relative distribution didn't change upon heat treatment at both 37°C and 55°C for 1 hour (Fig. 4.1A, compare lanes 2, 3 and 4).

To facilitate the identification of the histone content of the upper band and the lower band, florescent dye labeled H2B (Alexa Fluor 488-H2B) and H4 (Alexa Fluor 546-H4) were used in the Bbd-NCP reconstitution. It was shown that H2B and H4 were present in both bands based on visual examination of the dye (data not shown). The upper band and the lower band were separated by preparative gel electrophoresis. The upper band was determined to be Bbd-NCP [Bao et al., 2004]. In this study, the lower band was investigated further. The fractions for the upper band and the lower band of Bbd-NCP were analyzed by 18% SDS–PAGE (Fig. 4.1B). The lower band appeared to contain all four histone proteins (Fig. 4.1B, lane 4). Furthermore, the depletion of H2A.Bbd and H2B was evident in the lower band (compare lanes 1 and 4 of Fig. 4.1B). The bands were too closely spaced to be quantified.

To verify that the lower band is a complex with a depletion of H2A.Bbd-H2B dimer, a series of H2A.Bbd–H2B dimer titrations was performed during salt gradient reconstitution (Fig. 4.1C). When the molar ratio for tetramer, H2A.Bbd-H2B dimer and DNA (MT:BD:DNA) was 1:1:0.9, the quantity of the lower band was significant (Fig. 4.1C lanes 1 and 2). However, the intensity of the lower

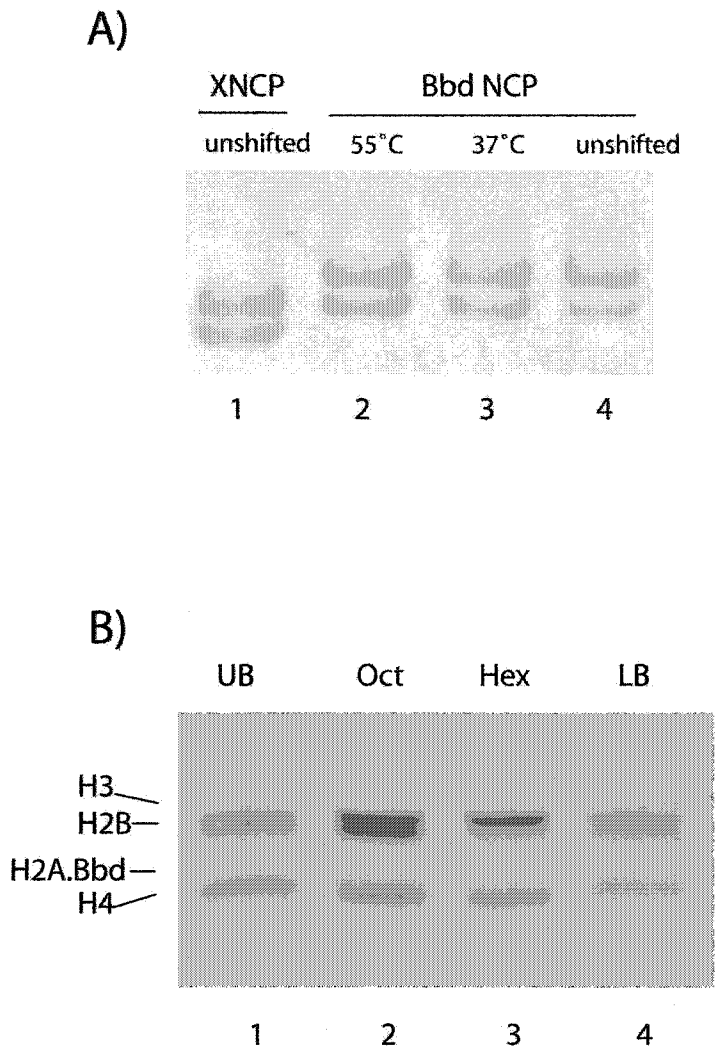

Figure 4.1: H2A.Bbd-H2B dimers deplete from Bbd-NCP spontaneously. A) Salt gradient reconstituted *Xenopus* NCP (XNCP), Bbd-NCP before (unshifted) and after a 1 h incubation at 37°C or 55°C, were analyzed by 5% native PAGE and stained with Coomassie blue. **B)** Analysis of the histone content of the two Bbd-NCP nucleosomal bands. The upper band (UB; lane 1) and lower band (LB; lane 4) of Bbd-NCP were excised from the native gel and analyzed by 18% SDS–PAGE. H2A.Bbd–H2B dimer, $(H3–H4)_2$ tetramer mixtures of 2:1 (Oct, lane 2) and1:1 (Hex, lane 3) were used as controls.

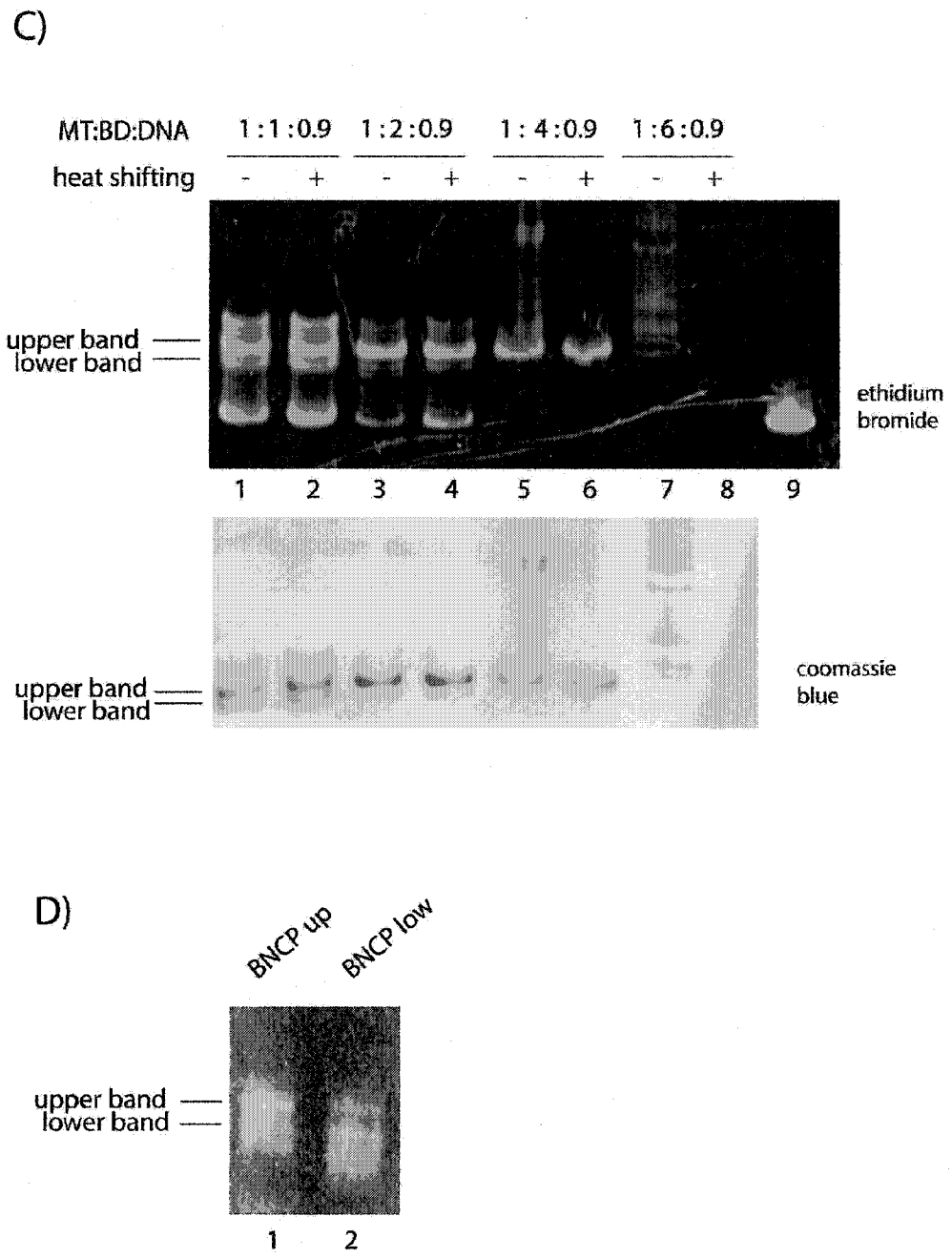

Figure 4.1: H2A.Bbd-H2B dimers deplete from Bbd-NCP spontaneously. C) Mouse $(H3–H4)_2$ tetramer: Bbd dimer: DNA (MT:BD:DNA) molar ratios were varied during the salt gradient reconstitution of Bbd-NCP. The molar ratios for MT:BD:DNA are labeled on the top of the figure. The reconstituted Bbd-NCP NCP before (-) and after (+) a 1 h incubation at 37°C, were analyzed by 5% native PAGE and stained with ethidium bromide (upper panel) and then with Coomassie blue (lower panel). **D)** The upper band and lower band of Bbd-NCP were purified from 5% native gel (see materials and methods) and analyzed by 5% native PAGE and stained with ethidium bromide.

band was diminished when more H2A.Bbd-H2B dimer was added to the reaction (compare lanes 1-6 of Fig. 4.1C). This result suggested that the extra H2A.Bbd-H2B dimers reacted with the complexes represented by the lower band to form Bbd-NCP, the upper band complex. Note that the intensity of the upper band was increased when MT:BD:DNA was 1:2:0.9 (compare lanes 1-4 of Fig. 4.1C). This is more evidence that the lower band involved a complex with H2A.Bbd-H2B dimer depleted. Too much extra H2A.Bbd-H2B dimer in the reconstitution reaction interacted with DNA and form aggregates (Fig.4.1C lanes 5-8). This complex in the lower band cannot be a tetrasome (one tetramer and DNA) since H2A.Bbd and H2B were present in the lower band (Fig. 4.1B). It could be a hexasome (one tetramer, one dimer and DNA) or a mixture of hexasome and tetrasome, which cannot be ruled out because tetramer alone and DNA can form a complex that migrates similar as that of the lower band on 5% native gel (see lanes 1 and 8 in Fig. 4.2C).

It was shown by gel filtration chromatography that the interaction between the H2A.Bbd–H2B dimer and the (H3–H4)2 tetramer is weak [Bao et al., 2004]. It has been suggested that the H2A.Bbd–H2B dimer exhibited a weaker interaction with the H3–H4 tetramer within the nucleosome than that of the conventional dimer, leading to a more efficient spontaneous transfer of the H2A.Bbd–H2B dimers [Angelov et al., 2004]. The lower band was always present with the upper band, and no redistribution occured upon heat treatment, even at 55°C (Fig. 4.1A). All these data suggest that the H2A.Bbd–H2B dimer is easily depleted. To investigate whether the H2A.Bbd–H2B dimer can be depleted spontaneously, the

upper band and lower band were purified by electroelution and analyzed again by 5% native gel. A lower band appeared in the purified upper band sample (Fig. 4.1D, lane 1). More interestingly, an upper band was also present in the purified lower band sample (Fig. 4.1D lane 2). Similar experiment has been done with MacroH2A-NCP and no re-distribution between the two bands was found (personal communication with Srinivas Chakravarthy). These results suggest that the H2A.Bbd–H2B dimer is readily depleted from Bbd-NCP, and also readily assembled into hexasome and/or tetrasome to form Bbd-NCP.

4.4b Bbd-NCP formed spontaneously *in vitro*

To study whether Bbd-NCP can be reconstituted spontaneously *in vitro*, Alexa Fluor 488 labeled H2A.Bbd–H2B dimer (or H2A-H2B dimer), Alexa Fluor 456 labeled (H3–H4)2 tetramer and DNA were mixed at a molar ratio of 2:1:0.8 in 100 mM KCl Tris EDTA buffer (pH 7.5). The mixtures were incubated at 4°C and 20°C for 90 min and incubated at 37°C for a time course (5 – 90 min). There was no detectable Bbd-NCP formed at 4°C (Fig. 4.2A, lane 1). Significant amounts of Bbd-NCP were formed at both 20°C and 37°C (Fig. 4.2A, lane 2-7). However, there was no detectable mouse NCP formed at either 4°C or 20°C (Fig. 4.2B, lane 1 and 2), and a very little at 37°C (Fig. 4.2B, lane 3-7). Additionally, it should be noted that only Bbd-NCP and a faint lower band were visible when the gel was viewed on a transilluminator without staining (upper panel of Fig. 4.2A). However, significant amounts of non-NCP complexes were formed in the mixture of H2A-H2B dimer, $(H3–H4)_2$ tetramer and DNA (upper panel of Fig. 4.2B).

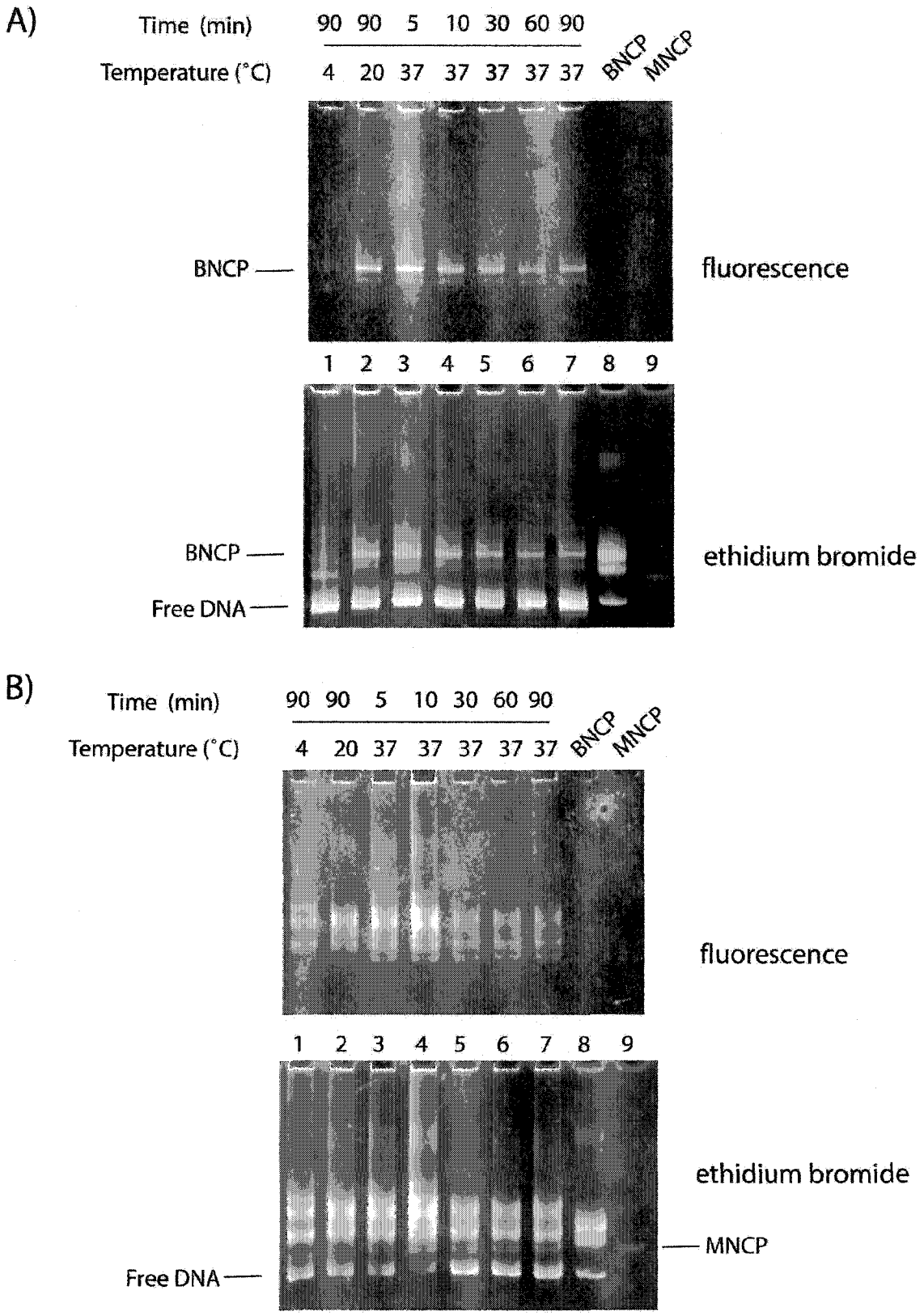

C)

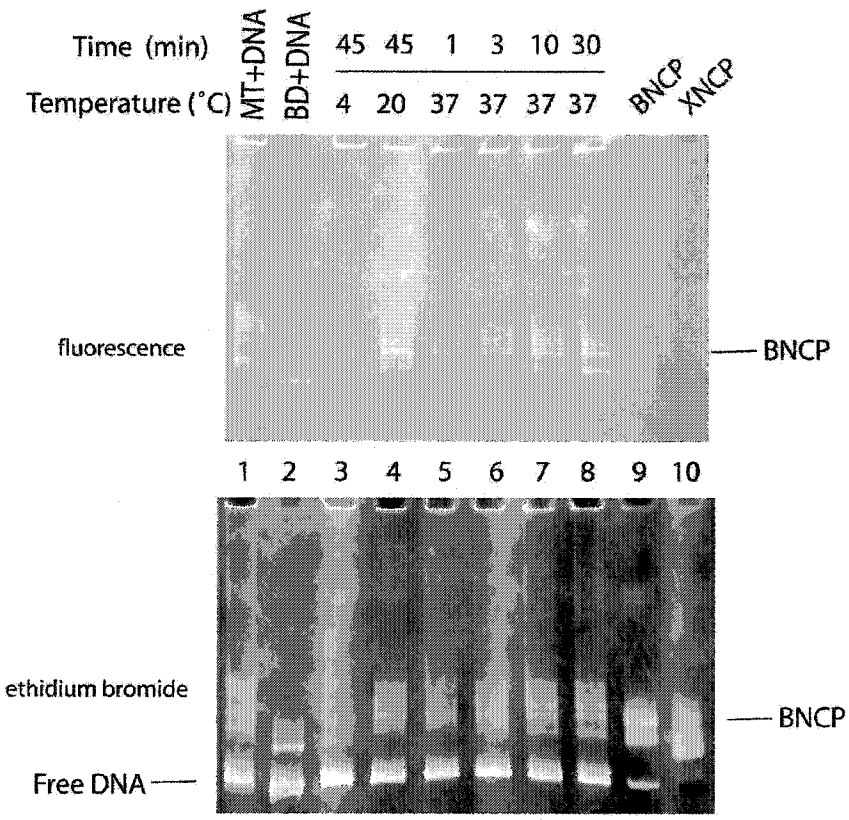

D)

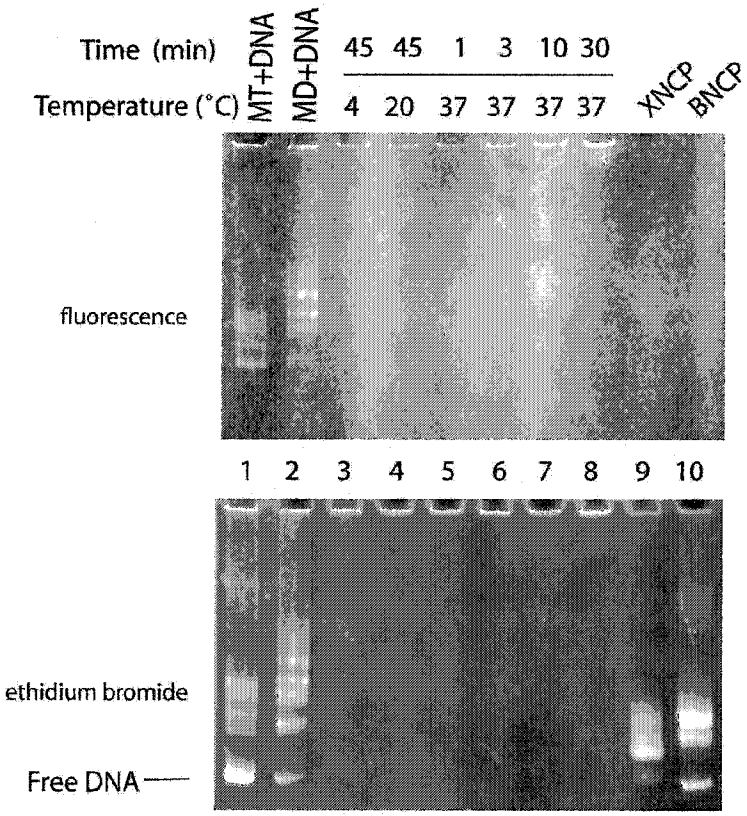

Figure 4.2: Bbd-NCP formed spontaneously at 37°C and 20°C. A) Alexa Fluor 546 labeled Mouse $(H3–H4)_2$ tetramer, Alexa Fluor 488 labeled H2A.Bbd-H2B dimer, and 146 bp DNA were mixed together at a 1:2:0.8 molar ratio in 100 mM KCl TE buffer. **B)** Alexa Fluor 546 labeled Mouse $(H3–H4)_2$ tetramer, Alexa Fluor 488 labeled H2A-H2B dimer, and 146 bp DNA were mixed together at a 1:2:0.8 molar ratio in 100 mM KCl TE buffer. The mixtures were incubated at 4°C (lane 1) and 20°C (lane 2) for 90 minutes and at 37°C for a time course (same amounts of samples were taken out at 5, 10, 30, 60, 90 min, lane 3-7). Bbd-NCP (BNCP, lane 8) and Mouse NCP (MNCP, lane 9) were used as controls. **C)** Alexa Fluor 546 labeled Mouse $(H3–H4)_2$ tetramer, Alexa Fluor 488 labeled H2A.Bbd-H2B dimer, and 146 bp DNA were mixed together at a 1:2:0.5 molar ratio in 100 mM KCl TE buffer. **D)** Alexa Fluor 546 labeled Mouse $(H3–H4)_2$ tetramer, Alexa Fluor 488 labeled H2A-H2B dimer, and 146 bp DNA were mixed together at a 1:2:0.5 molar ratio in 100 mM KCl TE buffer. The mixtures were incubated at 4°C (lane 3) and 20°C (lane 4) for 45 minutes and at 37°C for a time course (same amounts of samples were separately incubated for 1, 3, 10, and 30 min, lane 5-8). Labeled Mouse $(H3–H4)_2$ tetramer and 146 bp DNA at 1:0.5 molar ratio (MT+DNA), Labeled H2A.Bbd-H2B dimer and 146 bp DNA at 2:0.5 molar ratio (BD+DNA), Labeled H2A-H2B dimer and 146 bp DNA at 2:0.5 molar ratio (MD+DNA), Bbd-NCP (BNCP) and *Xenopus* NCP (XNCP) were used as controls. The samples were analyzed by 5% native PAGE and viewed on transilluminator (upper panel) and then stained with ethidium bromide (lower panel).

These non-NCP complexes could be formed by a strong interaction between the canonical dimers and tetrasomes located at different DNA positions. These results suggest that H2A.Bbd-H2B dimers readily move in and out of the complexes continually, and the complex with lowest free energy (central positioned Bbd-NCP) is preferred over others. That is the Bbd-NCP can be formed spontaneously *in vitro*. The efficiency of spontaneous assembly was lower than salt gradient reconstitution since there was much more free DNA (compare lane 7 and 8 in the lower panel of Fig. 4.1A). For the time course study, identical amounts of sample were removed at different times and put into ice to stop the reaction. Precipitate formed during incubation changed the concentration of Bbd-NCP and led to an inaccurate result, for example, there was more Bbd-NCP formed at 5 min than at 90 min (compare lanes 3 and 7 of Fig. 4.2A).

To perform a more accurate time course study, identical amounts of the mixture were separated into several tubes and then subjected to heating. The tubes were removed from water bath at different times. This approach showed that the quantity of Bbd-NCP increased with increased incubation time (Fig. 4.2C lanes 5-8). Note that tetramer and DNA formed a complex, which migrated in a manner similar to that of the lower band (Fig. 4.2C upper panel, lane 1 and 8). The molar ratio used here was 2:1:0.5 for dimer:tetramer:DNA. Everything aggregated at this ratio for the mixture of canonical dimer, tetramer and DNA (Fig. 4.2D).

4.4c Histone dimers exchange more readily into Bbd-NCP than into conventional NCP

In vivo, the depletion of H2A.Bbd-H2B dimers could provide an opportunity for canonical histone dimers and/or other variant histone dimers to be assembled into nucleosome. To investigate this hypothesis, the exchange of fluorescent dye labeled dimers into Bbd-NCP was studied. It has been shown that Yeast NAP1 (nucleosome assembly protein 1) possess a capability to exchange histone dimers within assembled nucleosomes [Park et al., 2004a]. The purified Bbd-NCP (or mouse NCP), Alexa Fluor 488 labeled H2A.Bbd-H2B dimer (or H2A-H2B dimer), and GST-yeast NAP1 were mixed at a 1:4:8 molar ratio and incubated at 4°C overnight. The samples were analyzed by 5% native PAGE. The fluorescence would appear in the nucleosome complex if the labeled histone dimer was exchanged into the nucleosome. Significant amounts of labeled H2A.Bbd dimer (BD*) and mouse dimer (MD*) were incorporated into Bbd-NCP (Fig. 4.3A lane 1 and 3). There was free DNA in Bbd-NCP exchanged with BD*, but no free DNA in Bbd-NCP exchanged with MD* (Fig. 4.3A lower panel, lane 1 and 3). These results are consistent with the spontaneous assembly experiment (Fig. 4.2), indicating that H2A-H2B dimers readily move in and out of complexes. Note that once the labeled mouse dimer was incorported into Bbd-NCP, the complex occupied a position between Bbd-NCP and mouse NCP (compare lanes 2,3, and 4 in the lower panel of Fig. 4.3A). This result is consistent with the previous studies of the hybrid nucleosome containing an H2A.Bbd-H2B dimer and a mouse dimer (Chapter 3 Fig. 3.6). However, very small amounts of

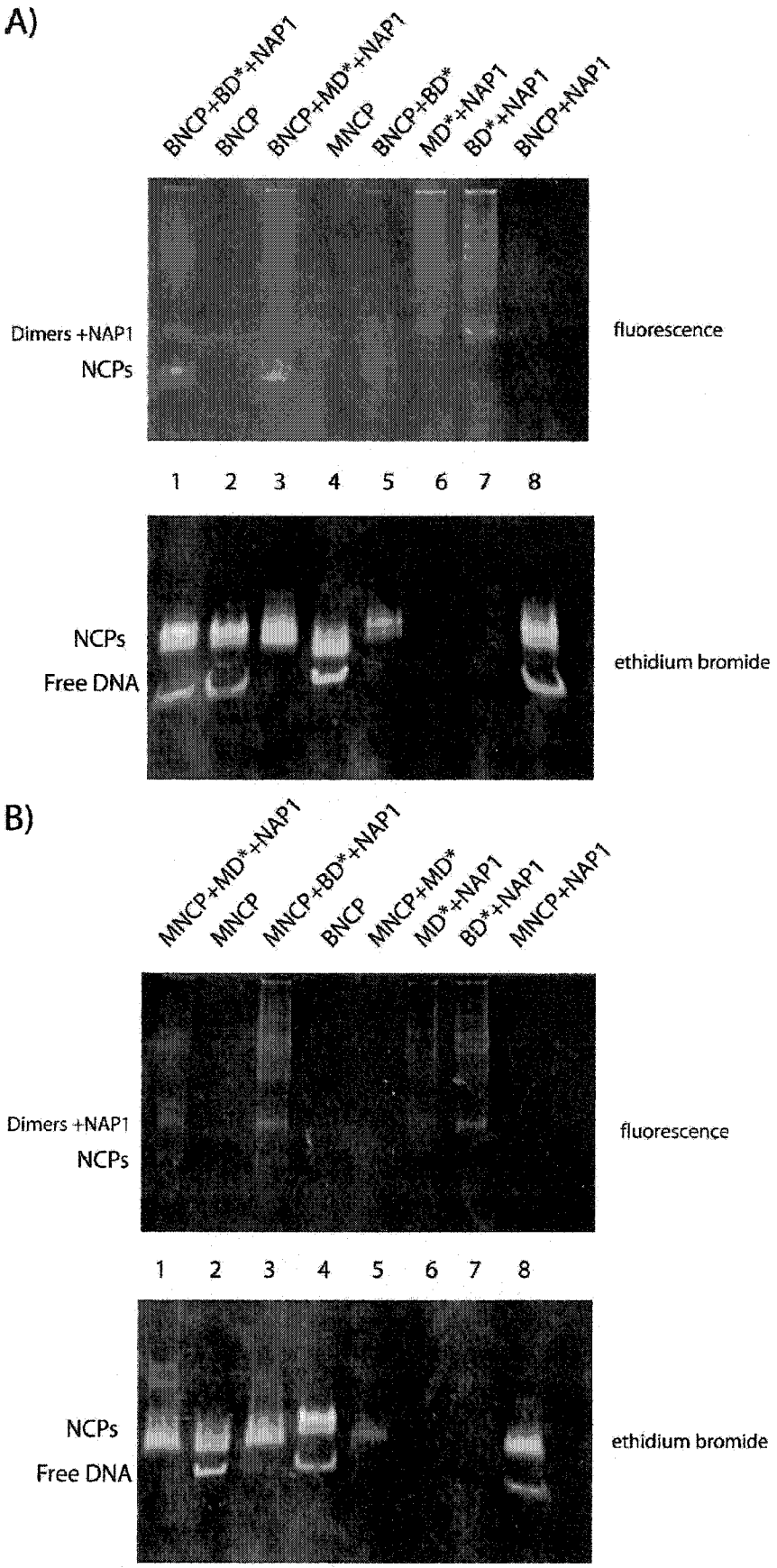

Figure 4.3: Histone dimers are easier to be exchanged into Bbd-NCP than into mouse NCP. A) Bbd-NCP, Alexa Fluor 488 labeled Bbd dimer and GST-NAP1 (BNCP+BD*+NAP1, lane 1); Bbd-NCP, Alexa Fluor 488 labeled Mouse dimer and GST-NAP1 (BNCP+MD*+NAP1, lane 3) were mixed at a 1: 4: 8 molar ratio in 100 mM KCl TE buffer and incubated at 4˚C overnight (see materials and methods). Bbd-NCP and Alexa Fluor 488 labeled Bbd dimer (BNCP+BD*, lane 5) were mixed at a 1: 4 molar ratio. The other controls (labeled on the top of the figure, lane 2, 4, 6, 7, 8) in the same buffer were incubated for the same time and analyzed by 5% native PAGE. **B)** Mouse NCP, Alexa Fluor 488 labeled mouse dimer and GST-NAP1 (MNCP+MD*+NAP1, lane 1); Mouse NCP, Alexa Fluor 488 labeled Bbd dimer and GST-NAP1 (MNCP+BD*+NAP1, lane 3) were mixed at a 1: 4: 8 molar ratio and incubated at 4˚C overnight. Mouse NCP and Alexa Fluor 488 labeled mouse dimer (MNCP+MD*, lane 5) were mixed at a 1: 4 molar ratio. The other controls (labeled on the top of the figure, lane 2, 4, 6, 7, 8) in the same buffer were incubated for the same time and analyzed by 5% native PAGE. Gels were first viewed on a transilluminator without staining (upper panel), followed by staining with ethidium bromide (lower panel).

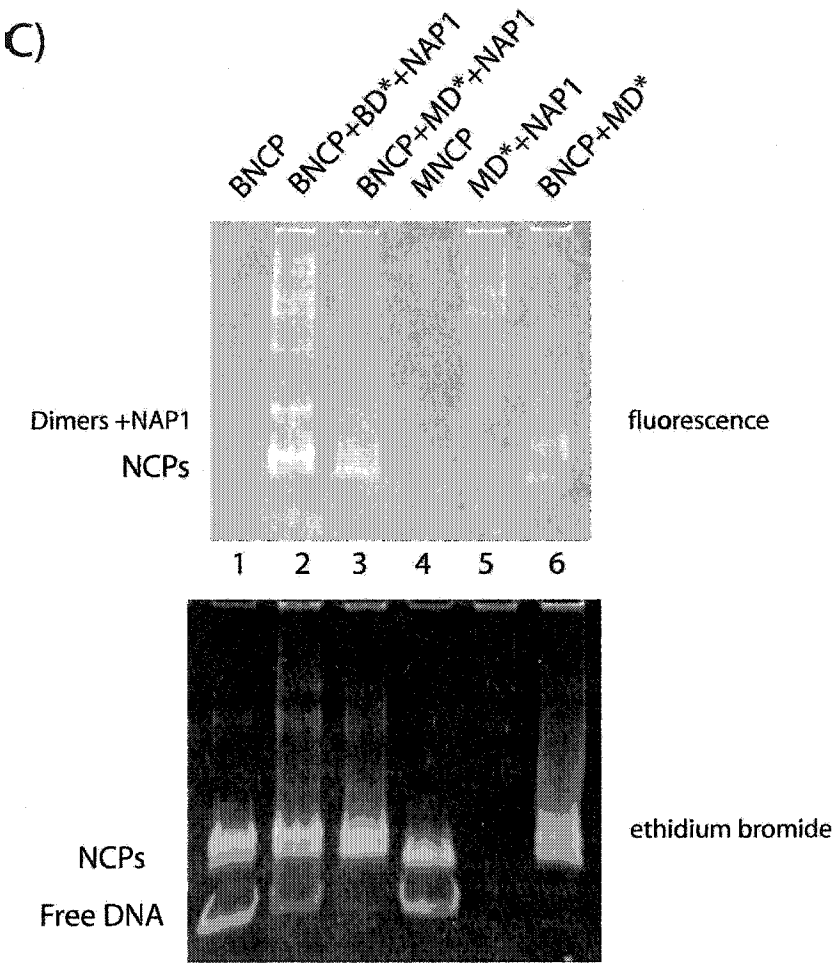

Figure 4.3: Histone dimers are easier to be exchanged into Bbd-NCP than into mouse NCP. C) Bbd-NCP, Alexa Fluor 488 labeled Bbd dimer and GST-NAP1 (BNCP+BD*+NAP1, lane 2); Bbd-NCP, Alexa Fluor 488 labeled Mouse dimer and GST-NAP1 (BNCP+MD*+NAP1, lane 3) were mixed at a 1: 4: 8 molar ratio in 100 mM KCl TE buffer and incubated at 4°C overnight. Bbd-NCP and Alexa Fluor 488 labeled Bbd dimer (BNCP+MD*, lane 6) were mixed at a 1: 4 molar ratio. The other controls (labeled on the top of the figure, lane 1, 4, 5) in the same buffer were incubated for the same time and analyzed by 5% native PAGE.

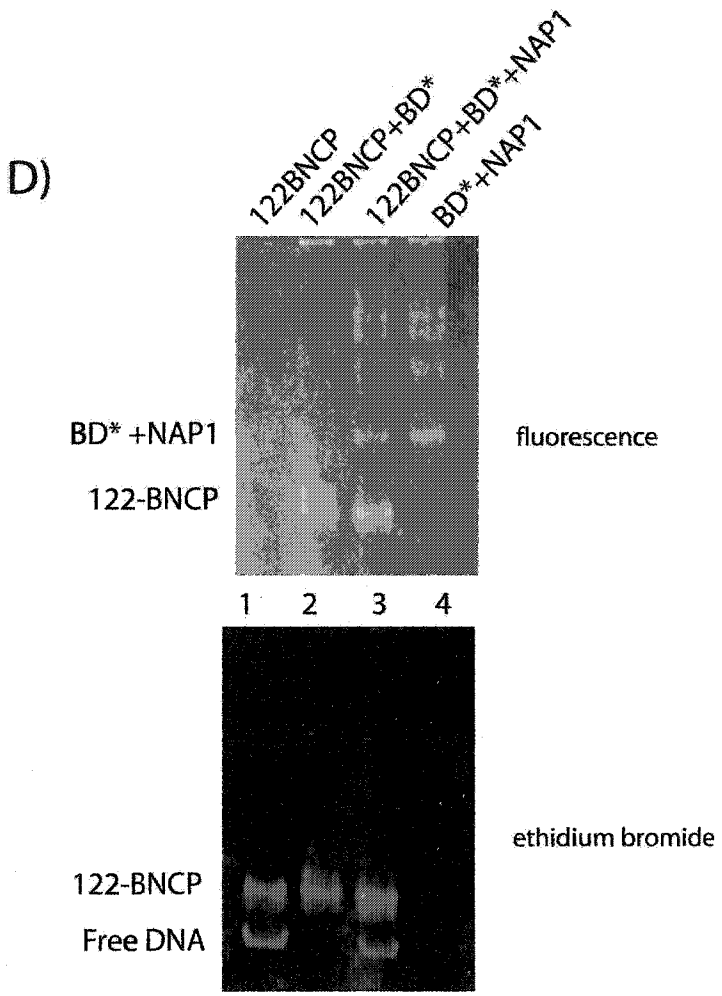

Figure 4.3: Histone dimers are easier to be exchanged into Bbd-NCP than into mouse NCP. D) 122 bp Bbd-NCP and Alexa Fluor 488 labeled Bbd dimer (122BNCP+BD*, lane 2) were mixed at a 1: 4 molar ratio; 122 bp Bbd-NCP, Alexa Fluor 488 labeled Bbd dimer and GST-NAP1 (122BNCP+BD*+NAP1, lane 3) were mixed at a 1: 4: 8 molar ratio. The samples and other controls (lane 1 and 4) in 100 mM KCl TE buffer were incubated at 4°C overnight and analyzed by 5% native PAGE. Gels were first viewed on a transilluminator without staining (upper panel), followed by staining with ethidium bromide (lower panel).

labeled dimers were exchanged into mouse NCP (Fig. 4.3B lane 1 and 3). More interestingly, in the absence of NAP1, both BD* and MD* were incorporated into the Bbd-NCP (Fig. 4.3A lane5, 4.3C lane 6). However, MD* wasn't exchanged into mouse NCP in the absence of NAP1 (Fig. 4.3B lane 5). Similarly, no BD* was incorporated into mouse NCP in the absence of NAP1 (data not shown). It has been shown that Bbd-NCP organizes about 118 bp DNA [Bao et al., 2004]. To rule out the possibility that the unbound nucleosomal DNA ends provide areas for nonspecific binding for labeled dimers, 122 bp α-satellite DNA was used to reconstitute 122 bp Bbd-NCP. This was then employed in the dimer exchange experiment. BD* was incorporated into 122 bp Bbd-NCP both in the presence and absence of NAP1 (Fig. 4.3D, lanes 2 and 3). These data indicate that the depletion of H2A.Bbd-H2B dimers provides an opportunity for labeled canonical and variant histone dimers to be assembled into Bbd-NCP. These data again suggest that the Bbd-NCP is more dynamic than canonical NCP.

4.5 Discussion

It has been suggested that the incorporation of H2A.Bbd into nucleosome leads to a more open structure and a lower inherent stability of the Bbd-NCP [Angelov et al., 2004; Bao et al., 2004; Gautier et al., 2004]. The stability of Bbd-NCP was investigated in this study. It was demonstrated by three different methods that the lower band, formed by *in vitro* reconstitution of Bbd-NCP, was a complex depleted in H2A.Bbd-H2B dimer. This complex could be a hexasome or a mixture of hexasome and tetrasome. It was also shown that Bbd-NCP could be

assembled spontaneously at both 20°C and 37°C without the salt gradient or histone chaperone protein driving force. These data suggest that H2A-H2B dimers readily move in and out of the complexes, with the lowest free energy complex (centrally positioned Bbd-NCP) preferred. Finally, histone dimers were found to be much more easily exchanged into Bbd-NCP than into conventional NCP. This result supports the hypothesis that the depletion of H2A.Bbd-H2B dimers from Bbd-NCPs *in vivo* would provide an opportunity for other histone dimers to be exchanged into nucleosomes.

The depletion of H2A.Bbd-H2B dimer from Bbd-NCP could be due to the weak interaction between the H2A.Bbd–H2B dimer and the $(H3–H4)_2$ tetramer, which has been shown by gel filtration chromatography [Bao et al., 2004]. The equilibrium and kinetic studies performed by Angelov and colleagues also suggested that the H2A.Bbd–H2B dimer exhibited a weaker interaction with the $(H3–H4)_2$ tetramer within the nucleosome than that of the conventional dimer [Angelov et al., 2004].

It has been suggested that the depletion of nucleosomes plays an important role in transcription activation and elongation. Recently, it was shown by ChIP assay that the positioned promoter nucleosomes are depleted during gene activation [Boeger et al., 2003; Boeger et al., 2004; Reinke and Horz, 2003]. FACT complex, RNA polymerase II and NAP1 have been found to be involved in histone dimers removal *in vivo* or *in vitro* [Belotserkovskaya et al., 2003; Kireeva et al., 2002; Park et al., 2004a]. The fact that H2A.Bbd-H2B dimer readily move out of Bbd-NCP makes the histone dimer depletion process less dependent on

the protein factors mentioned above. The H2A.Bbd-H2B dimer depletion would increase accessibility of the nucleosomal DNA to transcription factors and facilitate the transcription process. The present investigation sheds light on a cellular mechanism for regulation of transcription. That mechanism involves changing the biochemical makeup of nucleosomes by incorporation of special histone variant, H2A.Bbd, to reduce the inherent stability of nucleosomes and facilitate transcription processes.

In summary, we have shown that the replacement of H2A with H2A.Bbd significantly reduce the inherent stability of nucleosome. The properties of Bbd-NCPs described here have important implications for the in vivo function of this histone variant. Methods developed in this study could also be applied in the stability study of nucleosomes containing other histone variants.

4.6 Acknowledgements

This work was supported by a grant from the NIH (GM61909). We thank Jayanth V. Chodaparambil for help with histone labeling, Dr. Young-Jun Park for help with GST-NAP1 purification and discussion, Pamela N. Dyer for help with DNA purification, and Dr. Uma M. Muthurajan for critical reading of the manuscript.

CHAPTER 5

Studies on crystallization of Bbd-NCP and interactions between linker histone (H1) and Bbd-NCP

In this chapter I present my work done in the attempt to crystallize the Bbd-NCP and to test the hypothesis that the interaction between H1 and Bbd-NCP is changed due to the missing of C terminal tail in H2A.Bbd.

5.1 Introduction

It has been shown through the biochemical and biophysical studies described in Chapter 2 that Bbd-NCP possesses a relaxed structure. Further, *in vitro* biochemical studies in this investigation suggest that Bbd-NCP is highly dynamic (Chapter 4). These results offer insight on a previously unknown mechanism for transcription regulation. The mechanism involves changing the biochemical makeup of nucleosomes by incorporation of special histone variants (such as H2A.Bbd) to alter the inherent stability of nucleosomes. In order to understand the structural alteration and transcription regulation by incorporation of H2A.Bbd, an attempt was made to determine the X-ray crystal structure of Bbd-NCP. Methods have been developed to prepare highly diffracting crystals of NCP from recombinant histone proteins [Dyer et al., 2004; Luger et al., 1997b; Luger et al., 1999]. These methods have been used in the high-resolution structure determination of variant and yeast NCPs [Suto et al., 2000; White et al., 2001]. Most of these methods were directly applied to the 146 bp Bbd NCP investigation. The acidic patch on the surface of the nucleosome provides an important crystal contact with the H4 N terminal tail from a neighboring nucleosome and may be involved in nucleosome-nucleosome interaction [Luger and Richmond, 1998b; Suto et al., 2000]. However, in H2A-Bbd, three of the six conserved H2A residues that form the acidic patch are changed (H2A.1: Glu61 to Lys, Glu91 to Arg, Glu92 to Leu). The H2A.Bbd mutant, Bbd-3E, was constructed by Dr. Tremethick's laboratory. This mutant has 3 amino acids reverted back to acidic residues (glutamates, hence 3E, Fig. 5.1). The 147 bp Bbd-3E-NCP was

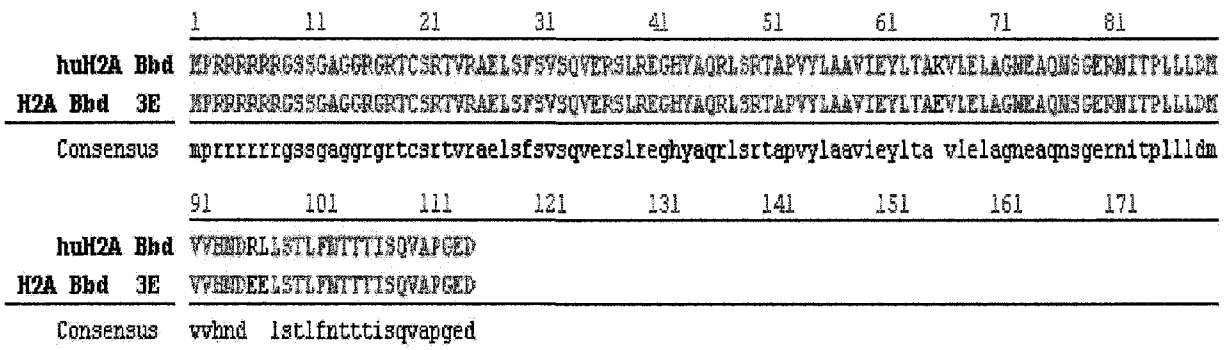

Figure 5.1: Sequence alignment of H2A.Bbd and H2A.Bbd-3E

subjected to a crystallization study in this research. MNase digestion experiments showed that Bbd-NCP binds less DNA than that of major-type NCP. This leaves "floppy ends" of DNA that might make it difficult to crystallize Bbd-NCP. Therefore, 122 bp Bbd-NCP and 122 bp Bbd-3E-NCP were also investigated.

Histone H1 is a representative of linker histones, which have been proposed to perform both architectural functions in chromatin structure, and regulatory functions in gene expression [Wolffe, 1997]. However, it is unclear how the linker histones manage the genome. To date, there are two models that have been developed to describe the interaction between H1 and nucleosomes. In one model, the globular domain of H1 is proposed to sit outside of the DNA coils and bind to DNA where it enters and exits the nucleosome [Staynov and Crane-Robinson, 1988]. In the other model, the globular domain lies asymmetrically inside the turns of nucleosomal DNA and contacts the core histones, especially H2A [Pruss et al., 1996]. Furthermore, studies carried out *in vitro* show that the C-terminal tail of H2A interacts with linker DNA [Lindsey et al., 1991]. However, it is not clear whether the C-terminal of H2A plays a direct role in nucleosome-linker histone interaction, as well as influencing chromatin folding through effects on linker DNA. The fact that H2A-Bbd has no C-terminal tail leads to the hypothesis that interaction between H1 and Bbd-NCP is changed and therefore gene regulation within the 'variant' chromatin is altered. In this study, gel shift assay was employed to investigate the interaction between Bbd-NCP and full length, or globular H1.

5.2 Materials and methods

5.2a Construction and amplification of the 122 bp DNA fragment

To amplify the 61 bp from the 84 mer α-satellite DNA template, which contains half of the 146 palindromic α-satellite DNA sequence, two oligo DNA fragments were designed and the PCR method was applied. Each designed oligo contained sites that would allow the sequence to be cut out and amplified. The insert containing the 61 bp α-satellite DNA was ligated into puc19 plasmid and further amplified to obtain a construct containing sixteen copies of the insert. This was done by using a cloning and duplication strategy reported earlier [Dyer et al., 2004]. The plasmid was purified in large scale. The 61 bp α-satellite DNA was cut out, purified, and ligated to obtain 122 bp palindromic α-satellite DNA according to the methods published previously [Dyer et al., 2004].

5.2b Nucleosome reconstitution

Human H2A.Bbd, H2A.Bbd-3E, and mouse histones were over-expressed in bacteria and purified using previously published protocols [Bao et al., 2004; Dyer et al., 2004]. 146 bp α-sat DNA was prepared as described previously [Dyer et al., 2004]. 196 bp DNA and 166 bp DNA were excised from the plasmid containing 208-12 template using EcorI and MavI respectively [Simpson et al., 1985]. The resulting fragments were purified by preparative gel electrophoresis. Mouse core histones were refolded into histone octamers and purified by gel filtration Dyer, 2004 #1605]. Mouse octamer and purified α-satellite 146 bp DNA were reconstituted into NCPs by salt gradient deposition to yield mouse-NCPs

[Dyer et al., 2004]. $(H3\text{-}H4)_2$ tetramer, H2A.Bbd-H2B dimer (or Bbd-3E-H2B dimer) and α-satellite 146 bp DNA (or other DNA fragments marked in figures) were mixed in a 1.2:3:1 molar ratio (or the ratio marked in figures), and reconstituted using salt gradient deposition to yield Bbd-NCPs. Samples were analyzed on a 5% polyacrylamide gel (acrylamide : bis-acrylamide 60:1) in 0.2 x TBE, run at a constant 150 V at 4°C.

5.2c 2D gel analysis of 123 bp Bbd-NCP and Bbd-3E-NCP

Nucleosomal bands on 5% polyacrylamide gel were excised, electro-eluted into 0.05 x TBE buffer, concentrated by Vivaspin 10K MWCO PES concentrator, and analyzed by 18% SDS polycacrylamide gel. Proteins were visualized by applying coomassie blue stain.

5.2d Histone labeling with fluorescent dye

H2B T112C and H4 E63C were unfolded in 6 M guanidinium HCl (20 mM Tris/HCl, pH 7.5, 0.4 mM TCEP), and Alexa Fluor 488 or Alexa Fluor were added at a 2:1 (dye:protein) molar ratio. The mixtures were incubated at room temperature overnight. Labeled histones were then separated from unreacted dyes by a Sephadex G-25 spin column.

5.2e MNase digestion of 123 bp Bbd-NCP

0.15U MNase (Worthington) was used to digest 10 μg of 123 bp Bbd-NCP at 37°C in 625 μl MNase buffer (0.6mM HEPES (pH 7.6), 52mM KCl, 5% (vol/vol)

glycerol, 1.4% (wt/vol) polyethylene glycol, 5.4mM $CaCl_2$). 122 µl aliquots were removed at 0, 2, 4, 8 and 16 min. The reactions were stopped and deproteinized as described previously [Bao et al., 2004]. DNA fragments were extracted, precipitated and analyzed on 10% polyacrylamide gels (in 0.5XTBE).

5.2f Crystallization trials of Bbd-NCPs

Milligram amounts of NCPs were purified by preparative gel electrophoresis [Dyer et al., 2004], or by the electroelution method described in 5.2c. Crystallization trials utilized the 'hanging drop' technique with vapor diffusion at NCP concentrations ranging from 4-8 mg/ml. A broad salt range (30 - 60mM KCl and 25 – 75 mM $MnCl_2$) was screened for 146 bp Bbd-NCP. 147 bp Bbd-3E-NCP was screened with salt concentration ranges of 20-37.5 mM KCl and 20-45 mM $MnCl_2$. The Natrix nucleic acid crystallization kit (Hampton research) was used to screen the crystallization conditions for 122 bp Bbd-3E-NCP. The crystallization conditions for 122 bp Bbd-NCP were screened by the Pegs crystallization kit (Nextal Biotech).

5.2g Gel shift assay for interactions between H1 and NCPs

Reconstituted mouse NCPs, or Bbd-NCPs, were mixed with full length Drosophila H1 or globular mouse $H1^0$ at a series of molar ratios (1:1, 1:2, and1:4) in Hepes buffer (20 mM Hepes pH 7.5, 50 mM NaCl, 0.03% NP-40). The mixtures were incubated at 4°C overnight and analyzed on a 5% polyacrylamide

gel (acrylamide : bis-acrylamide 60:1) in 0.2 x TBE, run at a constant 150 V at 4°C.

5.3 Results and discussion

5.3a Crystallization of 146 bp Bbd-NCP is in process

'Hanging drop' and 'sitting drop' vapor diffusion techniques were used to grow crystals of 146 bp mouse-NCP, under conditions described previously [Luger et al., 1997a; Suto et al., 2000; White et al., 2001]. A broad salt range (30 - 60mM KCl and 25 – 75 mM $MnCl_2$) was screened for 146 bp Bbd-NCP. It took longer time to get clear drops when the Bbd-NCPs were mixed with the same volume of stock solutions. The drops at low KCl concentration (30-40 mM) are clear and oil like, and the drops at high KCl concentration (40-60 mM) contain precipitate. The trays were incubated at 19°C for longer than six monthes. However, no crystal formed in the wide screening hanging drops for 146 bp Bbd-NCP. This could be due to at least two factors. First, H2A.Bbd has sequence dissimilarity from major H2A in its acidic patch, a region important for crystal contacts of neighboring nucleosomes. Second, the "floppy ends" of DNA in 146 bp Bbd-NCP might make crystallization difficult. Two methods are suggested in the next two sections for circumventing these difficulties.

5.3b Crystallization of 147 bp Bbd-3E-NCP is in process

H2A.Bbd has a much-reduced acidic patch when compared to major H2A. This acidic patch is important for crystal contacts, where the basic H4 tail of the

neighboring nucleosome interacts with the acidic patch within H2A. The human H2A.Bbd mutant, Bbd-3E, was constructed by Dr. Tremethick's laboratory. This mutant has 3 amino acids reverted back to acidic residues (glutamates, hence 3E). The Bbd-3E protein was purified and refolded with other histones. Similar to the refolding of H2A.Bbd and other core histones, only $(H3H4)_2$ tetramer and Bbd-3E-H2B dimer were obtained (data not shown). This result suggests that the regeneration of the acidic patch is not adequate to stabilize the interaction between the Bbd-3E-H2B dimer and the $(H3\text{-}H4)_2$ tetramer at high ionic strength. So, Bbd-3E-H2B dimer and $(H3\text{-}H4)_2$ tetramer and 146 bp palindromic α-satellite DNA were used to reconstitute the Bbd-3E-NCP. The 5% native gel showed that Bbd-3E-NCP has identical electrophoretic mobility to that of Bbd-NCP (Fig.5.2 A). 2D gel electrophoresis was used to confirm that the upper band of Bbd-3E-NCP contained all four histones, with no depletion of histone dimers (Fig.5.2 B). 147 bp palindromic α-satellite DNA was used to reconstitute Bbd-3E-NCP, since it is determined as the true amount of DNA bound to histone ocatmer, and can give high resolution diffraction. No difference was found between 146 bp and 147 bp Bbd-3E-NCPs on 5% native gel (data not shown). The 147 bp Bbd-3E-NCP was purified by electroelution. The vapor diffusion 'hanging drop' technique was used to crystallize the147 bp Bbd-3E-NCP. Wide screen crystallization tray was set up for the salt range of 20 to 37.5 mM KCl, 20 to 45 mM MnCl2, and 5mM K-cacodylate pH 6.0, which cover the previous conditions found for NCP crystallization. Similar to 146 bp Bbd-NCP, it took longer time to get clear drops when the 147 bp Bbd-3E-NCPs were mixed with the same volume of stock

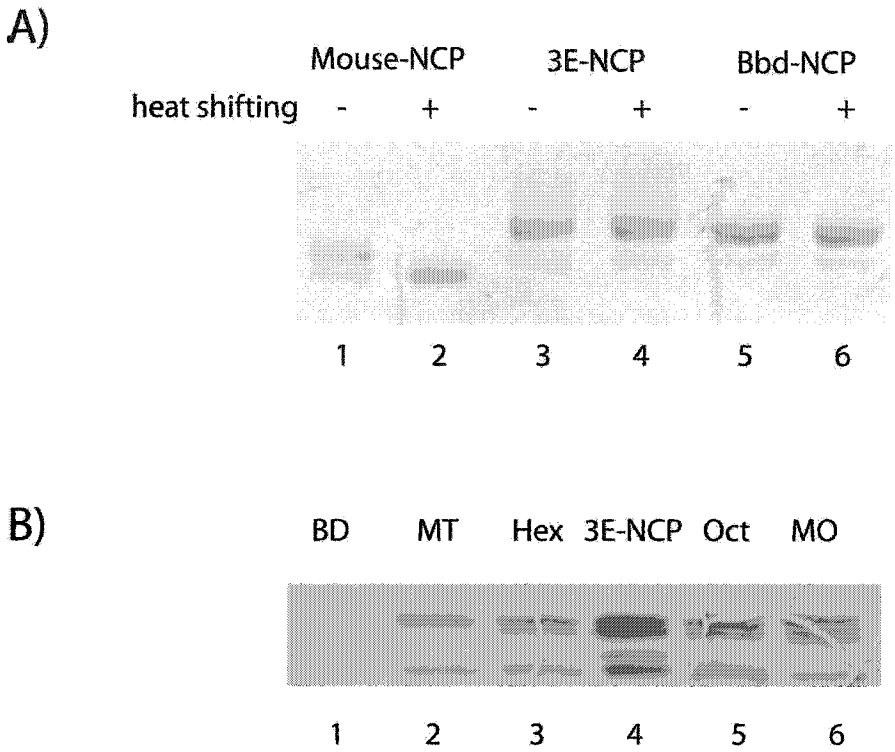

Figure 5.2: Reconstitution and characterization of Bbd-3E-NCP A) Salt gradient reconstituted Mouse-NCP, Bbd-NCP, and Bbd-3E-NCP (3E-NCP) before (-) and after (+) a 1 h incubation at 37°C, were analyzed by 5% native PAGE and stained with coomassie blue. **B)** Analysis of the histone content of the upper Bbd-3E-NCP nucleosomal band. The upper band (3E-NCP; lane 4) was excised from the native gel and analyzed by 18% SDS–PAGE. The mouse octamer(MO), H2A.Bbd–H2B dimer (BD), $(H3–H4)_2$ tetramer (MT), and their mixtures of 2:1 (Oct) and1:1 (Hex) were used as controls.

solutions. Most of the drops are clear and oil like, a few drops at high KCl concentration (37.5 mM) contain precipitate. The treys were incubated at 19°C for longer than six monthes. However, no crystal formed in the wide screening hanging drops for 147 bp Bbd-3E-NCP.

5.3c Crystallization of 122bp Bbd-NCP and 122 bp Bbd-3E-NCP are in process

Since no crystal has been formed in the crystallization trays of 146 bp Bbd-NCP and 147 bp Bbd-3E-NCP, another approach was pursued. It has been postulated that the failure to develop a Bbd-NCP crystal might be because the "floppy ends" of DNA make it difficult to crystallize. To overcome this obstacle, it was decided to use a shorter DNA to reconstitute the Bbd-NCP. In the preliminary study, a 123 bp DNA from the sea urchin 5s RNA gene was used. It was found that the 123bp DNA could be reconstituted with tetramer and Bbd dimer to form 123bp-Bbd-NCP (Fig.5.3A, lane 7 and 8). This 123bp-Bbd-NCP was observed to migrate a bit more slowly than mouse-NCP, but much faster than Bbd-NCP. The faster migration behavior of 123bp-Bbd-NCP could be because there are no "floppy ends" of DNA present. The 123 bp DNA can also form a complex with tetramer, but not with the mouse octamer (Fig.5.3A, lane 1-4). The 2D gel was used to confirm that the complex contained all histones with the proper stoichiometry (Fig.5.3B, lane 2). Micrococcal Nuclease (MNase) digestion was also used to check the DNA fragment stabilized by the octamer (Fig.5.3C). The observation that no clear stop band was formed during the

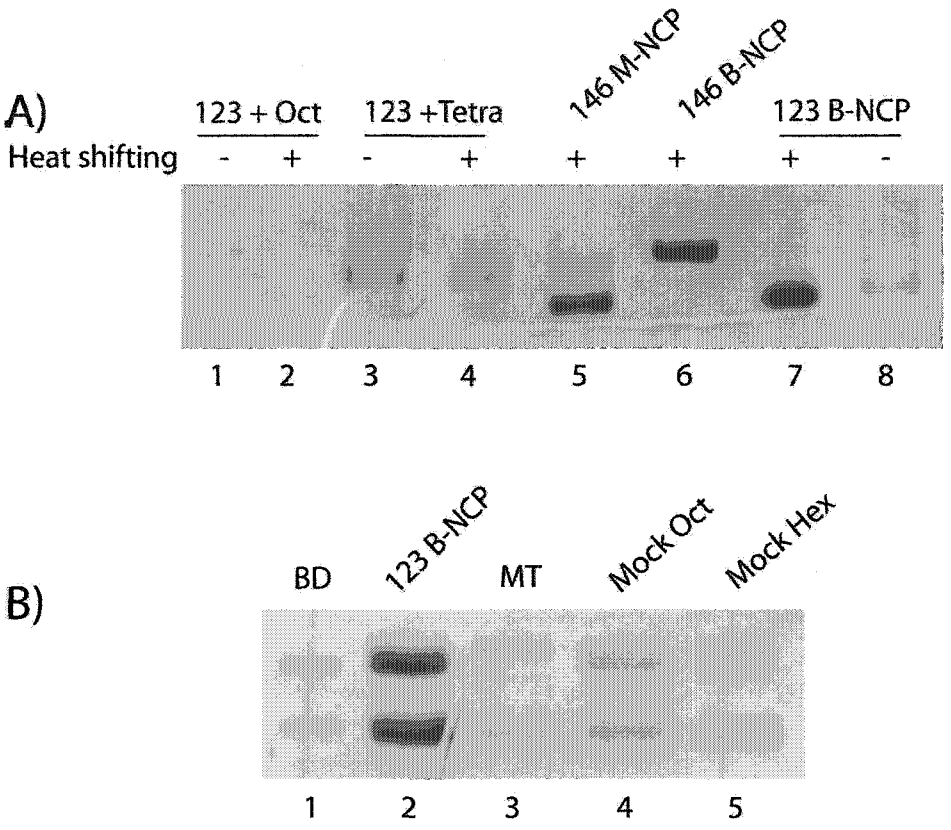

Figure 5.3: Reconstitution and characterization of 123 bp Bbd-NCP A) Salt gradient reconstituted 146 bp Mouse-NCP (146 M-NCP), 146 bp Bbd-NCP (146 B-NCP)Bbd-NCP, and 123 bp Bbd-NCP (123 B-NCP) before (-) and after (+) a 1 h incubation at 37°C, were analyzed by 5% native PAGE and stained with coomassie blue. 123 bp DNA fragment was also reconstituted with mouse octamer or mouse tetramer. The resulting complexes (123+Oct, 123+Tetra) were laded as control (lane 1-4). **B)** Analysis of the histone content of the upper 123 bp Bbd-NCP nucleosomal band. The upper band (123 B-NCP; lane 2) was excised from the native gel and analyzed by 18% SDS–PAGE. The H2A.Bbd-H2B dimer (BD), $(H3–H4)_2$ tetramer (MT), and their mixtures of 2:1 (Mock Oct) and1:1 (Mock Hex) were used as controls.

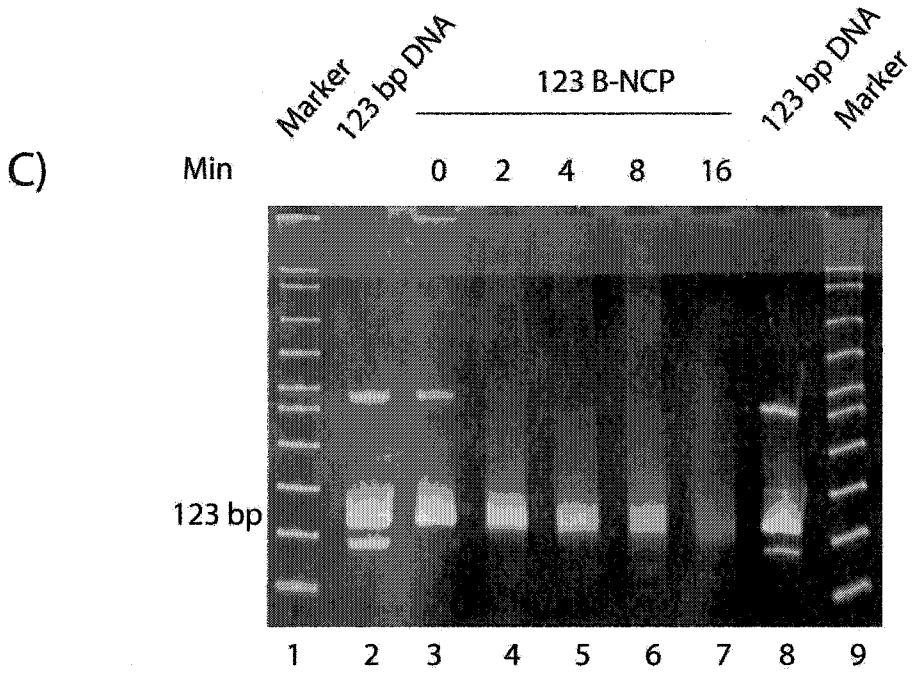

Figure 5.3: Reconstitution and characterization of 123 bp Bbd-NCP C) Micrococcal digestion of 123 Bbd-NCP: 10 ug of 123 B-NCP was digested with 0.15U MNase. Aliquots of 2 ug were removed after 0, 2, 4, 8 and 16 min. PAGE (10%) was used to check the deproteinized DNA fragments. 123 bp DNA with some 85 bp DNA was loaded as control.

MNase digestion, suggests that no significant floppy DNA was present in the complex. The results were as expected, and it was decided to make a 122 bp palindromic α-satellite DNA using the cloning and duplication strategy published previously [Dyer et al., 2004].

The 122 bp palindromic α-satellite DNA was made and reconstituted with mouse tetramer and H2A.Bbd-H2B dimer. The 122bp Bbd-NCP was analyzed on 5% native gel. As with 146 bp Bbd-NCP, there were upper and lower bands in the 122 bp Bbd-NCP prep and no redistribution happened upon heat treatment (Fig. 5.4 A). Alexa Fluor labeled mouse tetramer and Alexa Fluor labeled H2A.Bbd-H2B dimer were reconstituted separately into 122 bp Bbd-NCP and analyzed on 5% native gel. Both the tetramer and dimer were present in the upper and lower bands (Fig. 5.4 B, lane 3 and 4). These results are consistent with data described in Chapter 4, and suggest that the Bbd-NCP is highly dynamic regardless of the length of the nucleosomal DNA.

Both 122 bp Bbd-NCP and 122 bp Bbd-3E-NCP were reconstituted in large scale and purified by electroelution. The Natrix nucleic acid crystallization kit (Hampton research) was used to screen the crystallization conditions for 122 bp Bbd-3E-NCP. The crystallization conditions for 122 bp Bbd-NCP were screened by the Pegs crystallization kit (Nextal Biotech). The vapor diffusion 'hanging drop' technique was used to crystallize the 122 bp NCPs. About half of the drops are clear, and some of them are oil like. The other drops contain precipitate. The treys were incubated at 19°C and no crystal was formed in two monthes. Then, the treys were incubated at 4°C for about one month. Recently, the micro

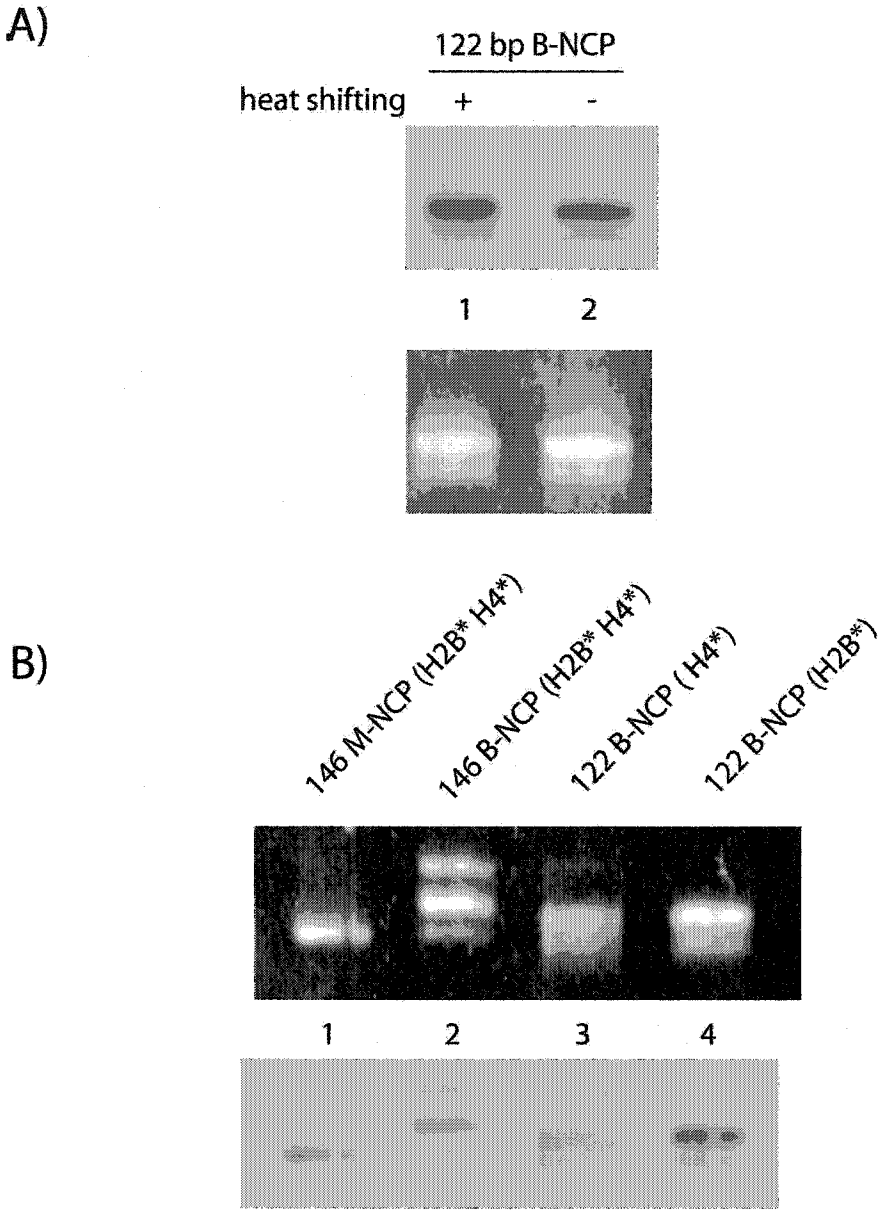

Figure 5.4: Reconstitution and characterization of 122 bp Bbd-NCP A) Salt gradient reconstituted 122 bp Bbd-NCP before (-) and after (+) a 1 h incubation at 37°C, were analyzed by 5% native PAGE and stained with ethidium bromide (lower panel) and coomassie blue (upper panel). **B)** 122 bp B-NCPs were reconstituted with Alexa Fluor 546 labeled Mouse $(H3–H4)_2$ tetramer (H4*, lane 3), or with Alexa Fluor 488 labeled H2A.Bbd-H2B dimer (H2B*, lane 4). The samples were analyzed by 5% native PAGE were first viewed on a transilluminator without staining (upper panel), followed by staining with coomassie blue (lower panel). The double labeled 146 bp M-NCP (H2B* H4*, lane 1) and 146 bp B-NCP (H2B* H4*,lane 2) were load as controls.

seeding technique was applied in the clear drops in the 122 bp Bbd-3E-NCP plates. No crystal has been formed at the time of this writing.

5.3d Both full length and globular H1 can bind to Bbd-NCP

It is not clear whether the C-terminal of H2A plays a direct role in nucleosome-linker histone interaction. The fact that H2A-Bbd has no C-terminal tail leads to the hypothesis that interaction between H1 and 'variant' nucleosome is changed, and therefore gene regulation within the 'variant' chromatin is altered. To test this hypothesis, gel shift assays were used to check the interaction between full length H1 and 146 bp Mouse-NCP, 146 bp Bbd-NCP, 196 bp Mouse-NCP, and 196 bp Bbd-NCP. It was shown that all the NCPs can be shifted by full length H1 (Fig. 5.5). That could be because there is a nonspecific binding between basic H1 tails and nucleosomal DNA. Therefore, we decide to use globular H1° (GH1°). In order to provide enough linker DNA for GH1° binding, a 166 bp DNA fragment was used, which was cut out from a 12-208 DNA template. The 5% native gel demonstrated that both 166 bp mouse-NCP and 166 bp Bbd-NCP can be shifted somewhat by GH1°. There was no supershift when more GH1° was added, suggesting that the binding is specific (Fig.5). The other weak bands in the gel are caused by impurities in the 166 bp DNA sample. To confirm the existence of GH1° in the complex, the bands should be electroeluted and subjected to 2D gel. These data suggest that there is no significant alteration in H1 binding with NCP once the H2A.Bbd is incorporated.

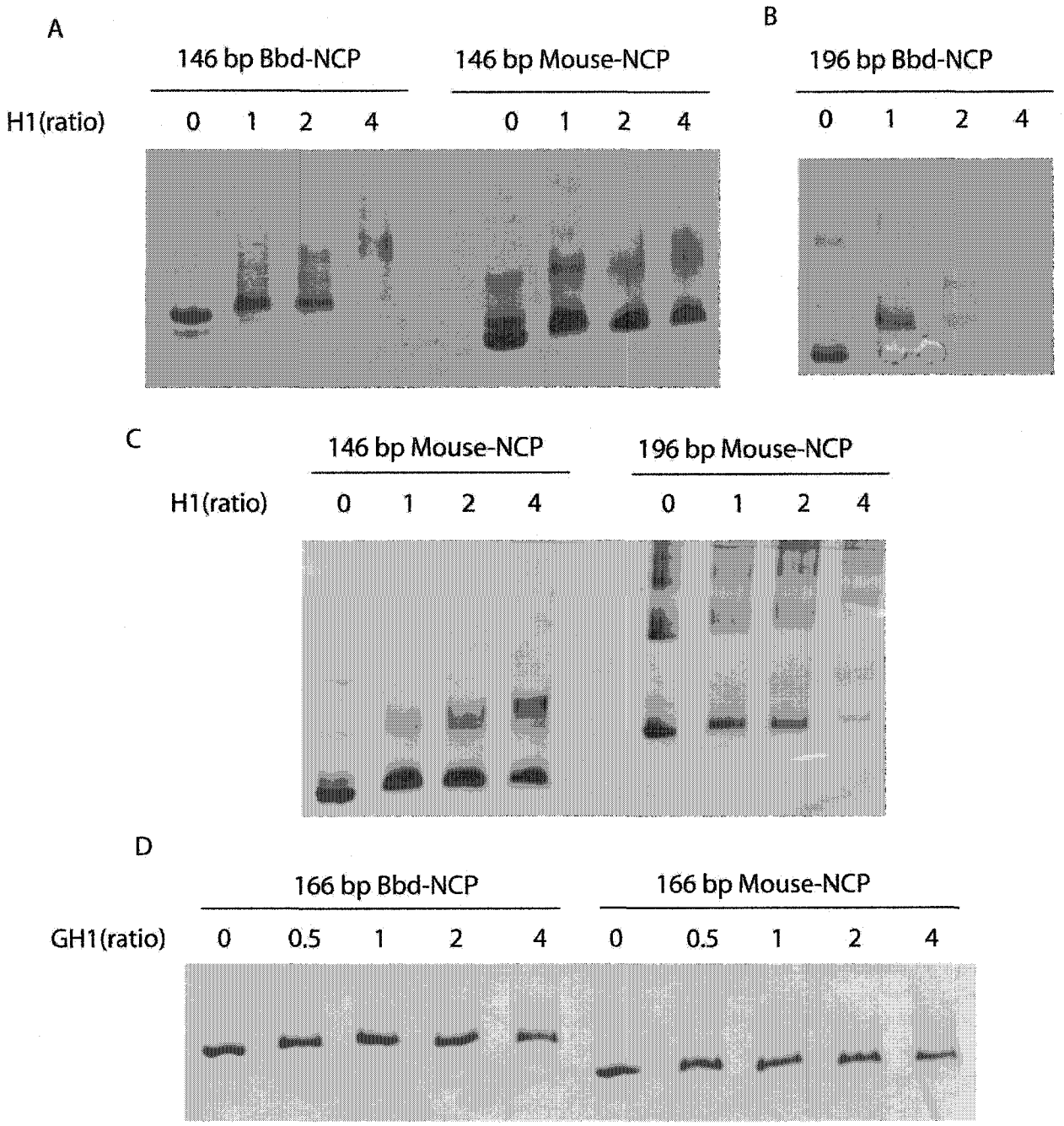

Figure 5.5: Gel shift assays show full length H1 binding with 146 bp Bbd-NCP and 146 bp Mouse-NCP **(A)**, 196 bp Bbd-NCP **(B)**, 146 bp Mouse-NCP and 196 bp Mouse-NCP **(C)**, Globular H1 (GH1) binding with 166 bp Bbd-NCP or 166 bp Mouse-NCP **(D)**. H1 or GH1 molar ratio to NCPs is shown on the top of each lane.

Other approaches, such as fluorescence anisotropy, might be needed to determine the binding affinity in detail.

5.4 Acknowledgement

We thank Dr. David Tremethick for kind gift of Bbd-3E construct, Kasey Konesky for a kind gift of Drosophila H1protein, Dr. Xu Lu for a kind gift of globular mouse H1° protein, Aaron B. Stephan for purification of Bbd-3E protein, Jayanth V. Chodaparambil for help with histone labeling, Pamela N. Dyer for help with DNA purification, Rajeswari S. Edayathumangalam and Dr. Srinivas Chakravarthy for help with crystallization trials.

CHAPTER 6

Nucleosome Core Particles Containing Poly (dA.dT) Element Possess a Local Distorted DNA Structure

The poly (dA·dT) elements common to many yeast promoter regions have been suggested to promote transcriptional activation by altering the stability or dynamics of nucleosomes. In order to study the role of poly (dA·dT) elements on nucleosomal DNA structure, we set out to determine the stability and crystal structure of a nucleosome core particle containing a 16 base pair poly (dA·dT) element. The data shown in this chapter will be written up for submission to *the Journal of Molecular Biology* as referenced below.

Yunhe Bao*, Cindy White*, Joel Gottesfeld, and Karolin Luger. Nucleosome core particles containing poly (dA.dT) element possess a local distorted DNA structure. The construction of the poly (dA·dT) element, the FRET study, and the crystallization trials were done by CW. JG helped in the DNase I footprinting experiments. The structural determination and analysis were performed by YB.

* YB and CW contributed equally to this work.

6.1 Abstract

The poly (dA·dT) elements have been suggested to promote transcription by altering the stability or dynamics of nucleosomes. In this study, the stability and structure of a nucleosome (A_{16} NCP) containing a 16 bp poly (dA·dT) element were investigated. It was found that a high temperature was required for histone octamer sliding within the A_{16} NCP *in vitro*. Fluorescence resonance energy transfer analyses showed that the interactions between the nucleosomal DNA ends and the histone octamer were destabilized in A_{16} NCPs. DNase I footprinting data indicated that hypersensitive sites were created by the A_{16} element. The A_{16} NCP was crystallized and the crystal structure was refined at 3.2 Å. This A_{16} NCP structure revealed that the overall structure was maintained except for some local structural alteration, especially in the poly (dA·dT) region. The results are consistent with the *in vivo* and *in vitro* observations that poly (dA·dT) elements caused modest changes in DNA accessibility and modest increases in steady-state transcript levels.

6.2 Introduction

The poly (dA·dT) elements (T-tracts) have been found to be greatly overrepresented in all eukaryotic species examined (from yeast to human), and particularly enriched in promoter regions [Behe, 1995]. It has been suggested that poly (dA·dT) promotes transcription by altering the stability or dynamics of nucleosomes and enhancing the binding between transcription activators and

their DNA targets, which lie close to the T-tracts. The mechanism of this transcription activation is not clear yet.

The poly (dA·dT) tracts have a straight and rigid DNA structure [Nelson et al., 1987], which is different from B-form DNA. Specifically, they have a narrow minor groove, 10 bp per helical turn, and additional bifurcated hydrogen bonds [Alexeev et al., 1987; Coll et al., 1987; Dickerson et al., 1982; Peck and Wang, 1981]. Because of these structural properties, it has been proposed that longer poly (dA·dT) tracts would not be able to conform well to the highly bent nucleosomal superhelix. Previous studies have shown that the poly (dA·dT) elements are resistant to nucleosome formation [Kunkel and Martinson, 1981; Rhodes, 1979]. A study in which hundreds of nucleosomal DNA fragments were sequenced showed that longer adenosine tracts (containing five or more contiguous adenosines) were underrepresented in nucleosomal DNA *in vivo* [Satchwell et al., 1986]. Additionally, many promoter regions which contain poly (dA·dT) elements have been shown to be nucleosome free *in vivo* [Filetici et al., 1998; Lascaris et al., 2000; Tanaka et al., 1996]. However, several research groups have recently shown that the poly (dA·dT) can be incorporated into nucleosomes both *in vitro* and *in vivo*. Using small DNA fragments from the NSR1 promoter, Losa et al. were able to demonstrate that the naturally occurring 34 bp poly (dA·dT) tract can be folded into nucleosomes *in vitro* [Losa et al., 1990]. It has been shown that the *Saccharomyces cerevisiae* DNA topoisomerase I promoter contains a 29 bp poly (dA·dT) tract within a nucleosome core [Rubbi et al., 1997]. In addition, the Thiele group found that a

16 bp poly (dA·dT) (A_{16}) element located adjacent to a metal response element (MRE) within the Amt1 gene promoter of *Candida glabrata* was incorporated into a positioned nucleosome *in vivo* [Liu and Thiele, 1997; Zhu and Thiele, 1996]. They also showed that this element is essential for rapid activation of the Amt1 promoter in response to a toxic copper level [Koch and Thiele, 1996]. Thus, poly (dA·dT) tracts alone are not sufficient to disrupt nucleosome formation, but might lead to local distortions in nucleosomal DNA, thereby permitting or enhancing the binding of regulatory factors.

To date, several studies have investigated the impact of poly (dA·dT) elements on the affinity of histone-DNA interactions. For example, one study reported that incorporation of a 16 bp poly (dA·dT) element at the end, and further in the middle of the nucleosomal DNA destabilized histone-DNA interactions and was accompanied by about a 1.6-fold increase in position-averaged equilibrium accessibility of nucleosomal DNA target sites [Anderson and Widom, 2001]. However, another study suggested the opposite effect: a 25 bp poly (dA·dT) tract stabilized the nucleosome [Mahloogi and Behe, 1997]. Therefore, the affects of poly (dA·dT) incorporation on histone-DNA interaction still remain uncertain.

To investigate the affects of poly (dA·dT) elements on nucleosome stability, White and Luger reconstituted nucleosomes with a 147 bp DNA containing an A_{16} element and the sequence recognition element (MRE) for Amt1 (Fig. 6.1). It was found that there was no preference for DNA sequences with or without the

Figure 6.1: Sequence alignment of A16 DNA and a-satellite DNA. The poly(dA·dT) element is shown in blue and the metal response element (MRE) for Amt1 is shown in red. The region of the A16 DNA sequence that matches the rest of the Amt1 gene promoter is shown in green. The rest of the DNA sequence is identical with human a-satellite DNA, which also contains two Amt1 binding sites (red). The position of the central base pair is indicated (Φ), and 10 bp increments from the dyad are indicated by black bullets. Reproduced from [White and Luger, 2004].

A_{16} element in the in vitro assembly system; the DNA binding domain of Amt1 bound to nucleosome containing the A_{16} element with only a 3-fold reduced affinity compared to free DNA; and no dissociation of histones was required for Amt1 binding [White and Luger, 2004].

In the present study, a more detailed analysis was performed of the nucleosome core particles containing an A_{16} element and the MRE (A_{16} NCP). Quantitative footprinting data showed that hypersensitive sites were created by the A_{16} element. Fluorescence resonance energy transfer (FRET) was utilized to compare the stability of NCPs reconstituted with either α-sat or A_{16} DNA. In order to determine the structural alteration caused by the incorporation of poly (dA·dT), the X-ray crystal structure of the A_{16} NCP was examined. We observe that some local areas of nucleosomal DNA were distorted. These results suggest that poly (dA·dT) elements are able to be incorporated into nucleosome and to cause some local structural alteration in DNA. Furthermore, this nucleosome crystal structure is the first one with a non-palindromic DNA sequence.

6.3 Materials and Methods

6.3a Reconstitution of NCPs

147 bp A_{16} DNA was designed and prepared as described in [White and Luger, 2004]. 146 bp α-sat DNA was prepared in a similar manner. Histones from *Xenopus laevis* were over-expressed in bacteria and purified using previously published protocols [Luger et al., 1999], and nucleosomes were prepared as described. Milligram amounts of NCPs were subjected to heat shifting (37°C for

α-sat NCPs, 55°C for A16 NCPs), and purified using preparative gel electrophoresis [Dyer et al., 2004].

6.3b DNase I footprinting

Nucleosomes were reconstituted by mixing ^{32}P end-labeled 147 bp A_{16} DNA, or 146 bp α-sat DNA with *Xenopus laevis* histone octamers at different ratios in 2M NaCl, and reconstituted as described [Gottesfeld and Luger, 2001]. Reactions were carried out in a 200 µl volume containing 2 - 5 nM labeled nucleosomes in 65 mM KCl, 5 mM $MgCl_2$, and 20 mM Tris/Cl pH 7.8. DNase I digestion was allowed to proceed for 5 minutes in the presence of 2.5 mM $CaCl_2$ with 0.02 units of DNase I (Roche Molecular Biochemicals). Samples were deproteinized and analyzed on an 8% sequencing gel.

6.3c Fluorescence labeling of DNA and histone proteins

The purified 147 bp A16 DNA and 146 bp α -sat DNA were labeled with the donor chromophore 7-diethylamino-3-(4'-maleimidylphenyl)- 4-methylcoumarin (CPM) as described earlier [White and Luger, 2004]. *Xenopus laevis* mutants H2B T112C were expressed and purified as described [Dyer et al., 2004]. The proteins were labeled with the acceptor chromophore fluorescein-5-maleimide (FM) as described [White and Luger, 2004].

6.3d Fluorescence Resonance Energy Transfer (FRET)

Nucleosomes containing donor (CPM) labeled DNA with acceptor (FM)-labeled H2B (for protein-DNA FRET) were mixed with 0.1 M NaCl to a final concentration of 28 µg/ml (1.33×10^{-7} M) and incubated for 30 minutes in a buffer containing 10 mM Tris/Cl (pH 8.0) and 0.1 mM EDTA. For stability measurements, donor emission quenching as a result of energy transfer to the nearby acceptor was monitored at 475 nm (excitation at 385 nm) in response to increased ionic strength up to 1.5 M. All experiments were carried out at 20°C, and each data set was corrected for dilution by dividing the raw signal by [1 – (injection volume / total volume)]. The data sets were then normalized to the same scale, and the average of the normalized data sets were plotted. Error bars of the standard deviation of the data sets were calculated and reported.

6.3e Crystallization of A_{16} NCP

Both vapor diffusion hanging and sitting drop techniques were used to crystallize A_{16} NCP. Diffraction-quality crystals were grown in 20 to 35 mM KCl, 34 to 48 mM $MnCl_2$, and 5mM K-cacodylate pH 6.0 at 19°C. The optimized protein concentration within the drop was 4 mg/ml. Crystals were harvested and soaked in a 24% methyl-pentane-diol cryo-protectant. Crystals were flash frozen in liquid propane before transferring to the cryo-stream, as previously described[Luger et al., 1997a].

6.3f Data Collection, Structure Refinement, and Validation

For initial screening, data were collected on a home source X-ray generator. Synchrotron Data were collected at Advanced Light Source beamline 8.2.2 in Berkeley. Data were indexed and scaled with DENZO and SCALEPACK [Otwinowski and Minor, 1997]. Molecular replacement was used to obtain crystal phases, using Protein Data Bank ID code 1KX5 (147 bp NCP) as the search model. Refinements were done with CNS [Brunger et al., 1998] and model building with O [Jones et al., 1991]. The model was checked by using stimulated annealing omit maps and validated using PROCHECK [Laskowski et al., 1993]. DNA was analyzed by 3DNA (v1.5) [Lu, XJ and Olson, WK, Rutgers university, http://rutchem.rutgers.edu/~xiangjun/3DNA/]. Some of the figures in this paper were made by using the molecular graphics program PYMOL [W. L. DeLano, PYMOL Molecular Graphics System (2002), www.pymol.org].

6.4 Results

6.4a High temperature is needed for histone octamer sliding on the A_{16} DNA *in vitro*

When DNA fragments reconstitute onto the histone octamer by salt-gradient deposition, the DNA adopts several translational positions with respect to the histone octamer. A simple heating step allows nucleosomes to attain the thermodynamically free energy minimum. It has been shown previously that α-sat NCPs completely shift by heating at 37° C after 30 minutes [Muthurajan et al.,

2003]. The A_{16} NCP requires higher temperatures for the DNA to attain the thermodynamically stable central position on the histone octamer. It was shown that three complexes were formed at 4°C after salt gradient reconstitution (Fig. 6.2A, lane 1). Most part of the upper band was shifted to the lower band at 37°C (Fig. 6.2A, lane 2). However, the middle band require heating at 55°C to be shifted to the lower band, which co-migrates with centrally positioned α-sat NCPs (Fig. 6.2A, lanes 3-5). Interestingly, this population of A_{16} NCP is similar to that of the NCP obtained by reconstitution onto an asymmetric 146 bp 5S DNA [Luger et al., 1999], indicating that the upper and middle bands are two electrophoretically distinguishable off-centered positioned A_{16}NCPs. For the NCPs prepared with a palindromic DNA fragment, the two off-centered positioned NCPs cannot be distinguished because they possess an identical exit angle of the ends of the DNA from the histone octamer [Luger et al., 1999] The rigid nature of poly dA·dT tracts may make it refractory to in vitro sliding. Only one of the off-centered A_{16}NCPs need high temperature to be shifted to centrally positioned NCP, suggesting that the relative positions of poly dA·dT tract (A_{16}) to the histone tetramer are important for its barrier role in nucleosome sliding by heat treatment. The time course study of shifting for A_{16} NCPs showed that majority of upper and middle bands were shifted to the lower band within 10 minutes at 55°C (Fig. 6.2B).

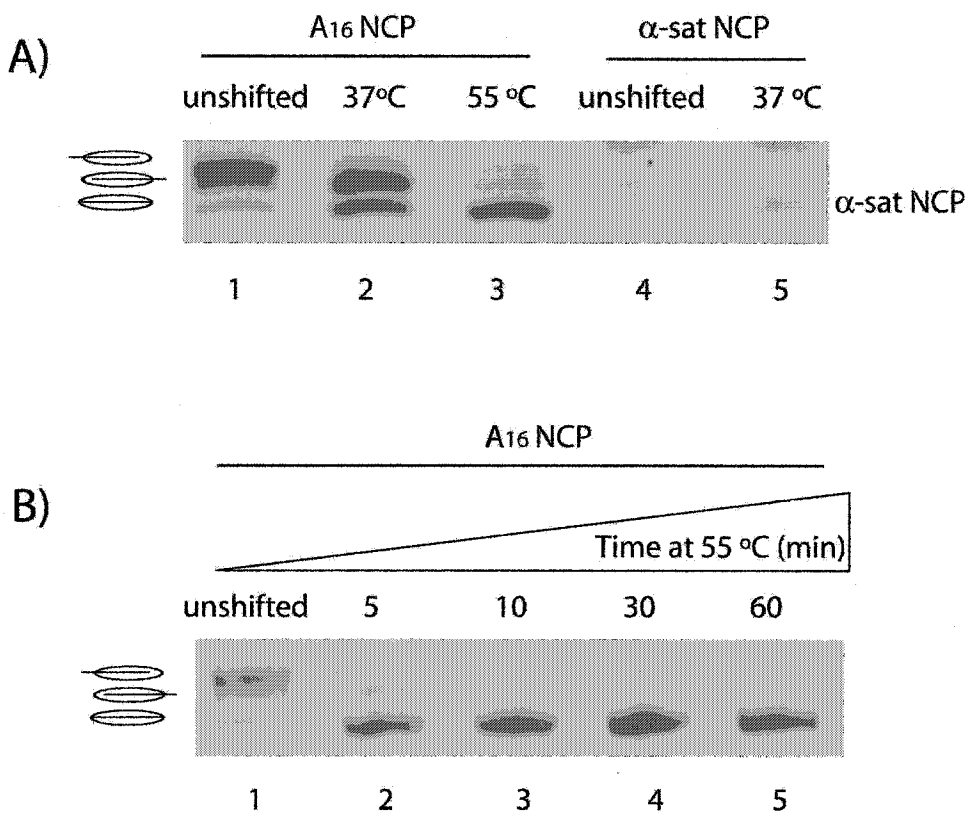

Figure 6.2: A_{16} NCPs require higher temperature to shift in vitro. A) Salt gradient reconstituted α-sat NCP, A_{16}NCP before (unshifted) and after a 1 h incubation at 37°C or 55°C, were analyzed by 5% native PAGE and stained with Coomassie blue. **B)** The A_{16}NCP was shifted at 55°C for a time course. Samples were analyzed by 5% native PAGE and stained with Coomassie blue.

6.4b The interactions between the nucleosomal DNA ends and the histone octamer are destabilized in A_{16} NCPs

The rigid nature of poly (dA·dT) tracts has the potential to destabilize nucleosomes [Lascaris et al., 2000; Suter et al., 2000]. On the other hand, highly stable nucleosomes appear to be formed on a 146 bp poly (dA·dT) tract at elevated temperatures [Puhl and Behe, 1995] To resolve this disparity, fluorescence resonance energy transfer (FRET) was utilized to compare the stability of NCPs reconstituted with either α-sat or A_{16} DNA. It has previously been shown that FRET can be used to study the salt-dependent dissociation of NCPs by monitoring the distance-dependent fluorescence emission of chromophores within the nucleosome [Muthurajan et al., 2003; Park et al., 2004b].

The ends of each DNA fragment were labeled with CPM (donor), and a histone H2B T112C mutant was labeled with FM (acceptor) prior to nucleosome assembly. In a completely assembled nucleosome, quenching of donor fluorescence emission is observed as a result of FRET, and this quenching effect disappears upon dissociation of the nucleosome at elevated salt concentrations (Fig. 6.3A). This property was utilized to monitor equilibrium dissociation curves of nucleosomes in response to elevated salt concentrations. When salt was added to nucleosomes containing only donor chromophore, no change in signal was detected (data not shown). The Luger group has repeatedly observed two distinct transitions of NCP dissociation when monitoring FRET between the DNA

A)

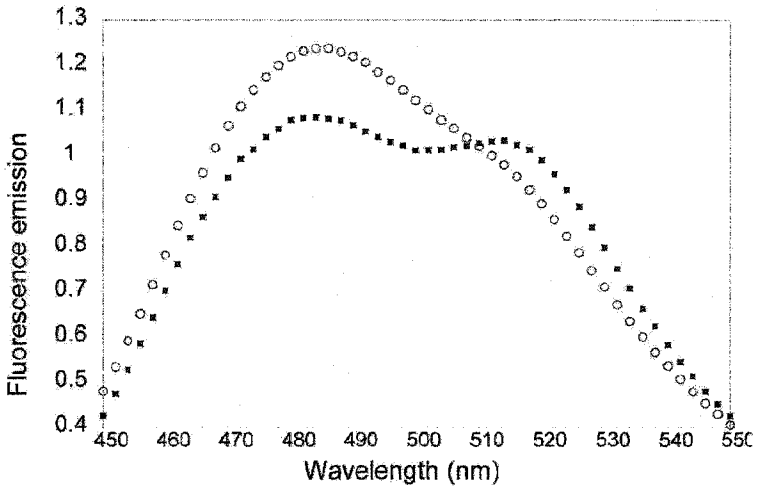

B)

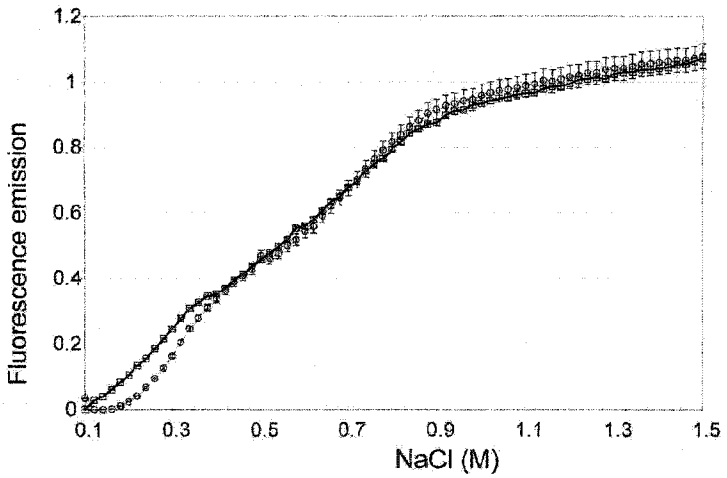

Figure 6.3: (A) Fluorescence emission spectra of A_{16} NCP, incubated for 30 min in either 0.1 M NaCl (filled squares) or 1.5 M NaCl (open circles). The ends of each DNA fragment were labeled with CPM (donor), and histone H2B T112C was labeled with FM (acceptor) prior to assembly. The excitation wavelength was set at 385 nm. **(B)** The salt dependent dissociation of A_{16}NCPs (squares) and α-sat NCPs (circles). NaCl was added up to 1.5 M in 0.02 M steps, and donor emission (475 nm) was recorded at each step upon excitation at 385 nm. Data was corrected for dilution before plotting. Standard deviations from three separate datasets were calculated and reported as error bars.

ends and the $(H3\text{-}H4)_2$ tetramer. This is confirmed for FRET between the ends of the DNA and the (H2A-H2B) dimer for α-sat NCPs, and is also apparent for the A_{16} NCPs (Fig. 6.3B). The first, fully reversible transition corresponds to the dissociation of the peripheral DNA ends [Park et al., 2004b]. The second transition is caused by the dissociation of the histone dimer from the $(H3\text{-}H4)_2$ – DNA complex. It was noted that the dissociation of the DNA ends from the histone octamer was initiated at a lower salt concentration for the A_{16} NCP (Fig. 1B), whereas the (H2A-H2B) dimer dissociated from the DNA at similar salt concentrations in the two nucleosomes. This result suggests that the DNA ends in A_{16} NCPs are more easily dissociated than those of α-sat NCPs. That is, the interactions between the nucleosomal DNA ends and the histone octamer are destabilized in the A_{16} NCPs. This data is consistent with the previous result that AMT1 binding with A_{16} NCP cause dissociation of DNA ends [White and Luger, 2004]. These results are consistent with the observation that the A_{16} is essential for rapid activation of the Amt1 promoter in response to a toxic copper level [Koch and Thiele, 1996]. Not that the 16 bp poly (dA·dT) element (36-51 bp) is not located at the ends of DNA, indicating that the incorporation of this A_{16} element into NCP may cause DNA distortions in different areas.

6.4c The A_{16} element creates areas of altered DNA accessibility

To determine if the A_{16} sequence element in this particular position results in localized distortions of nucleosomal DNA *in vitro* (as suggested in Zhu and Thiele, 1996), DNase I digestion was performed with either A_{16} NCP or with α-sat NCP. It was shown that there are differences in the digestion patterns of the A_{16} NCPs relative to α-sat NCPs throughout the entire sequence (indicated by stars, Fig. 6.4A). Note that because both 5' ends of the DNA were labeled and because the A_{16} 147mer is not a perfect palindrome (Fig. 6.1), the G-A tract and the footprinting pattern is actually a convolution of the two halves of nucleosomal DNA for A_{16} NCPs. Therefore, the Amt1 binding site and A_{16} element are shown on both sides of the dyad in A_{16} NCPs (Fig. 6.4A). Quantitative phosphorimaging shows that hypersensitive sites (HS) are created by the A_{16} element, whereas other areas (RS) are less sensitive to DNase I digestion compared to α-sat NCPs (Fig. 6.4B). One area of pronounced DNA hypersensitivity is located directly in the poly (dA·dT) element, indicating the local structure alteration caused by the A_{16} element. Other changes are located in the area of the Amt1 binding site (MRE) and the region between A_{16} and MRE. Structural analysis of the A_{16} NCPs confirms that the DNA position is maintained on the histone octamer (see next part). Thus, changes in the footprint of NCPs containing the poly (dA·dT) element are not the result of a different rotational or translational position of the DNA with respect to the histone octamer, as is also suggested from the similar pattern of the two nucleosomal footprints.

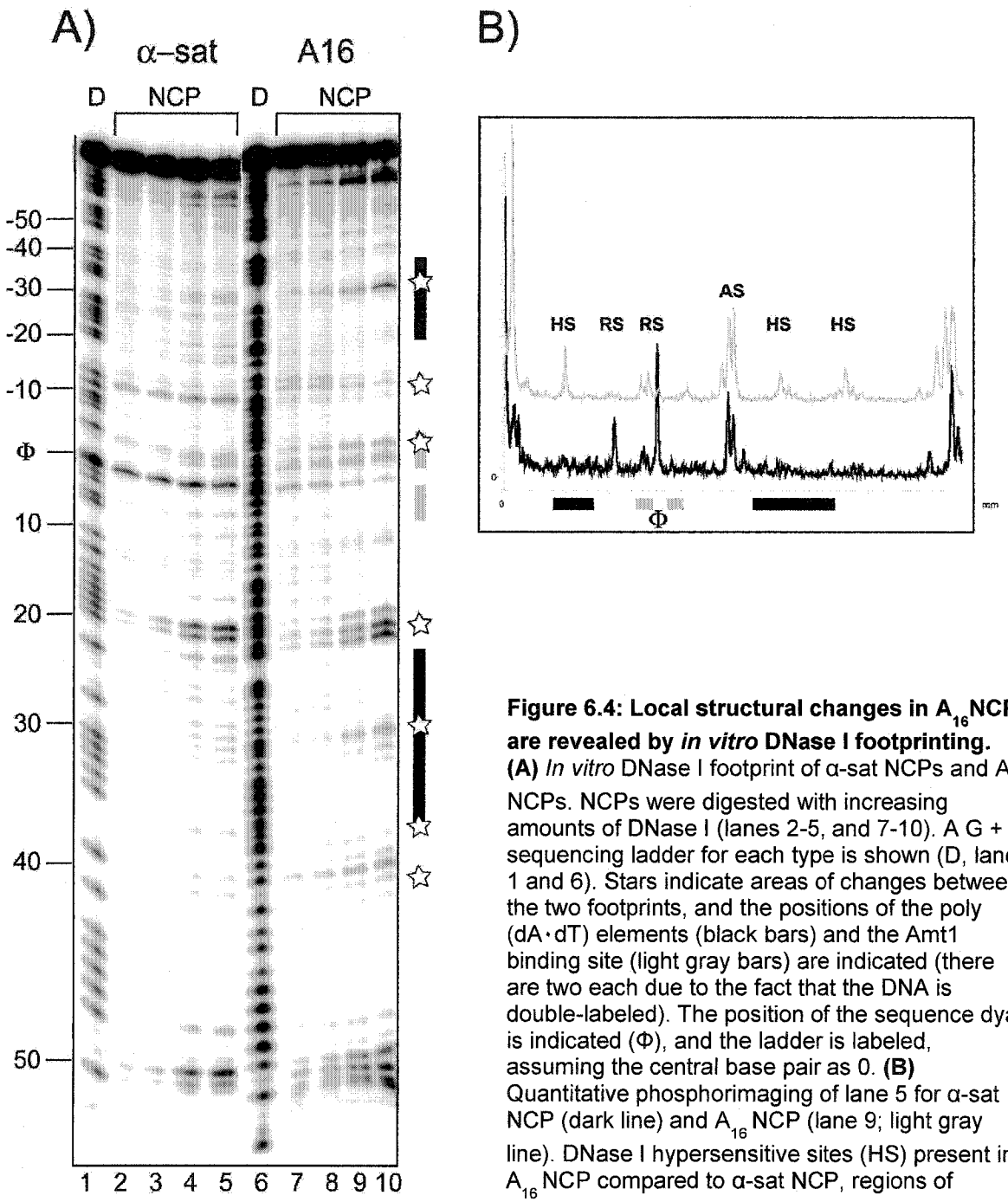

Figure 6.4: Local structural changes in A_{16} NCPs are revealed by *in vitro* DNase I footprinting. **(A)** *In vitro* DNase I footprint of α-sat NCPs and A_{16} NCPs. NCPs were digested with increasing amounts of DNase I (lanes 2-5, and 7-10). A G + A sequencing ladder for each type is shown (D, lanes 1 and 6). Stars indicate areas of changes between the two footprints, and the positions of the poly (dA·dT) elements (black bars) and the Amt1 binding site (light gray bars) are indicated (there are two each due to the fact that the DNA is double-labeled). The position of the sequence dyad is indicated (Φ), and the ladder is labeled, assuming the central base pair as 0. **(B)** Quantitative phosphorimaging of lane 5 for α-sat NCP (dark line) and A_{16} NCP (lane 9; light gray line). DNase I hypersensitive sites (HS) present in A_{16} NCP compared to α-sat NCP, regions of reduced sensitivity (RS), and regions areas of altered banding (AS), are indicated. The dyad is marked with Φ, and the positions of the poly (dA·dT) elements (black bars) and the Amt1 binding sites (light gray bars) are indicated.

6.4d The A_{16} fragment possesses a narrow minor groove in nucleosomal DNA

In order to investigate the detail of structural alteration caused by the incorporation of poly (dA·dT), the X-ray structure of the NCP containing A_{16} was studied. The A_{16} NCP is crystallized in the space group of $P2_12_12_1$ with a unit cell similar as that of the NCPs with α-satellite DNA (Table 6.1). Molecular replacement was used to obtain phases. The model for 147 bp NCP (PDBID: 1KX5, [Davey et al., 2002]) was used as a search model. The standard B form DNA base pairs A-T and G-C were used in the program O [Jones et al., 1991] to replace the original 1KX5 DNA according to the A_{16} DNA sequence. Convolution is a potential problem caused by the asymmetric character of A_{16} DNA. This means there could be a convolution between the two possible orientations of the A_{16} NCP with respect to the poly (dA·dT) element (Fig. 6.5). To test which orientation will give us a better model, the 'original-DNA' pdb file, which has the same DNA sequence shown in figure 6.1, was reversed to obtain the 'flip-DNA' file. The half of 'original-DNA' containing the A_{16} element was combined with the half of 'flip-DNA' containing the A_{16} element to obtain the 'both-DNA' file, which had two poly (dA·dT) elements (Fig. 6.5). These DNA pdb files were combined with the same protein pdb file individually and subjected to the same refinement procedures. It was found that 'flip-DNA' model was the best one by comparing r-frees obtained from the same refinement procedures: The r-free for 'flip-DNA' model is 0.364; the r-free for 'original-DNA' model is 0.376; the r-free for 'both-DNA' model is 0.462. However, this result doesn't mean that all the molecules in

Table 6.1: Crystallographic statistics

Space group	$P2_12_12_1$
Unit cell dimensions, Å	
a	104.9
b	109.6
c	178.0
Resolution range, Å	3.2-50.0
Unique reflections	34730
Redundancy (last shell)	7.1 (6.8)
Completeness (%)(last shell)	99.4 (99.8)
I/σ (last shell)	54.60 (10.23)
R_{merge} * (last shell)	0.067 (0.226)
R_{cryst} §	0.2816
R_{free} #	0.3507
Number of amino acids	758
Number of DNA base	*294*
rmsd ¥	
Bonds, Å	0.008
Angles, °	1.354
Average B-factors, $Å^2$	
Protein	84.52
DNA	168.17

Numerical values in parentheses are for highest resolution shell.

* $R_{merge} = \Sigma|I_h - \langle I_h \rangle| / \Sigma I_h$, where $\langle I_h \rangle$ is the mean of the measurements for a single hkl.

§ $R_{cryst} = \Sigma|F_{obs} - F_{calc}| / \Sigma F_{obs}$

Calculated using 5% data randomly chosen and omitted from the refinement.

¥ rmsd, rms deviation from ideal geometry

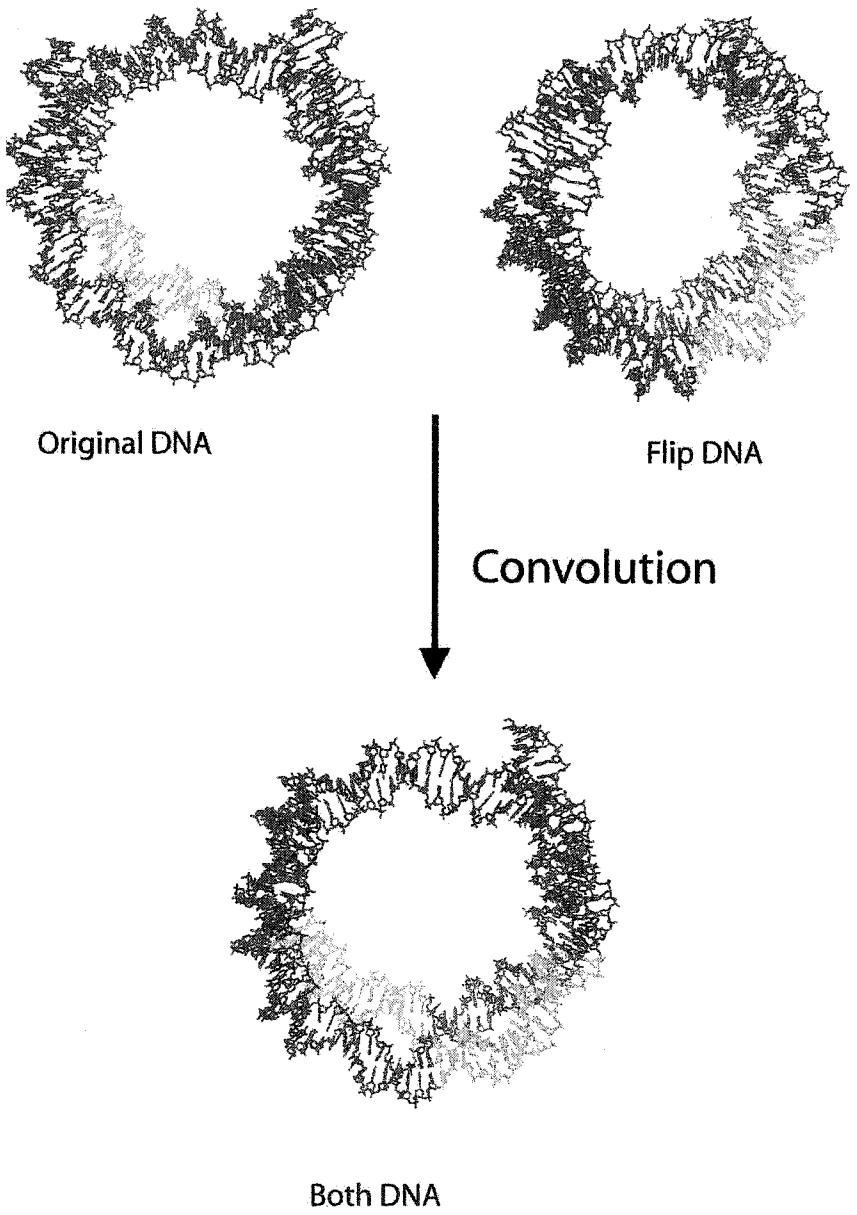

Figure 6.5: Two possible orientations of the A_{16} NCP with respect to the poly (dA·dT) element could lead to a convolution between the two in the crystal lattice. Red: non- poly (dA·dT) DNA; Green: 16 bp poly (dA·dT) element.

the crystal are 100% with 'flip-DNA' orientation. Maybe only 80 % of the molecules are with the 'flip-DNA' orientation. Therefore, the occupancy in 'original-DNA' and 'flip-DNA' pdb files was varied from 0.1 to 0.9 with a 0.1 step and from 0.9 to 0.1, respectively. Then the 'original-DNA' and the 'flip-DNA' pdb file were combined to obtain an occupancy as 1. For example, the 'original-DNA' pdb file with 0.1 occupancy should be combined with the 'flip-DNA' pdb file with 0.9 occupancy. The combined DNA pdb files were combined with the same protein pdb file individually and subjected to the same refinement procedures. It was found that none of these is better than 'flip-DNA' model by comparing the r-free. The 'original-DNA' model and 'flip-DNA' model were further compared by using the composite annealed omit map. The 'flip-DNA' model fits to the map much better than 'original-DNA' model. So, we decided to continue to rebuild 'flip-DNA' model with O and the r-free for the final model is 0.3507.

The structures of A_{16} NCP and 147 bp α-sat NCP were superimposed with an average root mean square deviation (rmsd) of 0.4 Å for protein and 1.3 Å for DNA. It can be seen that overall there is no significant difference in DNA path between the two models (Fig. 6.6A,B, The histone octamers in the two models are very similar and not shown). Surprisingly, the structure shows that the 16 bp poly (dA·dT) DNA fragment can be incorporated into NCP very well without any bulge formation, which was expected due to the rigid character of the poly (dA·dT) DNA structure [Zhu and Thiele, 1996]. The electron density map for part of the poly (dA·dT) element is shown (Fig. 6.6D).

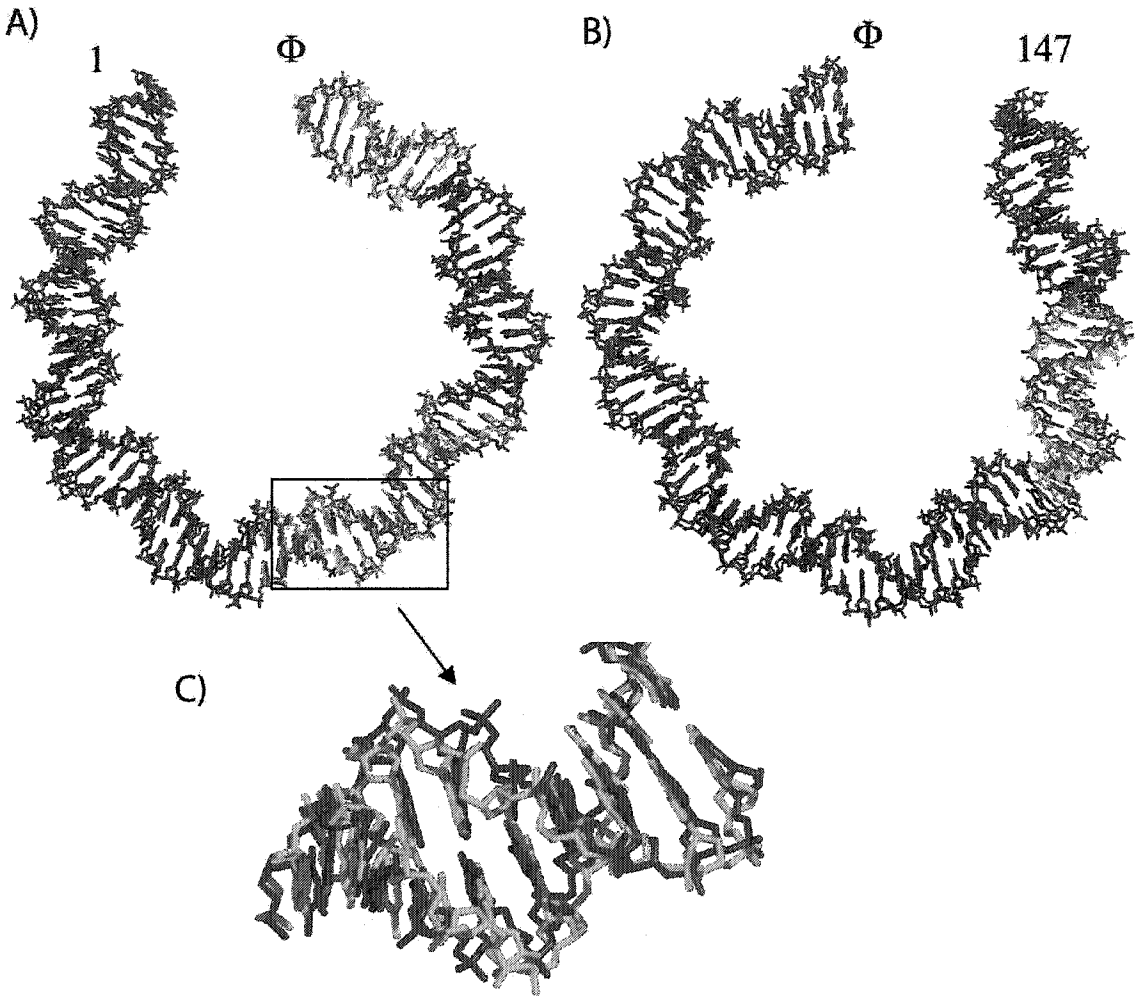

Figure 6.6: Overall comparison of DNA structure of A_{16} NCP and α-sat NCP. Partial structures, base pairs 1-74 **(A)** and base-pairs 75-147 **(B)** are viewed down the superhelical axis. The DNA of A_{16} NCP and α-sat NCP are colored in red and blue, respectively. Poly (dA·dT) element (36-51 bp, orange) and Amt1 binding site (66-74 bp, green), and 125-135 bp (cyan) are labeled. **(C)** Detail comparison of minor groove of Poly (dA·dT) element (base pairs 37-45) and that of α-sat NCP. The DNA of A_{16} NCP and α-sat NCP are colored in orange and blue, respectively.

D)

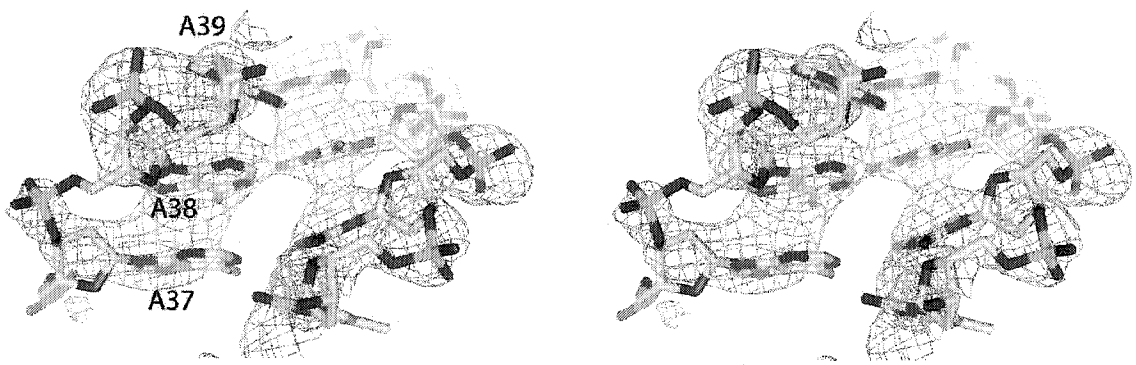

Figure 6.6: Overall comparison of DNA structure of A_{16} NCP and α-sat NCP. **(D)** Stereo view of a section of the |2Fo - Fc| electron density map, calculated at 3.2 Å and contoured at 1.2 σ, showing the part of Poly (dA·dT) element (37-39 bp).

The structure shows that the 16 bp poly (dA·dT) DNA fragment has a narrower minor groove than the α-sat 147 bp DNA in that region (Fig. 6.6C). This observation is consistent with the known poly (dA·dT) DNA structure [Alexeev et al., 1987]. Further, the minor groove width of the nucleosomal DNA was analyzed by 3DNA, a software program for analysis of nucleic acid structure (http://rutchem.rutgers.edu/~xiangjun/3DNA/). The minor groove width of the A_{16} DNA in the A_{16} NCP is compared with that of the 147 bp DNA in the α-sat NCP (Fig. 6.7 upper panel). Overall, the pattern of minor groove width of the A_{16} DNA is similar to that of the α-sat 147 bp DNA, except for a significant shift at the 16 bp poly (dA·dT) region (36- 51 bp) and some minor groove width variation regions (marked by stars). Most of these alterations in minor groove width correspond to regions of a high rmsd (Fig. 6.7 lower panel). The A_{16} DNA formed the two narrowest minor grooves in the A_{16} NCP. The minor groove width at base-pair 39^{th} in A_{16} NCP is much narrower than that of the α-sat NCP.

It has been suggested by co-crystal structure of DNA fragment and DNaseI that both minor groove width and DNA stiffness play an important role in determining the sequence-dependent DNase I sensitivity [Suck et al., 1988]. It has been suggested that the narrow minor groove and the rigid conformation of a poly (dA·dT) track are responsible for its low DNase I sensitivity [Fratini et al., 1982; Nelson et al., 1987; Suck et al., 1988]. However, it was shown in the present research that there were a hypersensitive site (around the 42^{nd} bp) for DNase I located in the A_{16} element (Fig. 6.4). This result suggests that the hypersensitive region in the A_{16} tract possesses a relative wide minor groove and

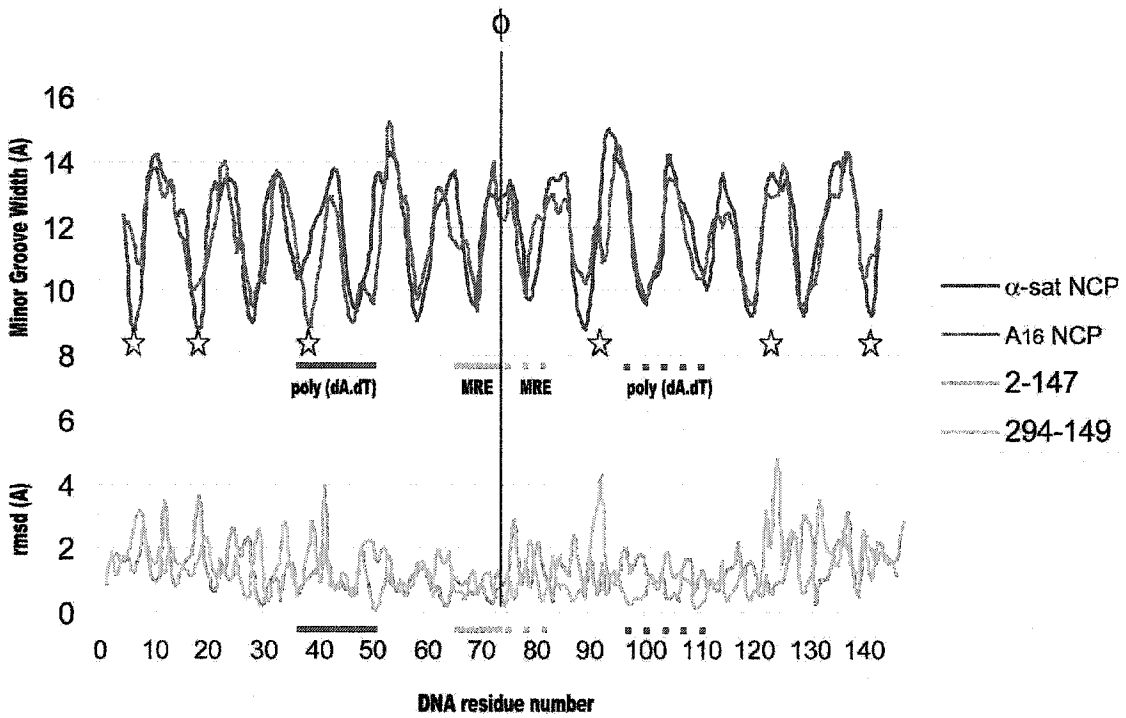

Figure 6.7: Minor groove widths are plotted against DNA residue number (upper panel). Values for A_{16} NCP model and α-sat NCP model are colored in magenta and blue, respectively. The position for16 bp poly (dA·dT) element (red bar) and Amt1 binding site (green) are labeled. The dashed red bar and green bar are convoluted positions for poly (dA·dT) element and Amt1 binding site. DNA was analyzed by 3DNA (v1.5) (See methods and materials). **The root mean square deviations (rmsd) for A_{16} DNA are plotted against DNAresidue number (lower panel).** Values for residues 2-147 and residues 294-149 are colored in orange and cyan, respectively.

bent conformation. The crystal structure of A_{16} NCP confirms this suggestion and shows that the A_{16} element is bent, and that the widest minor groove in the poly (dA·dT) is around 43rd bp, which is consistent with the DNaseI footprinting result. These results show that once the rigid poly (dA·dT) element is incorporated into nucleosome, the minor groove width and conformation will be altered and therefore its DNase I sensitivity will be changed.

The narrowest minor grove of α-sat NCP is at base-pair 90th, while the minor groove of this region is much wider in A_{16} NCP. Some minor groove variations are also located at the ends of DNA (Fig. 6.7). Another structural difference between the two models is located in 125-135 bp, the region just beside the poly (dA·dT) DNA fragment on the other gyre of the nucleosome (Fig. 6.6B). This observation is interesting because it appeared that the two most distorted DNA regions are physically close in the nucleosome, which might play a role in regulation of a binding of regulatory factors. However, there is no significant structural alteration in the MRE region (Fig. 6.6A).

It is difficult to recognize the detailed alteration in Protein-DNA interaction at this 3.2Å resolution. The average B factor for DNA is 168, which is higher than that of other NCP models. The high B factor for DNA might be caused by the potential convolution problem and/or by the dynamic and static disorder of DNA molecules. This also could be the intrinsic character of the A_{16} NCP, because previous study with another data set showed DNA is not visible in molecular replacement solution obtained by using only histone octamer (White, Ph.D. thesis 2003).

6.5 Discussion

It has been shown that long polypurine tracts are overrepresented in the genome of both simple and complex eukaryotes, particularly in promoter regions [Behe, 1995]. Poly (dA·dT) tracts have been suggested to alter the stability or dynamics of nucleosomes to facilitate transcription. To investigate the effects of poly (dA·dT) elements on nucleosome stability and structure, a 147 bp DNA containing a 16 bp Poly (dA·dT) element and the sequence recognition element (MRE) for Amt1 was prepared to reconstitute NCP in this study. The system under investigation here was selected because a positioned nucleosome encompassing the poly (dA·dT) element and the binding site for the transcription factor Amt1 has been mapped to high resolution in vivo [Zhu and Thiele, 1996].

Using the *in vitro* salt gradient reconstitution method, this study confirmed that a 147 bp DNA fragment containing a poly (dA·dT) tract of 16 bp in length can form stable folded nucleosomes (A_{16} NCPs). Higher temperature (55°C) was required for the DNA of the A_{16} NCP to attain the thermodynamically stable central position on the histone octamer *in vitro*. The rigid nature of the poly dA·dT tract, which is located at 36-51bp in the 147 bp A_{16} DNA, may introduce a free energy bias and make it refractory to *in vitro* sliding. This energy bias might be overcome by nucleosome remodeling complexes, and the centrally positioned A_{16} NCP could be formed *in vivo*.

The FRET study illustrated that the DNA ends were destabilized in the A_{16} NCPs. This result suggests that DNA accessibility is increased by the incorporation of a poly (dA·dT) tract into the nucleosome. In this study, it has also

shown by DNase I digestion that altered areas of DNA accessibility were caused by the poly (dA·dT) element. Previous research has shown that AMT1 binding with A_{16} NCP caused dissociation of DNA ends [White and Luger, 2004]. These findings suggest that there is a cooperative relationship between the poly (dA·dT) element, transcription factor, and DNA accessibility. That is, incorporation of the poly (dA·dT) element increases DNA accessibility, and further facilitates transcription factor binding, which in turn increases DNA accessibility. The results of this study are consistent with the observations that poly (dA·dT) elements are required for activated transcription of many genes in yeast [Filetici et al., 1998; Lascaris et al., 2000; Tanaka et al., 1996].

The crystal structure of A_{16} NCP reveals that overall structure is maintained except for some local structural alteration. One alteration is that the A_{16} region has a narrowed minor groove. The incorporation of A_{16} tract into NCP changes the minor groove width and the conformation of poly (dA·dT) DNA, and causes a pronounced DNA hypersensitivity located directly in the upstream of the poly (dA·dT) element. The other altered region is located just beside the poly (dA·dT) DNA fragment on the other gyre of the nucleosome, suggesting that this large altered DNA surface might play a role in permitting or enhancing the binding of regulatory factors. However, no significant structural alteration was observed in the MRE region. All the histone-DNA interactions are maintained within the A_{16} NCP structure. Therefore, the incorporation of the poly (dA·dT) DNA fragment results in a local subtly altered nucleosome structure, which is consistent with the *in vivo* and *in vitro* observations that modest changes in DNA accessibility and

modest increases in steady-state transcript levels are caused by poly (dA·dT) elements [Anderson and Widom, 2001; Iyer and Struhl, 1995; Mai et al., 2000; Zhu and Thiele, 1996].

The A_{16} NCP model is the first NCP structure with a non-palindromic DNA sequence. The overall structure is maintained as the NCP structure with palindromic DNA sequence, suggest that the overall NCP structure is not DNA sequence-dependent.

6.6 Acknowledgements

This work was supported by a grant from the NIH (GM61909). We thank Pamela N.Dyer for help with histones and DNA, Dr. Young-Jun Park for help with FRETstudies, and all Luger laboratory members for help and discussion. We acknowledge with gratitude Rajeswari S. Edayathumangalam's and Dr. Srinivas Chakravarthy's help with data collection, molecular replacement and structure refinement.

CHAPTER 7

X-ray Crystallographic Studies on the Complex of NCP and HMGN Nucleosome Binding Domain

The HMGN proteins bind specifically to nucleosomes. It has been suggested that HMGN proteins compete with H1 in binding with NCP via its nucleosome binding domain and further facilitate transcription. To test this hypothesis, we attempt to determine the co-crystal structure of the nucleosome core particle with a peptide comprises the nucleosome-binding domain of HMG-17.

7.1 Introduction

The high-mobility group (HMG) proteins are chromatin binding proteins that regulate gene expression by modifying the structure of DNA and chromatin and affecting the accessibility of the nucleosomal targets to their regulatory factors. The HMG superfamily is composed of three families: HMGB (previously termed HMG1/2), HMGA (formerly HMG-I/Y), and HMGN (formerly HMG-14/-17). Each family is characterized by a distinct DNA or chromatin binding motif.

The HMGN family is comprised of small, basic proteins that bind specifically to nucleosomes. They are highly conserved and found only in vertebrates. HMGN1 and HMGN2 (formerly named HMG-14 and HMG-17) have been studied extensively. These proteins have a molecular weight of~10 kDa, and contain three major functional motifs: a bipartite nuclear localization signal (NLS), a nucleosome-binding domain (NBD), and a chromatin unfolding domain (CHUD) [Bustin, 2001].

It has been shown that HMGN proteins bind specifically to the 147-base pair NCP [Shirakawa et al., 2000]. Furthermore, HMGN1 and HMGN2 bind to nucleosomes cooperatively and form complexes containing either two molecules of HMGN1 or two molecules of HMGN2 [Postnikov et al., 1995]. It has been suggested that the binding sites within the NCP are located in the two major grooves flanking the nucleosomal dyad axis and 25 bp from the end of the DNA (Fig. 7.1A) [Alfonso et al., 1994; Sandeen et al., 1980]. The main HMGN region responsible for binding nucleosomes is the nucleosomal-binding domain (NBD),

A

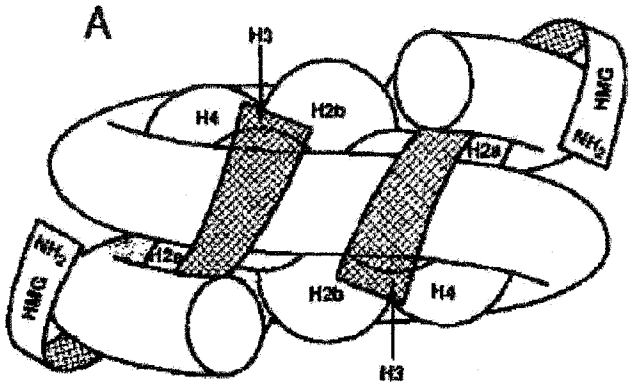

B

```
HMG-14 mpkrkv-ssaeg---aakeepkrrsarlsakp-pakveakpkkaaakdkssdkkv
HMG-17 mpkrkaegdakgdkakvkdepqrrsarlsakppapkpepkpkkapak-kge--kv

                                    peptide 2

HMG-14 qtkgkrgakgkqaevanqetkedlpaengetkteespasdeagekeaksd
HMG-17 p-kgkkg-kadagkegnn------paengdaktdqaqkaegagd--ak
```

Figure 7.1: A) Model of the location of the protein on the nucleosome core. The figure is reproduced from [Alfonso et al., 1994]. **B) Sequence alignment** of human HMG-14 (gi: 123101) and HMG-17 (gi: 123106). Peptide 2 was underlined.

a positively charged stretch of approximately 30 amino acids, rich in Arg, Lys and Pro residues [Crippa et al., 1992; Trieschmann et al., 1995].

The HMGN proteins are anchored to the NCPs by NBD to induce structural changes in chromatin fiber and to facilitate transcription and replication from chromatin templates [Bustin, 1999; Bustin and Reeves, 1996]. HMGN proteins have been shown to stimulate transcription from chromatin templates but not from deproteinized DNA, leading to the conclusion that the proteins are chromatin-specific effectors [Bustin, 2001]. Furthermore, most of the stimulatory effects were observed only when the HMGN proteins were incorporated into the nucleosomal arrays together with DNA and core histones rather than with preassembled chromatin. This suggested that a proper placement of the HMGN proteins into NCPs is required for their function [Bustin, 2001].

Interestingly, the HMGN-NCP complex appears more stable than NCP, as measured by nuclease digestion and thermal denaturation [Bustin and Reeves, 1996]. These observations seem to be inconsistent with the reported capability of HMGN proteins to enhance transcription or replication from chromatin templates. More and more evidence indicates that HMGN proteins decompact chromatin by competing with histone H1 and/or interacting with the amino termini of the core histones. For example, the nucleosomal footprint of HMGN proteins has been shown to partially overlap with that of histone H1 [Alfonso et al., 1994]; site-specific crosslinking experiments have indicated that the C-terminal region of HMGN1 interacts with the amino terminus of histone H3 [Trieschmann et al., 1998]; Catez and colleagues found that members of each of the three HMG

families weakened the binding of H1 to chromatin through a dynamic competition process [Catez et al., 2004]; and recent results have indicated that HMGN1 modulates histone H3 phosphorylation [Lim et al., 2004].

The structure of HMGN proteins is not known. A co-crystal structure of NCP and the nucleosomal-binding domain (NBD) of HMGNs would test the hypothesis that HMGN proteins compete with H1 in binding with NCP and provide insight on the binding mechanism. Knowledge of this mechanism would shed light on how the HMGN proteins de-compact chromatin fiber and further regulate transcription. In the present study, a 30-amino-acid peptide (peptide 2) was used. Peptide 2 comprises the nucleosome-binding domain of HMG-17 (amino acids 17-46, Fig 7.1B). It has been shown that peptide 2 and the intact HMG-17 protein protect the same nucleosomal DNA sites from DNase I digestion; and that digestion of the histone tails by trypsin weaken the binding of both the peptide 2 and the intact protein [Crippa et al., 1992]. Peptide 2 was incorporated into NCPs and the resulting Peptide2-NCP complex was subjected to crystallization trials. Crystals were obtained at optimized crystallization conditions for NCP. However, no electron density for peptide 2 was observed after molecular replacement.

7.2 Materials and methods

7.2a Gel shift assay for interactions between peptide 2 and NCP

Reconstituted Xenopus NCPs were mixed with peptide 2 or peptide C at a series of molar ratio (1:0.5, 1:1, and1:2) in the buffer (100 mM KCl, 20 mM K-Cacodylate, pH 6.0, 1mM EDTA). The mixtures were incubated in ice for 20

minutes and analyzed on a 5% polyacrylamide gel (acrylamide : bis-acrylamide 60:1) in 0.2 x TBE, run at a constant 150 V at 4°C.

7.2b salt gradient reconstitution of Peptide2-NCP complex

Xenopus histones were over-expressed in bacteria and purified using previously published protocols [Bao et al., 2004; Dyer et al., 2004].146 bp α-sat DNA was prepared as described previously[Dyer et al., 2004]. Xenopus core histones were refolded into histone octamers and purified by gel filtration[Dyer et al., 2004]. The peptide 2, Xenopus octamer and 146 bp α-sat DNA were mixed at different molar ratios and reconstituted by the salt gradient method [Dyer et al., 2004]. Samples were analyzed on a 5% polyacrylamide gel (acrylamide : bis-acrylamide 60:1) in 0.2 x TBE, run at a constant 150 V at 4°C. The Peptide2-NCP complexes resulting from large scale reconstitution were shifted at 37°C for 1 hour, and purified by preparative gel electrophoresis [Dyer et al., 2004].

7.2c Crystallographic procedures

The mixture of peptide 2 and purified Xenopus NCP at a 1.2:1 molar ratio (*co-crystallize*), and the purified Peptide2-NCP complexes (*co-reconstitution*) were crystallized using salting in vapor diffusion. The NCP concentrations ranged from 6-8 mg/ml, with salt concentrations of 40-60 mM KCl, and 40-50 mM $MnCl_2$. The Xenopus NCP crystals were soaked in a 24% 2-methyl-2,4-pentanediol and 5% trehalose solution with 1mM peptide 2 (*soaking*). For initial screening, data were collected on a home source X-ray generator. Synchrotron Data were

collected at Advanced Light Source beamline 5.0.2 in Berkeley. Data were indexed and scaled with DENZO and SCALEPACK [Otwinowski and Minor, 1997]. Molecular replacement was used to obtain crystal phases, using Protein Data Bank ID code 1AOI (146 bp Xenopus NCP) as the search model. Molecular replacement and subsequent rounds of refinement were performed with CNS [Brunger et al., 1998]. The program O was used to analyze the resulting |2Fo-Fc| and |Fo-Fc| electron density maps [Jones et al., 1991].

7.3 Results and discussion

7.3a Peptide 2 binds NCP specifically

In order to verify that peptide 2 can bind NCP specifically, various concentrations of peptide 2 were mixed with Xenopus NCP in 100 mM KCl, 20 mM K-Cacodylate, pH 6.0 buffer. Another peptide (peptide C), which has an identical amino acid composition but sequence different from that of peptide 2, was mixed with Xenopus NCP as a control. The mixtures were incubated in ice for 20 minutes and analyzed by 5% native gel. No clear shifted band was observed in the peptide C and NCP mixtures (Fig. 7.2 lane 5-7). However, there was a clear shift when the molar ratio of peptide 2 to NCP was approximately 1 (Fig. 7.2 lane 2), suggesting that peptide 2 binds NCP specifically. A shifted band with some smear was formed when the molar ratio of peptide 2 to NCP was about 2 (Fig. 7.2 lane 1), indicating that there was too much excess peptide.

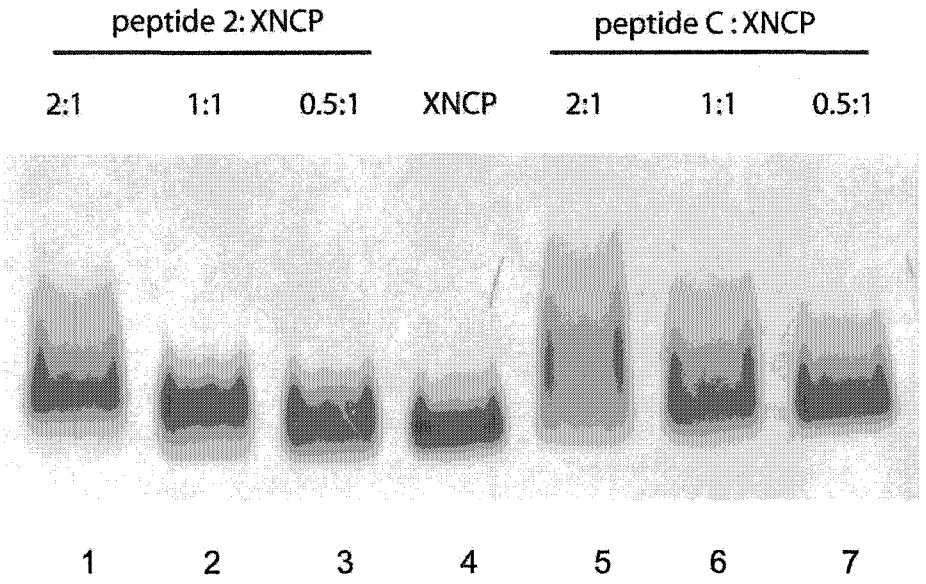

Figure 7.2: Gel shift assay shows peptide 2 binding with 146 bp Xenopus-NCP (lanes 1-3). Peptide C (scrambled peptide 2) was used as acontrol (lanes 5-7). The molar ratio of peptide 2 or peptide C (scrambled peptide 2) to NCPs is shown on the top of each lane.

Therefore, 1.2:1 was used as the molar ratio of peptide 2 to NCP for further crystallization trials.

7.3b Peptide 2 can be incorporated in NCP by salt gradient reconstitution

In order to obtain a pure Peptide2-NCP complex for crystallization screening studies, peptide 2, Xenopus octamer and 146 bp α-sat DNA were mixed at different molar ratios and reconstituted by the salt gradient method [Dyer et al., 2004]. It was shown that the same complex was formed when the molar ratios of peptide 2 to histone octamer were approximately 1, 2, or 4 (Fig. 7.3A lanes 5-10). The data also indicated that this Peptide2-NCP complex can be shifted by heat treatment (Fig. 7.3A lane 9, 10; Fig. 7.3B lane 3, 4). The shifted Peptide2-NCP complex occupied the same position as the upper band of unshifted Xenopus NCP (Fig. 7.3A lane 4, 5). Molar ratios of peptide 2 to histone octamer of 2:1 and 4:1 were used for large scale reconstitution. The resulting Peptide2-NCP complexes were purified by preparative gel electrophoresis and subjected to crystallization trials.

7.3c Crystallization of Peptide2-NCP complex

The mixture of peptide 2 and purified Xenopus NCP at a 1.2:1 molar ratio was subjected to a crystallization screen. Crystals were set up using a salting in vapor diffusion method with varying concentrations of KCl and $MnCl_2$. Single crystals were developed in salt concentrations of 40-60 mM KCl, and 40-50 mM

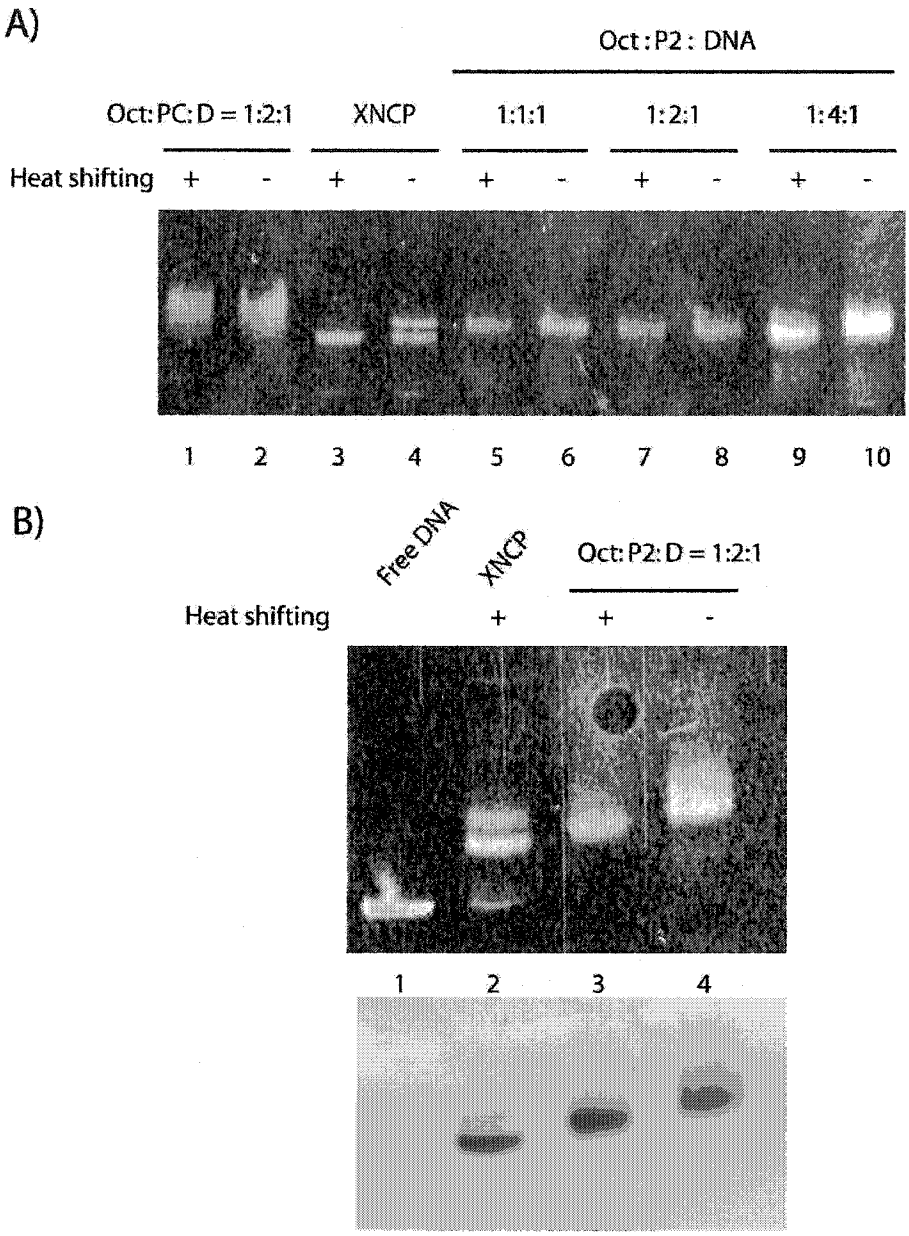

Figure 7.3: Reconstitution of Pepteide 2-NCP complex. A) Salt gradient reconstituted Peptide 2-NCP (lanes 5-10) before (-) and after (+) a 1 h incubation at 37°C, were analyzed by 5% native PAGE and stained with ethidium bromide. Peptide C was used as acontrol (lanes 1-2). The molar ratios of Xenopusoctamer: peptide 2 (or peptide C) : DNA is shown on the top of each lane. **B)** Large scale reconstituted Peptide 2-NCP complex (lanes 3, 4) before (-) and after (+) a 1 h incubation at 37°C, were analyzed by 5% native PAGE and stained with ethidium bromide (upper panel) and coomassie blue (lower panel). The molar ratios of Xenopus octamer : peptide 2 : DNA is 1:2:1.

$MnCl_2$, which are the optimum crystallization conditions for NCP. A crystallization screen was also set up with the purified Peptide2-NCP complexes. Single crystals were yielded at similar salt concentrations. The morphology of these crystals was similar to that of Xenopus NCP, having a long rod with a center hole down the middle from one end. Furthermore, single crystals of Xenopus NCP were also soaked in a 24% 2-methyl-2,4-pentanediol and 5% trehalose solution with 1mM peptide 2 for 5 days. Several of the crystals obtained by these methods diffracted to a resolution of ~3.0 Å with a home source X-ray generator. Several data sets were collected at the synchrotron (ALS-Berkeley-BL5.0.2). All the crystals crystallized in the orthorhombic space group $P2_12_12_1$ and have unit cell dimensions that resembled those of Xenopus NCPs. Molecular replacement with the Xenopus NCP (1AOI) as the search model yielded solutions with respectable R-factors (Table 7.1). However, no electron density for peptide 2 was observed in any of these crystals. These results suggest that the peptide 2 might dissociate from the Peptide 2-NCP complex during crystallization. It has been indicated that the HMGN binding sites within the NCP are located in the two major grooves flanking the nucleosomal dyad axis [Alfonso et al., 1994]. The DNA ends are crystal packing contacts of NCP [Luger et al., 1997a; White et al., 2001]. The crystal packing interactions might force the dissociation of peptide 2 in those optimized salt concentrations for NCP. Therefore, the crystallization conditions for Peptide 2-NCP complexes should be screened by the crystallization kits, such as the Natrix kit or the Pegs kit. Recently, a 23-amino-acid viral peptide was successfully co-crystallized with Xenopus NCP by soaking

Table 7.1: Summary of crystallographic analysis

	XNCP co-crystallized with peptide 2	Peptide 2 reconstituted with XNCP	XNCP soaked with peptide 2
Space group	$P2_12_12_1$	$P2_12_12_1$	$P2_12_12_1$
Unit cell dimensions (Å)	a =105.87, b = 109.633 c = 182.00	a = 106.00, b = 109.77, c = 181.70	a = 105.04, b = 109.09 c = 180.94
Reflections (total / unique)	178503 / 47686	265052 / 66149	120843 / 40606
Completeness (%) (overall / last shell)	99.3 / 94.3	99.4 / 99.9	95.7 / 89.7
R_{merge} (%) (over all/last shell)	7 / 26.1	7 / 39.3	7 / 45.2
Resolution (Å)	50 – 2.9	50 – 2.6	50 – 3.0
R-factor / R_{free}	0.229 / 0.278	0.228 / 0.264	0.234 / 0.276
Data collection	Home source	Synchrotron	Home source

at a 40:1 molar ratio of peptide: NCP (personal communication with Jayanth V. Chodaparambil). Consequently, it may be fruitful to increase the peptide 2 concentration in the soaking solution

7.4 Acknowledgements

We thank Dr. Micheal Bustin for kind gifts of peptide 2 and peptide C, Pamela N.Dyer for help with histones and DNA, We acknowledge with gratitude Rajeswari S. Edayathumangalam's and Dr. Srinivas Chakravarthy's help with data collection, molecular replacement and structure refinement.

CHAPTER 8

Contributions to Other Publications

1. Muthurajan, U.M., Bao, Y., Forsberg, L.J., Edayathumangalam, R.S., Dyer, P.N., White, C.L. and Luger, K. (2004) Crystal structures of histone Sin mutant nucleosomes reveal altered protein-DNA interactions. *Embo J*, 23, 260-271.

Eleven crystal structures of nucleosome core particles containing individual point mutations in the structured regions of histones H3 and H4 were described. The mutated residues are located at the two protein-DNA interfaces flanking the nucleosomal dyad. It was found that even nonconservative mutations of these residues have only moderate effects on global nucleosome structure. The number of lost protein-DNA interactions correlates directly with an increased propensity of the histone octamer to reposition with respect to the DNA, and with an overall destabilization of the nucleosome. Thus, the disruption of only two to six of the approximately 120 direct histone-DNA interactions within the nucleosome has a pronounced effect on nucleosome mobility and stability. I did site directed mutagenesis for H3 T118I, H3 R116A, H4 V43I, and H4 V43A. I also expressed and purified these proteins.

2. Park, Y.J., Chodaparambil, J.V., Bao, Y., McBryant, S.J. and Luger, K. (2004) Nucleosome assembly protein 1 exchanges histone H2A-H2B dimers and assists nucleosome sliding. *J Biol Chem.*

Here we show that the nucleosome assembly protein 1 (NAP-1) from yeast reversibly removes and replaces histone protein dimer H2A-H2B or histone variant dimers from assembled nucleosomes, resulting in active histone exchange. Transient removal of H2A-H2B dimers facilitates nucleosome sliding along the DNA to a thermodynamically favorable position. Histone exchange as well as nucleosome sliding is independent of ATP and relies on the presence of the C-terminal acidic domain of yeast NAP-1. I purified 196 bp DNA and did preliminary micrococcal nuclease digestion of 196 bp NCPs.

3. Kenny, J., Bao, Y., Hamm, B., Taylor, L., Toth, A., Wagers, B. and Curthoys, N.P. (2003) Bacterial expression, purification, and characterization of rat kidney-type mitochondrial glutaminase. *Protein ExPurif*, 31, 140-148.

In this study, a recombinant glutaminase, lacking the coding sequence contained in exon 1, was found to be fully active. An additional construct that corresponded to the sequence encoded by exons 2-14 also retained full activity. Both of the fully active, truncated proteins were purified. The K(M) values for glutamine of the native and recombinant forms of glutaminase were nearly identical. However, the two truncated forms of the glutaminase exhibit the characteristic phosphate activation profile only when dialyzed into a buffer

lacking phosphate. Dialysis versus 10mM Tris-phosphate was sufficient to form an active tetramer. Thus, the deleted N-terminal sequence may contribute to the phosphate-dependent oligomerization and activation of the native glutaminase. I cloned the N terminal truncated glutaminase gene into bacterial expression vector and expressed the protein. I also did preliminary protein and enzyme assay.

CHAPTER 9

Summary and Future Considerations

The main conclusion that can be drawn from the results of my thesis work is that incorporation of a histone variant, H2A.Bbd, into a nucleosome results in a more open structure and reduced inherent stability (Chapter 2 and Chapter 4). The results presented in this thesis support the hypothesis that H2A.Bbd is localized in transcriptionally active chromatin, and facilitates the process of transcription. This research sheds light on another cellular mechanism for regulation of transcription. The mechanism involves changing the biochemical makeup of nucleosomes by incorporation of special histone variant, H2A.Bbd, to reduce the inherent stability of nucleosomes and facilitate transcription.

The residues within the docking domain of H2A.Bbd differ significantly from those of H2A. It was demonstrated that the H2A.Bbd docking domain is responsible for the reduced interaction between H2A.Bbd-H2B dimer and $(H3\text{-}H4)_2$ tetramer, and the loose DNA organization observed in Bbd-NCP (Chapter 2). The N terminal region (1- 51) of H2A.Bbd, including αN helix, α1 helix, and L1 loop, is another domain altered significantly from the canonical H2A. This domain could be exchanged into the canonical H2A and the hybrid protein could be subjected to the biochemical and biophysical studies employed in Chapter 2 and 4. Results from such studies would indicate the importance of this N terminal

domain of H2A.Bbd in dimer-tetramer interaction, nucleosome structure, and inherent stability.

The crystal structure of Bbd-NCP would provide valuable information in understanding the functional significance of H2A.Bbd. However, no crystal has been obtained from the crystallization trays of 146 bp Bbd-NCP, 147 bp Bbd-3E-NCP, 122 bp Bbd-NCP, or 122 bp Bbd-3E-NCP (Chapter 5). It has been shown that H2A.Bbd dimer readily exchanges in and out of the Bbd-NCP. This reduced inherent stability could result in a mixture of nucleosome, hexasome, and tetrosome. This problem might explain the difficulty of Bbd-NCP crystallization. Addition of extra H2A.Bbd-H2B dimer that would interact with hexasome and tetrasome to form nucleosome, and further increase the sample homogeneity. Therefore, addition of extra H2A.Bbd-H2B dimer to the purified 122 bp Bbd-NCP could solve the crystallization problem. Careful dimer and NCP titration would be necessary since it has been shown that too much excess H2A.Bbd-H2B dimer could result in aggregation (Chapter 4). It has been shown that the docking of H2A-H2B dimer against $(H3\text{-}H4)_2$ tetramer is highly consistent between the octamer structure and nucleosome structure [Chantalat et al., 2003]. Crystal structure of H2A.Bbd-H2B dimer would provide important insights regarding dimer-tetramer interactions and the Bbd-NCP structure. Consequently, crystallization of H2A.Bbd-H2B dimer would be a future research effort.

To test the hypothesis that incorporation of H2A-Bbd may alter the nucleosome surface and change the nucleosome-nucleosome interactions, a highly defined in vitro chromatin model system has been employed by one of our

collaborators, Dr. Tremethick. This model system utilizes the 208-12 DNA template, which consists of twelve 208 base pair repeats of a nucleosome positioning sequence from the *Lytechinus* 5S rRNA gene. The major advantage of using this system is that one can produce highly homogenous nucleosomal arrays that can be characterized by a rigorous analytical method [Carruthers et al., 1998; Carruthers and Hansen, 2000; Fan et al., 2002; Fletcher and Hansen, 1995; Tse and Hansen, 1997]. The sedimentation velocity analyses of Bbd nucleosomal arrays and mouse nucleosomal arrays are in process in Dr. Tremethick's laboratory. Comparing the sedimentation coefficient distribution profiles [Schwarz and Hansen, 1994] of both arrays, they can address whether H2A-Bbd containing array has a less folded conformation than the 'major' chromatin array.

MNase digestion H2A.Bbd nucleosomal array assembled on a supercoiled plasmid DNA showed that H2A.Bbd was assembled onto a regularly spaced nucleosomal array with a shorter repeat length (~126 bp, Chapter 2). This result leads to the hypothesis that more nucleosomes will be formed in Bbd arrays than in conventional arrays. To test this hypothesis, quantitative agarose gel electrophoresis (QAGE), which provides a direct measure of macromolecular surface charge density, would be employed [Georgel and Hansen, 2003; Hansen et al., 1997]. We expect to see a higher surface charge density on the Bbd arrays. Furthermore, atomic force microscopy (AFM) or cryo-electron microscopy (cryo-EM) would be applied to observe the Bbd nucleosomal array.

Theoretically, it is possible to have a nucleosome with one $(H3\text{-}H4)_2$ tetramer, one canonical H2A-H2B dimer and one variant H2A-H2B dimer *in vivo*. However, it will be extremely difficult to investigate the distribution of histone variants in a single-nucleosome level *in vivo* due to the technical challenge. We investigated this possibility in vitro and found that H2A.Bbd was capable of forming hybrid nucleosome (Chapter 3). The structure and stability of this hybrid nucleosome could be evaluated, once it is purified and subjected to the series of biochemical and biophysical studies applied in Chapter 2 and 4.

The work presented in this thesis provided the first clear insight into the structure and inherent stability of nucleosomes containing H2A.Bbd. These results offer some guidance for future functional and structural studies of H2A.Bbd and Bbd-NCP. To date, our knowledge of the functional, mechanistic and structural aspects of H2A.Bbd and Bbd-NCP are very limited. Clearly, much more needs to be done before we can fully understand its structure, function and cellular mechanism.

The poly (dA·dT) elements have been suggested to promote transcription by altering the stability or dynamics of nucleosomes. The crystal structure of a nucleosome (A_{16} NCP) containing a 16 bp poly (dA·dT) element was solved in this thesis (Chapter 6). This structure would be useful in guiding the functional studies of poly (dA·dT) elements. To understand structural changes caused by transcription factor binding to a nuclesosome, the co-crystal structure of Amt1 and A_{16} NCP would need to be investigated.

HMGN proteins bind specifically to nucleosomes. Knowledge of the co-crystal structure of NCP and the nucleosomal-binding domain (NBD) of HMGNs would shed light on the mechanism of HMGN binding with NCP. This knowledge would be very useful in understanding how the HMGN proteins decompact chromatin fiber and further facilitate transcription. In this thesis, crystals of NBD and NCP complex (Peptide2-NCP) were obtained at optimized crystallization conditions for NCP. However, no electron density for peptide 2 was observed after molecular replacement (Chapter 7). Crystallization kits and an optimized soaking method would be used to screen the crystallization conditions for Peptide2-NCP complex.

In summary, this thesis research endeavored to define the impacts on nucleosome core particle structure and stability by histone variant incorporation; rigid DNA element incorporation; and interaction with nucleosome binding protein. The results presented herein provide significant information on nucleosome structure and stability and transcription regulation within a chromatin context, and may offer direction for additional functional and structural studies in the chromatin field.

REFERENCES

Adkins, N.L., Watts, M. and Georgel, P.T. (2004) To the 30-nm chromatin fiber and beyond. *Biochim Biophys Acta*, 1677, 12-23.

Ahmad, K. and Henikoff, S. (2002) Histone H3 variants specify modes of chromatin assembly. *Proc Natl Acad Sci U S A*, 99 Suppl 4, 16477-16484.

Akey, C.W. and Luger, K. (2003) Histone chaperones and nucleosome assembly. *Curr Opin Struct Biol*, 13, 6-14.

Alexeev, D.G., Lipanov, A.A. and Skuratovskii, I. (1987) Poly(dA).poly(dT) is a B-type double helix with a distinctively narrow minor groove. *Nature*, 325, 821-823.

Alfonso, P.J., Crippa, M.P., Hayes, J.J. and Bustin, M. (1994) The footprint of chromosomal proteins HMG-14 and HMG-17 on chromatin subunits. *J Mol Biol*, 236, 189-198.

Allan, J., Mitchell, T., Harborne, N., Bohm, L. and Crane-Robinson, C. (1986) Roles of H1 domains in determining higher order chromatin structure and H1 location. *J Mol Biol*, 187, 591-601.

Anderson, J.D. and Widom, J. (2000) Sequence and position-dependence of the equilibrium accessibility of nucleosomal DNA target sites. *J Mol Biol*, 296, 979-987.

Anderson, J.D. and Widom, J. (2001) Poly(dA-dT) promoter elements increase the equilibrium accessibility of nucleosomal DNA target sites. *Mol Cell Biol*, 21, 3830-3839.

Angelov, D., Molla, A., Perche, P.Y., Hans, F., Cote, J., Khochbin, S., Bouvet, P. and Dimitrov, S. (2003) The histone variant macroH2A interferes with transcription factor binding and SWI/SNF nucleosome remodeling. *Mol Cell*, 11, 1033-1041.

Angelov, D., Verdel, A., An, W., Bondarenko, V., Hans, F., Doyen, C.M., Studitsky, V.M., Hamiche, A., Roeder, R.G., Bouvet, P. and Dimitrov, S. (2004) SWI/SNF remodeling and p300-dependent transcription of histone variant H2ABbd nucleosomal arrays. *Embo J*, 23, 3815-3824.

Angelov, D., Vitolo, J.M., Mutskov, V., Dimitrov, S. and Hayes, J.J. (2001) Preferential interaction of the core histone tail domains with linker DNA. *Proc Natl Acad Sci U S A*, 98, 6599-6604.

Arents, G., Burlingame, R.W., Wang, B.C., Love, W.E. and Moudrianakis, E.N. (1991) The nucleosomal core histone octamer at 3.1 A resolution: a tripartite protein assembly and a left-handed superhelix. *Proc Natl Acad Sci U S A*, 88, 10148-10152.

Aviles, F.J., Chapman, G.E., Kneale, G.G., Crane-Robinson, C. and Bradbury, E.M. (1978) The conformation of histone H5. Isolation and characterisation of the globular segment. *Eur J Biochem*, 88, 363-371.

Baer, B.W. and Rhodes, D. (1983) Eukaryotic RNA polymerase II binds to nucleosome cores from transcribed genes. *Nature*, 301, 482-488.

Bao, Y., Konesky, K., Park, Y.J., Rosu, S., Dyer, P.N., Rangasamy, D., Tremethick, D.J., Laybourn, P.J. and Luger, K. (2004) Nucleosomes containing the histone variant H2A.Bbd organize only 118 base pairs of DNA. *Embo J*, 23, 3314-3324.

Bassing, C.H., Suh, H., Ferguson, D.O., Chua, K.F., Manis, J., Eckersdorff, M., Gleason, M., Bronson, R., Lee, C. and Alt, F.W. (2003) Histone H2AX: a dosage-dependent suppressor of oncogenic translocations and tumors. *Cell*, 114, 359-370.

Becker, P.B. and Horz, W. (2002) ATP-dependent nucleosome remodeling. *Annu Rev Biochem*, 71, 247-273.

Behe, M.J. (1995) An overabundance of long oligopurine tracts occurs in the genome of simple and complex eukaryotes. *Nucleic Acids Res*, 23, 689-695.

Belotserkovskaya, R., Oh, S., Bondarenko, V.A., Orphanides, G., Studitsky, V.M. and Reinberg, D. (2003) FACT facilitates transcription-dependent nucleosome alteration. *Science*, 301, 1090-1093.

Berger, S.L. (2002) Histone modifications in transcriptional regulation. *Curr Opin Genet Dev*, 12, 142-148.

Black, B.E., Foltz, D.R., Chakravarthy, S., Luger, K., Woods, V.L., Jr. and Cleveland, D.W. (2004) Structural determinants for generating centromeric chromatin. *Nature*, 430, 578-582.

Boeger, H., Griesenbeck, J., Strattan, J.S. and Kornberg, R.D. (2003) Nucleosomes unfold completely at a transcriptionally active promoter. *Mol Cell*, 11, 1587-1598.

Boeger, H., Griesenbeck, J., Strattan, J.S. and Kornberg, R.D. (2004) Removal of promoter nucleosomes by disassembly rather than sliding in vivo. *Mol Cell*, 14, 667-673.

Brooks, W. and Jackson, V. (1994) The rapid transfer and selective association of histones H2A and H2B onto negatively coiled DNA at physiological ionic strength. *J Biol Chem*, 269, 18155-18166.

Brunger, A.T., Adams, P.D., Clore, G.M., DeLano, W.L., Gros, P., Grosse-Kunstleve, R.W., Jiang, J.S., Kuszewski, J., Nilges, M., Pannu, N.S., Read, R.J., Rice, L.M., Simonson, T. and Warren, G.L. (1998) Crystallography & NMR system: A new software suite for macromolecular structure determination. *Acta Crystallogr D Biol Crystallogr*, 54 (Pt 5), 905-921.

Bruno, M., Flaus, A. and Owen-Hughes, T. (2004) Site-specific attachment of reporter compounds to recombinant histones. *Methods Enzymol*, 375, 211-228.

Bruno, M., Flaus, A., Stockdale, C., Rencurel, C., Ferreira, H. and Owen-Hughes, T. (2003) Histone H2A/H2B dimer exchange by ATP-dependent chromatin remodeling activities. *Mol Cell*, 12, 1599-1606.

Bustin, M. (1999) Regulation of DNA-dependent activities by the functional motifs of the high-mobility-group chromosomal proteins. *Mol Cell Biol*, 19, 5237-5246.

Bustin, M. (2001) Chromatin unfolding and activation by HMGN(*) chromosomal proteins. *Trends Biochem Sci*, 26, 431-437.

Bustin, M. and Reeves, R. (1996) High-mobility-group chromosomal proteins: architectural components that facilitate chromatin function. *Prog Nucleic Acid Res Mol Biol*, 54, 35-100.

Carruthers, L.M., Bednar, J., Woodcock, C.L. and Hansen, J.C. (1998) Linker histones stabilize the intrinsic salt-dependent folding of nucleosomal arrays: mechanistic ramifications for higher-order chromatin folding. *Biochemistry*, 37, 14776-14787.

Carruthers, L.M. and Hansen, J.C. (2000) The core histone N termini function independently of linker histones during chromatin condensation. *J Biol Chem*, 275, 37285-37290.

Carter, G.J. and van Holde, K. (1998) Self-association of linker histone H5 and of its globular domain: evidence for specific self-contacts. *Biochemistry*, 37, 12477-12488.

Catez, F., Yang, H., Tracey, K.J., Reeves, R., Misteli, T. and Bustin, M. (2004) Network of dynamic interactions between histone H1 and high-mobility-group proteins in chromatin. *Mol Cell Biol*, 24, 4321-4328.

Celeste, A., Difilippantonio, S., Difilippantonio, M.J., Fernandez-Capetillo, O., Pilch, D.R., Sedelnikova, O.A., Eckhaus, M., Ried, T., Bonner, W.M. and Nussenzweig, A. (2003a) H2AX haploinsufficiency modifies genomic stability and tumor susceptibility. *Cell*, 114, 371-383.

Celeste, A., Fernandez-Capetillo, O., Kruhlak, M.J., Pilch, D.R., Staudt, D.W., Lee, A., Bonner, R.F., Bonner, W.M. and Nussenzweig, A. (2003b) Histone H2AX phosphorylation is dispensable for the initial recognition of DNA breaks. *Nat Cell Biol*, 5, 675-679.

Chadwick, B.P., Valley, C.M. and Willard, H.F. (2001) Histone variant macroH2A contains two distinct macrochromatin domains capable of directing macroH2A to the inactive X chromosome. *Nucleic Acids Res*, 29, 2699-2705.

Chadwick, B.P. and Willard, H.F. (2001) A Novel Chromatin Protein, Distantly Related to Histone H2A, Is Largely Excluded from the Inactive X Chromosome. *J Cell Biol*, 152, 375-384.

Chadwick, B.P. and Willard, H.F. (2002) Cell cycle-dependent localization of macroH2A in chromatin of the inactive X chromosome. *J Cell Biol*, 157, 1113-1123.

Chakravarthy, S., Bao, Y., Roberts, V.A., Tremethick, D. and Luger, K. (2004) Structural Charavterization of histone H2A variants. *Cold Spring Harbor Symposia on Quantitative Biology* (Accepted).

Chang, L., Loranger, S.S., Mizzen, C., Ernst, S.G., Allis, C.D. and Annunziato, A.T. (1997) Histones in transit: cytosolic histone complexes and diacetylation of H4 during nucleosome assembly in human cells. *Biochemistry*, 36, 469-480.

Chantalat, L., Nicholson, J.M., Lambert, S.J., Reid, A.J., Donovan, M.J., Reynolds, C.D., Wood, C.M. and Baldwin, J.P. (2003) Structure of the

histone-core octamer in KCl/phosphate crystals at 2.15 A resolution. *Acta Crystallogr D Biol Crystallogr*, 59, 1395-1407.

Chen, T.A., Smith, M.M., Le, S.Y., Sternglanz, R. and Allfrey, V.G. (1991) Nucleosome fractionation by mercury affinity chromatography. Contrasting distribution of transcriptionally active DNA sequences and acetylated histones in nucleosome fractions of wild-type yeast cells and cells expressing a histone H3 gene altered to encode a cysteine 110 residue. *J Biol Chem*, 266, 6489-6498.

Cheung, P., Tanner, K.G., Cheung, W.L., Sassone-Corsi, P., Denu, J.M. and Allis, C.D. (2000a) Synergistic coupling of histone H3 phosphorylation and acetylation in response to epidermal growth factor stimulation. *Mol Cell*, 5, 905-915.

Cheung, W.L., Briggs, S.D. and Allis, C.D. (2000b) Acetylation and chromosomal functions. *Curr Opin Cell Biol*, 12, 326-333.

Clark, K.L., Halay, E.D., Lai, E. and Burley, S.K. (1993) Co-crystal structure of the HNF-3/fork head DNA-recognition motif resembles histone H5. *Nature*, 364, 412-420.

Clarkson, M.J., Wells, J.R., Gibson, F., Saint, R. and Tremethick, D.J. (1999) Regions of variant histone His2AvD required for Drosophila development. *Nature*, 399, 694-697.

Coll, M., Frederick, C.A., Wang, A.H. and Rich, A. (1987) A bifurcated hydrogen-bonded conformation in the d(A.T) base pairs of the DNA dodecamer d(CGCAAATTTGCG) and its complex with distamycin. *Proc Natl Acad Sci U S A*, 84, 8385-8389.

Costanzi, C. and Pehrson, J.R. (1998) Histone macroH2A1 is concentrated in the inactive X chromosome of female mammals. *Nature*, 393.

Costanzi, C. and Pehrson, J.R. (2001) MacroH2A2, a new member of the MacroH2A core histone family. *J Biol Chem*, 21, 21.

Crane Robinson, C. (1997) Where is the globular domain of linker histone located on the nucleosome? *Trends Biochem Sci*, 22, 75-77.

Crippa, M.P., Alfonso, P.J. and Bustin, M. (1992) Nucleosome core binding region of chromosomal protein HMG-17 acts as an independent functional domain. *J Mol Biol*, 228, 442-449.

Cui, Y. and Bustamante, C. (2000) Pulling a single chromatin fiber reveals the forces that maintain its higher-order structure. *Proc Natl Acad Sci U S A*, 97, 127-132.

d'Adda di Fagagna, F., Reaper, P.M., Clay-Farrace, L., Fiegler, H., Carr, P., Von Zglinicki, T., Saretzki, G., Carter, N.P. and Jackson, S.P. (2003) A DNA damage checkpoint response in telomere-initiated senescence. *Nature*, 426, 194-198.

Davey, C.A., Sargent, D.F., Luger, K., Maeder, A.W. and Richmond, T.J. (2002) Solvent mediated interactions in the structure of the nucleosome core particle at 1.9 a resolution. *J Mol Biol*, 319, 1097-1113.

Dickerson, R.E., Drew, H.R., Conner, B.N., Wing, R.M., Fratini, A.V. and Kopka, M.L. (1982) The anatomy of A-, B-, and Z-DNA. *Science*, 216, 475-485.

Dillon, P.J. and Rosen, C.A. (1990) A rapid method for the construction of synthetic genes using the polymerase chain reaction. *Biotechniques*, 9, 298, 300.

Dong, F. and van Holde, K.E. (1991) Nucleosome positioning is determined by the (H3-H4)2 tetramer. *Proc Natl Acad Sci U S A*, 88, 10596-10600.

Dorigo, B., Schalch, T., Kulangara, A., Duda, S., Schroeder, R.R. and Richmond, T.J. (2004) Nucleosome arrays reveal the two-start organization of the chromatin fiber. *Science*, 306, 1571-1573.

Dyer, P.N., Edayathumangalam, R.S., White, C.L., Bao, Y., Chakravarthy, S., Muthurajan, U.M. and Luger, K. (2004) Reconstitution of nucleosome core particles from recombinant histones and DNA. *Methods Enzymol*, 375, 23-44.

Eberharter, A. and Becker, P.B. (2004) ATP-dependent nucleosome remodelling: factors and functions. *J Cell Sci*, 117, 3707-3711.

Edayathumangalam, R.S., Weyermann, P., Gottesfeld, J.M., Dervan, P.B. and Luger, K. (2004) Molecular recognition of the nucleosomal "supergroove". *Proc Natl Acad Sci U S A*, 101, 6864-6869.

Faast, R., Thonglairoam, V., Schulz, T., Wells, J.R.E., Rathjen, P.D., Tremethick, D.J. and Lyons, I. (1999) H2AZ is essential for early mouse development. *(manuscript in preparation).*

Fan, J.Y., Gordon, F., Luger, K., Hansen, J.C. and Tremethick, D.J. (2002) The essential histone variant H2A.Z regulates the equilibrium

between different chromatin conformational states. *Nat Struct Biol*, 19, 19.

Fazzio, T.G. and Tsukiyama, T. (2003) Chromatin remodeling in vivo: evidence for a nucleosome sliding mechanism. *Mol Cell*, 12, 1333-1340.

Filetici, P., Aranda, C., Gonzalez, A. and Ballario, P. (1998) GCN5, a yeast transcriptional coactivator, induces chromatin reconfiguration of HIS3 promoter in vivo. *Biochem Biophys Res Commun*, 242, 84-87.

Finch, J.T. and Klug, A. (1976) Solenoidal model for superstructure in chromatin. *Proc. Natl. Acad. Sci. U. S. A.*, 73, 1897-1901.

Flaus, A. and Owen-Hughes, T. (2004) Mechanisms for ATP-dependent chromatin remodelling: farewell to the tuna-can octamer? *Curr Opin Genet Dev*, 14, 165-173.

Fletcher, T.M. and Hansen, J.C. (1995) Core histone tail domains mediate oligonucleosome folding and nucleosomal DNA organization through distinct molecular mechanisms. *J Biol Chem*, 270, 25359-25362.

Fratini, A.V., Kopka, M.L., Drew, H.R. and Dickerson, R.E. (1982) Reversible bending and helix geometry in a B-DNA dodecamer: CGCGAATTBrCGCG. *J Biol Chem*, 257, 14686-14707.

Gautier, T., Abbott, D.W., Molla, A., Verdel, A., Ausio, J. and Dimitrov, S. (2004) Histone variant H2ABbd confers lower stability to the nucleosome. *EMBO Rep*, 5, 715-720.

Georgel, P., Demeler, B., Terpening, C., Paule, M.R. and van Holde, K.E. (1993) Binding of the RNA polymerase I transcription complex to its promoter can modify positioning of downstream nucleosomes assembled in vitro. *J Biol Chem*, 268, 1947-1954.

Georgel, P.T. and Hansen, J.C. (2003) Quantitative characterization of specific genomic promoters using agarose gel electrophoresis. *Biopolymers*, 68, 557-562.

Georges, S.A., Kraus, W.L., Luger, K., Nyborg, J.K. and Laybourn, P.J. (2002) p300-Mediated Tax Transactivation from Recombinant Chromatin: Histone Tail Deletion Mimics Coactivator Function. *Mol Cell Biol*, 22, 127-137.

Gottesfeld, J.M. and Luger, K. (2001) Energetics and Affinity of the Histone Octamer for Defined DNA Sequences. *Biochemistry*, 40, 10927-10933.

Hamiche, A., Carot, V., Alilat, M., De Lucia, F., O'Donohue, M.F., Revet, B. and Prunell, A. (1996) Interaction of the histone (H3-H4)2 tetramer of the nucleosome with positively supercoiled DNA minicircles: Potential flipping of the protein from a left- to a right-handed superhelical form. *Proc Natl Acad Sci U S A*, 93, 7588-7593.

Hansen, J.C. (2002) Conformational dynamics of the chromatin fiber in solution: determinants, mechanisms, and functions. *Annu Rev Biophys Biomol Struct*, 31, 361-392.

Hansen, J.C., Kreider, J.I., Demeler, B. and Fletcher, T.M. (1997) Analytical ultracentrifugation and agarose gel electrophoresis as tools for studying chromatin folding in solution. *Methods*, 12, 62-72.

Harp, J.M., Hanson, B.L., Timm, D.E. and Bunick, G.J. (2000) Asymmetries in the nucleosome core particle at 2.5 A resolution. *Acta Crystallogr D Biol Crystallogr*, 56 Pt 12, 1513-1534.

Hartman, P.G., Chapman, G.E., Moss, T. and Bradbury, E.M. (1977) Studies on the role and mode of operation of the very-lysine-rich histone H1 in eukaryote chromatin. The three structural regions of the histone H1 molecule. *Eur J Biochem*, 77, 45-51.

Hayes, J.J., Clark, D.J. and Wolffe, A.P. (1991) Histone contributions to the structure of DNA in the nucleosome. *Proc Natl Acad Sci U S A*, 88, 6829-6833.

Hayes, J.J. and Wolffe, A.P. (1993) Preferential and asymmetric interaction of linker histones with 5S DNA in the nucleosome. *Proc Natl Acad Sci U S A*, 90, 6415-6419.

Henikoff, S., Ahmad, K. and Malik, H.S. (2001) The centromere paradox: stable inheritance with rapidly evolving DNA. *Science*, 293, 1098-1102.

Henikoff, S., Furuyama, T. and Ahmad, K. (2004) Histone variants, nucleosome assembly and epigenetic inheritance. *Trends Genet*, 20, 320-326.

Howman, E.V., Fowler, K.J., Newson, A.J., Redward, S., MacDonald, A.C., Kalitsis, P. and Choo, K.H. (2000) Early disruption of centromeric chromatin organization in centromere protein A (Cenpa) null mice. *Proc Natl Acad Sci U S A*, 97, 1148-1153.

Hoyer-Fender, S., Costanzi, C. and Pehrson, J.R. (2000) Histone macroH2A1.2 is concentrated in the XY-body by the early pachytene stage of spermatogenesis. *Exp Cell Res*, 258, 254-260.

Ito, T., Bulger, M., Kobayashi, R. and Kadonaga, J.T. (1996) Drosophila NAP-1 is a core histone chaperone that functions in ATP-facilitated assembly of regularly spaced nucleosomal arrays. *Mol Cell Biol*, 16, 3112-3124.

Ito, T., Bulger, M., Pazin, M.J., Kobayashi, R. and Kadonaga, J.T. (1997) ACF, an ISWI-containing and ATP-utilizing chromatin assembly and remodeling factor. *Cell*, 90, 145-155.

ito, T., Ikehara, T., Nakagawa, T., Kraus, W.L. and Muramatsu, M. (2000) p300-mediated acetylation facilitates the transfer of histone H2A-H2B dimers from nucleosomes to a histone chaperone. *Genes Dev*, 14, 1899-1907.

Iyer, V. and Struhl, K. (1995) Poly(dA:dT), a ubiquitous promoter element that stimulates transcription via its intrinsic DNA structure. *Embo J*, 14, 2570-2579.

Jackson, V. (1990) In vivo studies on the dynamics of histone-DNA interaction: evidence for nucleosome dissolution during replication and transcription and a low level of dissolution independent of both. *Biochemistry*, 29, 719-731.

Jenuwein, T. and Allis, C.D. (2001) Translating the histone code. *Science*, 293, 1074-1080.

Jones, T.A., Zou, J.Y., Cowan, S.W. and Kjeldgaard. (1991) Improved methods for building protein models in electron density maps and the location of errors in these models. *Acta Crystallogr A*, 47 (Pt 2), 110-119.

Kaufman, P.D., Kobayashi, R., Kessler, N. and Stillman, B. (1995) The p150 and p60 subunits of chromatin assembly factor I: a molecular link between newly synthesized histones and DNA replication. *Cell*, 81, 1105-1114.

Kerrigan, L.A. and Kadonaga, J.T. (1992) Periodic binding of individual core histones to DNA: inadvertent purification of the core histone H2B as a putative enhancer-binding factor. *Nucleic Acids Res*, 20, 6673-6680.

Kimura, H. and Cook, P.R. (2001) Kinetics of core histones in living human cells: little exchange of H3 and H4 and some rapid exchange of H2B. *J Cell Biol*, 153, 1341-1353.

Kireeva, M.L., Walter, W., Tchernajenko, V., Bondarenko, V., Kashlev, M. and Studitsky, V.M. (2002) Nucleosome remodeling induced by RNA polymerase II: loss of the H2A/H2B dimer during transcription. *Mol Cell*, 9, 541-552.

Kobor, M.S., Venkatasubrahmanyam, S., Meneghini, M.D., Gin, J.W., Jennings, J.L., Link, A.J., Madhani, H.D. and Rine, J. (2004) A Protein Complex Containing the Conserved Swi2/Snf2-Related ATPase Swr1p Deposits Histone Variant H2A.Z into Euchromatin. *PLoS Biol*, 2, E131.

Koch, K.A. and Thiele, D.J. (1996) Autoactivation by a Candida glabrata copper metalloregulatory transcription factor requires critical minor groove interactions. *Mol Cell Biol*, 16, 724-734.

Kornberg, R.D. (1974) Chromatin structure: a repeating unit of histones and DNA. *Science*, 184, 868-871.

Kornberg, R.D. and Lorch, Y. (1999) Twenty-five years of the nucleosome, fundamental particle of the eukaryote chromosome. *Cell*, 98, 285-294.

Kouzarides, T. (2002) Histone methylation in transcriptional control. *Curr Opin Genet Dev*, 12, 198-209.

Kraus, W.L. and Kadonaga, J.T. (1998) p300 and estrogen receptor cooperatively activate transcription via differential enhancement of initiation and reinitiation. *Genes Dev*, 12, 331-342.

Krogan, N.J., Keogh, M.C., Datta, N., Sawa, C., Ryan, O.W., Ding, H., Haw, R.A., Pootoolal, J., Tong, A., Canadien, V., Richards, D.P., Wu, X., Emili, A., Hughes, T.R., Buratowski, S. and Greenblatt, J.F. (2003) A Snf2 family ATPase complex required for recruitment of the histone H2A variant Htz1. *Mol Cell*, 12, 1565-1576.

Krude, T. (1999) Chromatin assembly during DNA replication in somatic cells. *Eur J Biochem*, 263, 1-5.

Kunkel, G.R. and Martinson, H.G. (1981) Nucleosomes will not form on double-stranded RNa or over poly(dA).poly(dT) tracts in recombinant DNA. *Nucleic Acids Res*, 9, 6869-6888.

Lascaris, R.F., Groot, E., Hoen, P.B., Mager, W.H. and Planta, R.J. (2000) Different roles for abf1p and a T-rich promoter element in nucleosome organization of the yeast RPS28A gene. *Nucleic Acids Res*, 28, 1390-1396.

Laskowski, R., MacArthur, M., Moss, D. and Thornton, J. (1993) PROCHECK: a program to evaluate stereochemical quality of protein structures. *J. Appl. Crystallogr.*, 26, 283-291.

Lee, H., Habas, R. and Abate-Shen, C. (2004) MSX1 cooperates with histone H1b for inhibition of transcription and myogenesis. *Science*, 304, 1675-1678.

Leuba, S.H., Yang, G., Robert, C., Samori, B., van Holde, K., Zlatanova, J. and Bustamante, C. (1994) Three-dimensional structure of extended chromatin fibers as revealed by tapping-mode scanning force microscopy. *Proc Natl Acad Sci U S A*, 91, 11621-11625.

Lim, J.H., Catez, F., Birger, Y., West, K.L., Prymakowska-Bosak, M., Postnikov, Y.V. and Bustin, M. (2004) Chromosomal protein HMGN1 modulates histone H3 phosphorylation. *Mol Cell*, 15, 573-584.

Lindsey, G.G., Orgeig, S., Thompson, P., Davies, N. and Maeder, D.L. (1991) Extended C-terminal tail of wheat histone H2A interacts with DNA of the "linker" region. *J Mol Biol*, 218, 805-813.

Litt, M.D., Simpson, M., Gaszner, M., Allis, C.D. and Felsenfeld, G. (2001) Correlation between histone lysine methylation and developmental changes at the chicken beta-globin locus. *Science*, 293, 2453-2455.

Liu, X., Li, B. and Gorovsky, M.A. (1996) Essential and nonessential histone H2A variants in Tetrahymena thermophila. *Mol Cell Biol*, 16, 4305-4311.

Liu, X.D. and Thiele, D.J. (1997) Yeast metallothionein gene expression in response to metals and oxidative stress. *Methods*, 11, 289-299.

Lohr, D. and Van Holde, K.E. (1975) Yeast chromatin subunit structure. *Science*, 188, 165-166.

Losa, R., Omari, S. and Thoma, F. (1990) Poly(dA).poly(dT) rich sequences are not sufficient to exclude nucleosome formation in a constitutive yeast promoter. *Nucleic Acids Res*, 18, 3495-3502.

Louters, L. and Chalkley, R. (1985) Exchange of histones H1, H2A, and H2B in vivo. *Biochemistry*, 24, 3080-3085.

Luger, K. (2003) Structure and dynamic behavior of nucleosomes. *Curr Opin Genet Dev*, 13, 127-135.

Luger, K., Maeder, A.W., Richmond, R.K., Sargent, D.F. and Richmond, T.J. (1997a) X-ray structure of the nucleosome core particle at 2.8 Å resolution. *Nature*, 389, 251-259.

Luger, K., Rechsteiner, T.J., Flaus, A.J., Waye, M.M. and Richmond, T.J. (1997b) Characterization of nucleosome core particles containing histone proteins made in bacteria. *J Mol Biol*, 272, 301-311.

Luger, K., Rechsteiner, T.J. and Richmond, T.J. (1999) Preparation of nucleosome core particle from recombinant histones. *Methods Enzymol*, 304, 3-19.

Luger, K. and Richmond, T.J. (1998a) DNA binding within the nucleosome core. *Current Opinion in Structural Biology*, 8, 33-40.

Luger, K. and Richmond, T.J. (1998b) The histone tails of the nucleosome. *Curr Opin Genet Dev*, 8, 140-146.

Mahloogi, H. and Behe, M.J. (1997) Oligoadenosine tracts favor nucleosome formation. *Biochem Biophys Res Commun*, 235, 663-668.

Mai, X., Chou, S. and Struhl, K. (2000) Preferential accessibility of the yeast his3 promoter is determined by a general property of the DNA sequence, not by specific elements. *Mol Cell Biol*, 20, 6668-6676.

Malik, H.S. and Henikoff, S. (2003) Phylogenomics of the nucleosome. *Nat Struct Biol*, 10, 882-891.

Maman, J.D., Yager, T.D. and Allan, J. (1994) Self-association of the globular domain of histone H5. *Biochemistry*, 33, 1300-1310.

McBryant, S.J., Park, Y.J., Abernathy, S.M., Laybourn, P.J., Nyborg, J.K. and Luger, K. (2003) Preferential binding of the histone (H3-H4)2 tetramer by NAP1 is mediated by the amino-terminal histone tails. *J Biol Chem*, 278, 44574-44583.

Mello, J.A. and Almouzni, G. (2001) The ins and outs of nucleosome assembly. *Curr Opin Genet Dev*, 11, 136-141.

Meneghini, M.D., Wu, M. and Madhani, H.D. (2003) Conserved histone variant H2A.Z protects euchromatin from the ectopic spread of silent heterochromatin. *Cell*, 112, 725-736.

Mizuguchi, G., Shen, X., Landry, J., Wu, W.H., Sen, S. and Wu, C. (2004) ATP-driven exchange of histone H2AZ variant catalyzed by SWR1 chromatin remodeling complex. *Science*, 303, 343-348.

Muchardt, C. and Yaniv, M. (1999) ATP-dependent chromatin remodelling: SWI/SNF and Co. are on the job. *J Mol Biol*, 293, 187-198.

Muthurajan, U.M., Park, Y.J., Edayathumangalam, R.S., Suto, R.K., Chakravarthy, S., Dyer, P.N. and Luger, K. (2003) Structure and dynamics of nucleosomal DNA. *Biopolymers*, 68, 547-556.

Nelson, H.C., Finch, J.T., Luisi, B.F. and Klug, A. (1987) The structure of an oligo(dA).oligo(dT) tract and its biological implications. *Nature*, 330, 221-226.

Noll, M. and Kornberg, R.D. (1977) Action of micrococcal nuclease on chromatin and the location of histone H1. *J Mol Biol*, 109, 393-404.

Noma, K., Allis, C.D. and Grewal, S.I. (2001) Transitions in distinct histone H3 methylation patterns at the heterochromatin domain boundaries. *Science*, 293, 1150-1155.

Otwinowski, Z. and Minor, W. (1997) *Processing of X-ray diffraction data collected in oscillation mode.* Academic Press, New York.

Oudet, P., Gross-Bellard, M. and Chambon, P. (1975) Electron microscopic and biochemical evidence that chromatin structure is a repeating unit. *Cell*, 4, 281-300.

Owen-Hughes, T. and Bruno, M. (2004) Molecular biology. Breaking the silence. *Science*, 303, 324-325.

Palmer, D.K., O'Day, K., Trong, H.L., Charbonneau, H. and Margolis, R.L. (1991) Purification of the centromere-specific protein CENP-A and demonstration that it is a distinctive histone. *Proc Natl Acad Sci U S A*, 88, 3734-3738.

Park, Y.J., Chodaparambil, J.V., Bao, Y., McBryant, S.J. and Luger, K. (2004a) Nucleosome assembly protein 1 exchanges histone H2A-H2B dimers and assists nucleosome sliding. *J Biol Chem.*

Park, Y.J., Dyer, P.N., Tremethick, D.J. and Luger, K. (2004b) A new fluorescence resonance energy transfer approach demonstrates that the histone variant H2AZ stabilizes the histone octamer within the nucleosome. *J Biol Chem*, 279, 24274-24282.

Parthun, M.R., Widom, J. and Gottschling, D.E. (1996) The major cytoplasmic histone acetyltransferase in yeast: links to chromatin replication and histone metabolism. *Cell*, 87, 85-94.

Peck, L.J. and Wang, J.C. (1981) Sequence dependence of the helical repeat of DNA in solution. *Nature*, 292, 375-378.

Pehrson, J.R., Costanzi, C. and Dharia, C. (1997) Developmental and tissue expression patterns of histone macroH2A1 subtypes. *Cell Biochem*, 65, 107-113.

Pehrson, J.R. and Fried, V.A. (1992) MacroH2A, a core histone containing a large nonhistone region. *Science*, 257, 1398-1400.

Perche, P., Vourc'h, C., Konecny, L., Souchier, C., Robert-Nicoud, M., Dimitrov, S. and Khochbin, S. (2000) Higher concentrations of histone macroH2A in the barr body are correlated with higher nucleosome density [In Process Citation]. *Curr Biol*, 10, 1531-1534.

Peterson, C.L. (2000) ATP-dependent chromatin remodeling: going mobile. *FEBS Lett*, 476, 68-72.

Postnikov, Y.V., Trieschmann, L., Rickers, A. and Bustin, M. (1995) Homodimers of chromosomal proteins HMG-14 and HMG-17 in nucleosome cores. *J Mol Biol*, 252, 423-432.

Protacio, R.U. and Widom, J. (1996) Nucleosome transcription studied in a real-time synchronous system: test of the lexosome model and direct measurement of effects due to histone octamer. *J Mol Biol*, 256, 458-472.

Pruss, D., Bartholomew, B., Persinger, J., Hayes, J., Arents, G., Moudrianakis, E.N. and Wolffe, A.P. (1996) An asymmetric model for the nucleosome: a binding site for linker histones inside the DNA gyres [see comments]. *Science*, 274, 614-617.

Puhl, H.L. and Behe, M.J. (1995) Poly(dA).poly(dT) forms very stable nucleosomes at higher temperatures. *J Mol Biol*, 245, 559-567.

Ramakrishnan, V. (1995) The histone fold: evolutionary questions. *Proc Natl Acad Sci U S A*, 92, 11328-11330.

Ramakrishnan, V. (1997) Histone structure and the organization of the nucleosome. *Annu Rev Biophys Biomol Struct*, 26, 83-112.

Ramakrishnan, V., Finch, J.T., Graziano, V., Lee, P.L. and Sweet, R.M. (1993) Crystal structure of globular domain of histone H5 and its implications for nucleosome binding. *Nature*, 362, 219-223.

Rangasamy, D., Berven, L., Ridgway, P. and Tremethick, D.J. (2003) Pericentric heterochromatin becomes enriched with H2A.Z during early mammalian development. *Embo J*, 22, 1599-1607.

Rangasamy, D., Greaves, I. and Tremethick, D.J. (2004) RNA interference demonstrates a novel role for H2A.Z in chromosome segregation. *Nat Struct Mol Biol*, 11, 650-655.

Rasmussen, T.P., Huang, T., Mastrangelo, M.A., Loring, J., Panning, B. and Jaenisch, R. (1999) Messenger RNAs encoding mouse histone macroH2A1 isoforms are expressed at similar levels in male and female cells and result from alternative splicing. *Nucleic Acids Res*, 27, 3685-3689.

Reinke, H. and Horz, W. (2003) Histones are first hyperacetylated and then lose contact with the activated PHO5 promoter. *Mol Cell*, 11, 1599-1607.

Rhodes, D. (1979) Nucleosome cores reconstituted from poly (dA-dT) and the octamer of histones. *Nucleic Acids Res*, 6, 1805-1816.

Richler, C., Dhara, S.K. and Wahrman, J. (2000) Histone macroH2A1.2 is concentrated in the XY compartment of mammalian male meiotic nuclei. *Cytogenet Cell Genet*, 89, 118-120.

Richmond, T.J., Davey, C.A. (2003) The structure of DNA in the nucleosome core. *Nature*, 423, 145-150.

Richmond, T.J., Searles, M.A. and Simpson, R.T. (1988) Crystals of a nucleosome core particle containing defined sequence DNA. *J Mol Biol*, 199, 161-170.

Rothkamm, K. and Lobrich, M. (2003) Evidence for a lack of DNA double-strand break repair in human cells exposed to very low x-ray doses. *Proc Natl Acad Sci U S A*, 100, 5057-5062.

Rubbi, L., Camilloni, G., Caserta, M., Di Mauro, E. and Venditti, S. (1997) Chromatin structure of the Saccharomyces cerevisiae DNA topoisomerase I promoter in different growth phases. *Biochem J*, 328 (Pt 2), 401-407.

Rydberg, B., Holley, W.R., Mian, I.S. and Chatterjee, A. (1998) Chromatin conformation in living cells: support for a zig-zag model of the 30 nm chromatin fiber. *J Mol Biol*, 284, 71-84.

Sandeen, G., Wood, W.I. and Felsenfeld, G. (1980) The interaction of high mobility proteins HMG14 and 17 with nucleosomes. *Nucleic Acids Res*, 8, 3757-3778.

Sanner, M.F., Olson, A.J. and Spehner, J.C. (1996) Reduced surface: an efficient way to compute molecular surfaces. *Biopolymers*, 38, 305-320.

Santos-Rosa, H., Schneider, R., Bannister, A.J., Sherriff, J., Bernstein, B.E., Emre, N.C., Schreiber, S.L., Mellor, J. and Kouzarides, T. (2002) Active genes are tri-methylated at K4 of histone H3. *Nature*, 419, 407-411.

Satchwell, S.C., Drew, H.R. and Travers, A.A. (1986) Sequence periodicities in chicken nucleosome core DNA. *J Mol Biol*, 191, 659-675.

Schwarz, P.M. and Hansen, J.C. (1994) Formation and stability of higher order chromatin structures. Contributions of the histone octamer. *J Biol Chem*, 269, 16284-16289.

Shelby, R.D., Vafa, O. and Sullivan, K.F. (1997) Assembly of CENP-A into centromeric chromatin requires a cooperative array of nucleosomal DNA contact sites. *J Cell Biol*, 136, 501-513.

Shibahara, K. and Stillman, B. (1999) Replication-dependent marking of DNA by PCNA facilitates CAF-1-coupled inheritance of chromatin. *Cell*, 96, 575-585.

Shirakawa, H., Herrera, J.E., Bustin, M. and Postnikov, Y. (2000) Targeting of high mobility group-14/-17 proteins in chromatin is independent of DNA sequence. *J Biol Chem*, 275, 37937-37944.

Simpson, R.T. (1978) Structure of the chromatosome, a chromatin particle containing 160 base pairs of DNA and all the histones. *Biochemistry*, 17, 5524-5531.

Simpson, R.T., Thoma, F. and Brubaker, J.M. (1985) Chromatin reconstituted from tandemly repeated cloned DNA fragments and core histones: a model system for study of higher order structure. *Cell*, 42, 799-808.

Smith, S. and Stillman, B. (1991) Stepwise assembly of chromatin during DNA replication in vitro. *Embo J*, 10, 971-980.

Stargell, L.A., Bowen, J., Dadd, C.A., Dedon, P.C., Davis, M., Cook, R.G., Allis, C.D. and Gorovsky, M.A. (1993) Temporal and spatial association of histone H2A variant hv1 with transcriptionally competent chromatin during nuclear development in Tetrahymena thermophila. *Genes Dev*, 7, 2641-2651.

Staynov, D.Z. and Crane-Robinson, C. (1988) Footprinting of linker histones H5 and H1 on the nucleosome. *Embo J*, 7, 3685-3691.

Strahl, B.D. and Allis, C.D. (2000) The language of covalent histone modifications. *Nature*, 403, 41-45.

Suck, D., Lahm, A. and Oefner, C. (1988) Structure refined to 2A of a nicked DNA octanucleotide complex with DNase I. *Nature*, 332, 464-468.

Sullivan, K. (1998) A moveable feast: the centromere/-kinetochore complex in cell division. *Frontiers in Molecular Biology: Cell Division Glover, D., Endow, S., Eds.*

Sullivan, K.F., Hechenberger, M. and Masri, K. (1994) Human CENP-A contains a histone H3 related histone fold domain that is required for targeting to the centromere. *J Cell Biol*, 127, 581-592.

Sullivan, S., Sink, D.W., Trout, K.L., Makalowska, I., Taylor, P.M., Baxevanis, A.D. and Landsman, D. (2002) The Histone Database. *Nucleic Acids Res*, 30, 341-342.

Suter, B., Schnappauf, G. and Thoma, F. (2000) Poly(dA.dT) sequences exist as rigid DNA structures in nucleosome-free yeast promoters in vivo. *Nucleic Acids Res*, 28, 4083-4089.

Suto, R.K., Clarkson, M.J., Tremethick, D.J. and Luger, K. (2000) Crystal structure of a nucleosome core particle containing the variant histone H2A.Z. *Nat Struct Biol*, 7, 1121-1124.

Suto, R.K., Edayathumangalam, R.S., White, C.L., Melander, C., Gottesfeld, J.M., Dervan, P.B. and Luger, K. (2003) Crystal structures of nucleosome core particles in complex with minor groove DNA-binding ligands. *J Mol Biol*, 326, 371-380.

Tagami, H., Ray-Gallet, D., Almouzni, G. and Nakatani, Y. (2004) Histone H3.1 and H3.3 complexes mediate nucleosome assembly pathways dependent or independent of DNA synthesis. *Cell*, 116, 51-61.

Tanaka, S., Livingstone-Zatchej, M. and Thoma, F. (1996) Chromatin structure of the yeast URA3 gene at high resolution provides insight into structure and positioning of nucleosomes in the chromosomal context. *J Mol Biol*, 257, 919-934.

Thomas, J.O. and Wilson, C.M. (1986) Selective radiolabelling and identification of a strong nucleosome binding site on the globular domain of histone H5. *Embo J*, 5, 3531-3537.

Trieschmann, L., Martin, B. and Bustin, M. (1998) The chromatin unfolding domain of chromosomal protein HMG-14 targets the N-terminal tail of histone H3 in nucleosomes. *Proc Natl Acad Sci U S A*, 95, 5468-5473.

Trieschmann, L., Postnikov, Y.V., Rickers, A. and Bustin, M. (1995) Modular structure of chromosomal proteins HMG-14 and HMG-17: definition of a transcriptional enhancement domain distinct from the nucleosomal binding domain. *Mol Cell Biol*, 15, 6663-6669.

Tse, C. and Hansen, J.C. (1997) Hybrid trypsinized nucleosomal arrays: identification of multiple functional roles of the H2A/H2B and H3/H4 N-termini in chromatin fiber compaction. *Biochemistry*, 36, 11381-11388.

van Daal, A. and Elgin, S.C. (1992) A histone variant, H2AvD, is essential in Drosophila melanogaster. *Mol Biol Cell*, 3, 593-602.

Van Holde, K.E. (1988) *Chromatin*. Springer-Verlag, New York.

Van Holde KE, Weischet WO (1978) Boundary analysis of sedimentation velocity experiments with monodisperse and paucidisperse solutes. *Biopolymers* 17: 1387–1403

Varga-Weisz, P., van Holde, K. and Zlatanova, J. (1993) Preferential binding of histone H1 to four-way helical junction DNA. *J Biol Chem*, 268, 20699-20700.

Varga-Weisz, P., Zlatanova, J., Leuba, S.H., Schroth, G.P. and van Holde, K. (1994) Binding of histones H1 and H5 and their globular domains to four-way junction DNA. *Proc Natl Acad Sci U S A*, 91, 3525-3529.

Vermaak, D., Hayden, H.S. and Henikoff, S. (2002) Centromere targeting element within the histone fold domain of Cid. *Mol Cell Biol*, 22, 7553-7561.

Vermaak, D. and Wolffe, A.P. (1998) Chromatin and chromosomal controls in development. *Dev Genet*, 22, 1-6.

Verreault, A. (2000) De novo nucleosome assembly: new pieces in an old puzzle. *Genes Dev*, 14, 1430-1438.

Verreault, A., Kaufman, P.D., Kobayashi, R. and Stillman, B. (1996) Nucleosome assembly by a complex of CAF-1 and acetylated histones H3/H4. *Cell*, 87, 95-104.

White, C.L. and Luger, K. (2004) Defined structural changes occur in a nucleosome upon Amt1 transcription factor binding. *J Mol Biol*, 342, 1391-1402.

White, C.L., Suto, R.K. and Luger, K. (2001) Structure of the yeast nucleosome core particle reveals fundamental changes in internucleosome interactions. *Embo J*, 20, 5207-5218.

Widom, J. (1998a) Chromatin structure: linking structure to function with histone H1. *Curr Biol*, 8, R788-791.

Widom, J. (1998b) Structure, Dynamics, and function of chromatin in vitro. *Annu. Rev. Biophys.*, 27, 285-387.

Widom, J. (2001) Role of DNA sequence in nucleosome stability and dynamics. *Q Rev Biophys*, 34, 269-324.

Wolffe, A. (1998) *Chromatin: Structure and Function.* Academic Press.

Wolffe, A.P. (1997) Histone H1. *Int J Biochem Cell Biol*, 29, 1463-1466.

Wolffe, A.P. and Pruss, D. (1996) Deviant nucleosomes: the functional specialization of chromatin. *Trends Genet*, 12, 58-62.

Woodcock, C.L., Grigoryev, S.A., Horowitz, R.A. and Whitaker, N. (1993) A chromatin folding model that incorporates linker variability generates fibers resembling the native structures. *Proc Natl Acad Sci U S A*, 90, 9021-9025.

Xie, X., Kokubo, T., Cohen, S.L., Mirza, U.A., Hoffmann, A., Chait, B.T., Roeder, R.G., Nakatani, Y. and Burley, S.K. (1996) Structural similarity between TAFs and the heterotetrameric core of the histone octamer [see comments]. *Nature*, 380, 316-322.

Zhang, Y. (2003) Transcriptional regulation by histone ubiquitination and deubiquitination. *Genes Dev*, 17, 2733-2740.

Zhang, Y. and Reinberg, D. (2001) Transcription regulation by histone methylation: interplay between different covalent modifications of the core histone tails. *Genes Dev*, 15, 2343-2360.

Zhu, Z. and Thiele, D.J. (1996) A specialized nucleosome modulates transcription factor access to a C. glabrata metal responsive promoter. *Cell*, 87, 459-470.

Zlatanova, J. and van Holde, K. (1996) The linker histones and chromatin structure: new twists. *Prog Nucleic Acid Res Mol Biol*, 52, 217-259.